ORNL
MASTER COPY

OAK RIDGE NATIONAL LABORATORY
operated by
UNION CARBIDE CORPORATION
for the
U. S. ATOMIC ENERGY COMMISSION

UNION CARBIDE

ORNL - TM - 603

15

WASTE TREATMENT AND DISPOSAL QUARTERLY PROGRESS REPORT

FEBRUARY-APRIL 1963

This document has been approved for release
to the public by:

David R Hamrin 7/28/95
Technical Information Officer Date
ORNL Site

NOTICE

This document contains information of a preliminary nature and was prepared primarily for internal use at the Oak Ridge National Laboratory. It is subject to revision or correction and therefore does not represent a final report. The information is not to be abstracted, reprinted or otherwise given public dissemination without the approval of the ORNL patent branch, Legal and Information Control Department.

LEGAL NOTICE

This report was prepared as an account of Government sponsored work. Neither the United States, nor the Commission, nor any person acting on behalf of the Commission:

A. Makes any warranty or representation, expressed or implied, with respect to the accuracy, completeness, or usefulness of the information contained in this report, or that the use of any information, apparatus, method, or process disclosed in this report may not infringe privately owned rights; or

B. Assumes any liabilities with respect to the use of, or for damages resulting from the use of any information, apparatus, method, or process disclosed in this report.

As used in the above, "person acting on behalf of the Commission" includes any employee or contractor of the Commission, or employee of such contractor, to the extent that such employee or contractor of the Commission, or employee of such contractor prepares, disseminates, or provides access to, any information pursuant to his employment or contract with the Commission, or his employment with such contractor.

ORNL-TM-603

CHEMICAL TECHNOLOGY DIVISION

HEALTH PHYSICS DIVISION

WASTE TREATMENT AND DISPOSAL QUARTERLY PROGRESS REPORT FEBRUARY-APRIL 1963

R. E. Blanco F. L. Parker

DATE ISSUED

DEC 16 1963

OAK RIDGE NATIONAL LABORATORY
Oak Ridge, Tennessee
operated by
UNION CARBIDE CORPORATION
for the
U. S. ATOMIC ENERGY COMMISSION

ABSTRACT

High-Level Waste Pot Calcination. Three continuous evaporator-pot calcination tests using simulated FTW-65 Purex waste were completed. The average feed rates varied from 31 liters/hr to 49 liters/hr, and the maximum hourly rates from 125 to 190 liters/hr. The average feed rate is a function of the amount of concentration in the evaporator and the degree of filling of the calciner pot. The calcined solids had densities of 1.23 to 1.30. The residual nitrate composition for the calcined solids varied from 100 to 400 ppm and decreased with time that the calcined solid was above 600°C. The sulfate retention in the calciner was high, only 0.3% to 2% of the sulfate was lost. This loss is attributed to entrainment since similar values were obtained for nonvolatile ions such as iron and sodium. A catch tank, tested as a method of isolating mercury, collected only 27% of the mercury. The amount of mercury caught was proportional to the amount in the last fraction of the calciner condensate. A ruthenium decontamination factor of 3×10^3 (using non-radioactive ruthenium) was obtained in test R-72 across the continuous evaporator using an impingement plate de-entrainer.

Fixation of High Level Waste in Glass. Simulated Hanford formaldehyde-treated 1965 waste solution (FTW-65 waste) was evaporated to 1/4 of original volume without precipitation of solids. Experimental phosphate glassy melts were made by addition of phosphate, sodium and calcium to FTW-65. Generally, these melts were too soluble in water or lost SO_3 readily, but a few appeared to be insoluble and were relatively stable at high temperatures. Two semicontinuous, semiengineering scale experiments were successful although excessive solids entrainment caused an operating problem. The product contained 45% waste oxides and represented a volume reduction factor of 30. Sulfate loss was less than 2% and 24% of the ruthenium volatilized. An electrical resistance probe for sensing levels of solution, calcine and melt in the pot performed satisfactorily.

Imposition of a small cathodic current decreased the time necessary for removal of >99% of the mercury in a copper column from FTW-65 waste solution from about 25 to 12 minutes or less. More current was required than the minimum to remove the mercury to prevent dissolution of excess copper.

Exposure of 304L specimens at 300°C in bedded salt (NaCl) containing natural occurring impurities showed corrosion rates of about 0.03 mil/mo. Type 304 stainless steel and titanium 45A, both coupled and uncoupled to each other, showed low rates for exposure in refluxing FTW-65 waste solution and vapors; the maximum rate was on the coupled 304L and amounted to 0.3 mil/mo with no local attack.

The thermal conductivity characteristics of powdered MgO, Al_2O_3, and ZrO_2 were investigated as a function of void space and temperature. Over the temperature range studied (200 to 1500°F), the thermal conductivity increased quadratically with the temperature.

Low-Level Waste Treatment: Scavenging-Precipitation--Ion Exchange. The phosphate concentration of ORNL low level waste was successfully reduced from $\geq$3 ppm phosphate to 0.2-0.5 ppm during treatment of greater than 8,666 volumes of waste with one bed volume of alumina. This treatment permitted more quantitative precipitation of calcium carbonate in the scavenging-precipitation clarifier, i.e. reduction in hardness of clarified product from 70 ppm to < 10 ppm. A significant but unknown fraction of the ruthenium was also adsorbed on the alumina.

Low Level Waste Treatment: Foam Separation. Initial tests of a two-step process for decontamination of low-level waste, consisting of sludge column precipitation of calcium carbonate and magnesium hydroxide followed by a countercurrent foam column for strontium removal, were performed with Sr^{85}-spiked ORNL tap water and ORNL low-level process waste water in laboratory-scale equipment. With tap water as feed, strontium decontamination factors in the foam column and in the overall process were 2 to greater than 400 and 320 to greater than 15,000, respectively, depending on operating conditions. With process waste water, foam column and overall strontium decontamination factors were 11 to 16 and about 250, respectively, which are close to those obtained with tap water under the same operating conditions. Also tested with simulated and actual ORNL low level process waste was a one-step process which involves precipitation of calcium as orthophosphate in a small mixer and then feeding solution and solids to a foam column where flotation and foam separation occur. Strontium decontamination factors with simulated and actual ORNL waste water were, respectively, in excess of 1000 and 200 to 300.

Studies were performed of the biological degradation in ORNL process waste water of the alkylbenzenesulfonate already present in the waste water (primarily from Fab), of the alkylbenzenesulfonate in Fab, and of the branched chain sodium dodecylbenzenesulfonate of Trepolate F-95. After 2 to 3 weeks the respective amounts of degradation from existing bacteria were 20, 25 to 30, and 60 to 65%.

A 24-in.-diam foam column was operated with liquid feed introduced through tubes on a 5-in. triangular spacing; channeling was observed for 10 to 30 inches below the feed tubes. Twenty-mesh screens across the column cross sections were not effective liquid distributors since they accumulated liquid which dumped through periodically. Good drainage of foam was obtained in a horizontal drainage section. The experimentally measured foam densities agreed well with a foam drainage model. Air operated sonic whistles condensed 0.05 to 0.10 ft^3 of foam per standard cubic foot of operating air. The experimentally observed concentrations for a three-stage surfactant recovery system agreed well with concentrations calculated by using a distribution coefficient of 7×10^{-4} $(moles/cm^2)/(moles/cc)$ for the dodecylbenzenesulfonate.

Engineering, Economics, and Safety Evaluation. Atmospheric contamination from an assumed continuous accidental release of fission products at a rate of 1 curie/sec from a hypothetical storage-tank site at ORNL results in a downwind concentration of 2.5×10^{-6} and 7.5×10^{-7} μc/cc at ground level at 5 and 10 miles for typical daytime meteorological conditions. For an instantaneous release of 1 curie for daytime and

nighttime meteorological conditions, the concentrations at 10 miles downstream are 3×10^{-9} and 5×10^{-7} μc/cc.

Disposal in Deep Wells. With reference to the mix, the effect on the pumping characteristics of several contaminants and variations in the waste composition was evaluated by the Halliburton Company. It was confirmed that the proposed mix will be usable over the range of these expected variations and in the presence of these contaminants.

An analysis of the fluid lost from the proposed mix prior to setting showed that cesium and strontium were preferentially retained; the concentration of these elements in the fluid was less than 10% of their concentration in the original waste solution. In a 17-day leach test made on a five-day-cured specimen, only 7% of the cesium was leached; neither strontium or ruthenium was detected.

Detail design of the mixing and injecting equipment is in progress. The installation of the waste tanks and pumps is 80% completed.

Drilling has started on the injection and observation wells. The surface casing of the injection well was cemented; the well is at a depth of 668 ft. The observation well was drilled to a depth of 518 ft.

Disposal in Natural Salt Formations. Fuel elements of the ETR have been selected as the heat and radiation sources for the demonstration of the disposal of solid, high-level waste. The purposes of the demonstration are to perfect the equipment and method, and to investigate the combined effects of heat, radiation, and pressure on plastic flow, salt stability, and chlorine production. The demonstration will consist of a 7-can array of fuel elements, an electrical-heat-equivalent array, and two sets of electrical heaters to heat a pillar between the two arrays.

The Carey mine at Lyons, Kansas, will have its hoist and shaft renovated to handle the 7-ton loads required for the demonstration.

The heated-room model at the Hutchinson mine showed that the hole is closing at a unit rate 100 times faster at 160°C than at ambient temperature (about 10^{-4} in. in.$^{-1}$ day^{-1} vs 10^{-6} in. in.$^{-1}$ day^{-1}).

Experimental work on KCl has been used to calculate total production of chlorine in irradiated NaCl. After 200 days, 1.8 moles of oxidizing agent per can could be produced. Irradiation of NaCl indicates that these values are conservative and that for short-term storage of high-level wastes in salt, little or no production of free chlorine can be expected.

Clinch River Study. A regression analysis of bottom-sediment samples from the Clinch and Tennessee Rivers showed a strong correlation of Ru^{106}, total rare earths, and Co^{60} with Cs^{137}, indicating that similar mechanisms control the longitudinal

distribution of these nuclides. The correlation for Zr^{95}-Nb^{95} and Sr^{90} with Cs^{137} is not as good, indicating that different mechanisms may be controlling their distribution.

Pontacyl Pink was injected into White Oak Lake along the face of the dam to determine whether there was any large-scale seepage through the dam. Though small amounts of seepage were indicated, no dye passed through the dam. Other potential sources of contamination proved to be negligible.

A code was developed for calculating critical-organ burdens and dose received, taking into account individuals of different age groups in comparison to standard man, for those consuming Clinch and Tennessee river water for various periods of time.

Bottom sediments from the Clinch River were selectively leached. Salts between pH of 6 and 8 removed less than 10% of Co^{60}, Ru^{106}, and Cs^{137}. At lower pH's, ruthenium is not removed though cobalt is. At higher pH ruthenium is leached, though only moderate amounts of cobalt are released.

Mineral Exchange Studies. Sorption of trace quantities of cesium by vermiculite can be improved by pretreatment with potassium to increase the number of collapsed lattices available for edge fixation. Continued leaching of the treated vermiculite with 0.5 M $NaNO_3$, containing traces of cesium (1.7×10^{-7} M), releases the interlayer potassium and negates the pretreatment. Addition of potassium in the influent was found effective in maintaining potassium-treated vermiculite in a collapsed state. A concentration of 0.0005 M KNO_3 in 0.5 M $NaNO_3$ gave optimum cesium sorption (K_d = 366 ml/g) and a final exchange capacity of 46.8 meq/100 g compared to the initial exchange capacity of the potassium-saturated vermiculite of 5.9 meq/100 g. Higher concentrations of potassium were more effective in maintaining lattice collapse, but reduced cesium sorption due to increased ion competition.

Interlayer fixation of trace quantities of strontium was not observed when the vermiculite lattice was collapsed by addition of 0.01 to 0.04 M KNO_3 to 0.5 M $NaNO_3$ influent. The sorption of strontium was reduced by increases in the potassium concentration of the influent, and about 80% of the strontium was removed during the determination of the exchange capacity following column saturation.

White Oak Creek Basin Study. The average concentration of Cs^{137} in the upper 6 in. of soil in the bed of White Oak Lake is approximately 100 times that of Sr^{90}. In general, the highest concentrations of Cs^{137} are restricted to areas where lacustrine sediment is thickest, while the highest concentration of Sr^{90} occurs in the inundated area immediately behind White Oak Dam.

CONTENTS

	Page
1. Introduction	6
2. High-Level-Waste Calcination	7
2.1 Engineering Development	7
2.2 Laboratory Scale Development	18
2.3 Corrosion Studies	28
2.4 Thermal Conductivity	33
3. Low-Level-Waste Treatment	36
3.1 Pilot Plant Tests	36
3.2 Laboratory Development	36
3.3 Foam Separation	37
4. Engineering, Economics and Safety Evaluation	54
4.1 Safety of Tank Storage of High-Level Liquid Wastes	54
5. Disposal in Deep Wells	56
5.1 Mix Development for Hydrofracture	56
5.2 Design of Hydrofracturing Pilot Plant	62
5.3 Hydrofracture Well Construction	64
6. Disposal in Natural Salt Formations	66
6.1 Demonstration of the Disposal of Solid, High-Level Waste in Salt Mines	66
6.2 Heated-Model Room	77
6.3 Chlorine Release from Gamma Irradiated Salt	91
7. Clinch River Study	92
7.1 Bottom Sediments	92
7.2 Calcite Precipitation	97
7.3 Sources of Release to Clinch River	98
7.4 Hazards Analyses	98
7.5 Desorption of Radionuclides from River Sediments	103
8. Mineral Exchange Studies	107
8.1 Cesium Exchange by Potassium-Treated Vermiculite	107
8.2 Strontium Exchange by Vermiculite with Potassium Added to the Influent	108
9. White Oak Creek Basin Study	109
9.1 Distribution and Transport of Radionuclides in the Bed of Former White Oak Lake	109
9.2 Movement of Radionuclides in White Oak Creek	113
9.3 Geology and Hydrology of White Oak Creek Basin	113
10. References	116

1. INTRODUCTION

This report is the eleventh* in a series of reports on progress in the ORNL development program, the objective of which is to develop and demonstrate, on a pilot-plant scale, integrated processes for the treatment and ultimate disposal of radioactive wastes resulting from reactor operations and reactor fuel processing in the forthcoming nuclear power industry. The wastes include those of high, intermediate, and low levels of radioactivity in liquid, solid, or gaseous states.

Principal current emphasis is on the high- and low-activity liquid wastes. Under the integrated plan, low-activity wastes, consisting of very dilute salt solutions, such as cooling water and canal water, would be treated by scavenging and ion exchange processes to remove radioactive constituents, and the water would be discharged to the environment. The retained waste solids or slurries would be combined with the high-activity wastes. Alternatively, the retained solids or the untreated waste could be discharged to the environment in deep geologic formations. The high-activity wastes would be stored at their sites of origin for economic periods to allow for radioactive decay and artificial cooling.

Two methods are being investigated for the permanent disposal of high-activity wastes. One approach is conversion of the waste liquids to solids by high-temperature "pot" calcination or fixation in the final storage container (pot), itself, and storage in a permanently dry place, such as a salt mine. This is undoubtedly the safest method because complete control of radioactivity can be ensured within present technology during treatment, shipping, and storage. Another approach is the disposal of the liquid directly into sealed or vented salt cavities. Research and development work is planned to determine the relative feasibility, safety, and economics of these methods, although the major effort will be placed on conversion to and final storage as solids.

Tank storage or high-temperature calcination of intermediate-activity wastes may be unattractive because of their large volumes, and other disposal methods will be studied. One method, for example, the addition of solidifying agents prior to direct disposal is being given to the engineering design and construction of an experimental fracturing plant to dispose of ORNL intermediate-activity wastes by this method if proved workable.

Environmental research on the Clinch River, motivated by the need for safe and realistic permissible limits of waste releases, is included in this program. The objective is to obtain a detailed characterization of fission product distribution, transport, and accumulation in the physical, chemical, and biological segments of the environment.

---

*ORNL-CF-61-7-3, ORNL-TM-15, ORNL-TM-49, ORNL-TM-133, ORNL-TM-169, ORNL-TM-252, ORNL-TM-376, ORNL-TM-396, ORNL-TM-482, and ORNL-TM-516.

2. HIGH-LEVEL-WASTE CALCINATION

The pot-calcination process for converting high-activity-level wastes to solids is being studied on both a laboratory and engineering scale to provide design information for the construction of a pilot plant. Development work has been with synthetic Purex, Darex, and TBP-25 wastes. The first phase of the program is concerned with direct calcination processes where melting does not occur and little or no additives are combined with the wastes. In the second phase, enough additives are used to induce melting to form a glass-like material in which the fission products are fixed.

2.1 Engineering Development

J. C. Suddath C. W. Hancher

Three continuous evaporator-calcination tests (R-72, R-73, and R-74) were made with simulated formaldehyde treated Hanford purex waste (FTW-65) to test methods of adding calcium and the effect of fluoride concentration on corrosion. Details are reported elsewhere.[1-3]

2.1.1. Test Conditions and Results

Waste evaporator-calciner tests R-72, R-73, and R-74 were made using FTW-65 Purex waste with the following molar composition:

Nitrate	1.2
Iron	0.2
Sodium	0.3
Mercury	0.0016
Sulfate	0.15
Phosphate	0.005
Fluoride	0.005

(Note: R-74 feed contained only a trace of fluoride from drinking water and makeup chemicals.)

The total amount of feed fed to the system for tests R-72, R-73, and R-74 was 1912, 1838, and 1968 liters, respectively (Table 1.A). The average system feed rates were 40, 31, and 49 liters/hr, respectively, with a maximum hourly feed rate as high as 190 liters/hr. In test R-72, the feed line plugged temporarily during the 5th hour of operation and reduced the feed rate for a period of time making a low average for the entire run. Test R-73 had a low overall feed rate because the concentration in the evaporator was lower than for Run R-74 (Table 1.B). The material balances for these tests are about the same. The mercury material balance was variable because of deposits which were not removed between tests (Table 2).

The calcined solids had a nitrate composition that varied from 100 to 400 ppm (Table 3) and was inversely related to the total calcination time (Table 4). Thus, the

Table 1.A. Operating Conditions for Evaporation-Calcination Tests

HOURLY SYSTEM VARIABLES AND PARAMETERS - PART A

TEST NO R-72 FEED TYPE - PUREX OPERATION MODE - CONTINUOUS

RUN TIME HOURS	FEED LITERS	WATER LITERS	CALCINER ADDITIVE LITERS	EVAP. COND. LITERS	CALCINER FURNACE (HUNDRED-THOUSANDS OF BTUS)	CALCINER COND.	EVAP. COND.	SYSTEM OFF-GAS CU FT	EVAP. DENSITY GM/CC
1	70.	4.	0.	74.	0.	0.	0.80	26.	1.05
2	125.	8.	0.	133.	1.43	0.80	4.05	52.	1.08
3	213.	10.	0.	223.	2.97	1.71	5.71	78.	1.26
4	241.	12.	0.	253.	4.51	1.94	5.71	106.	1.25
5	241.	14.	0.	255.	5.19	2.34	7.49	133.	1.18
6	366.	16.	2.	384.	5.81	3.44	11.26	160.	1.20
7	467.	23.	4.	494.	7.38	4.70	12.88	188.	1.12
8	565.	25.	6.	596.	8.81	5.99	14.39	215.	1.18
9	663.	27.	8.	698.	10.42	7.31	19.41	242.	1.14
10	731.	32.	10.	773.	12.12	8.41	19.41	269.	1.19
11	773.	36.	12.	821.	13.42	9.56	23.97	296.	1.19
12	870.	40.	12.	922.	14.65	10.31	24.37	323.	1.19
13	891.	45.	12.	948.	16.02	11.13	26.44	350.	1.20
14	969.	49.	12.	1030.	16.90	11.93	27.10	377.	1.21
15	987.	51.	12.	1050.	18.10	12.68	28.74	404.	1.18
16	1078.	56.	12.	1146.	19.02	13.45	29.84	431.	1.20
17	1125.	58.	12.	1195.	19.91	14.13	31.07	458.	1.19
18	1182.	62.	12.	1256.	21.04	14.85	32.33	485.	1.19
19	1209.	67.	12.	1288.	21.75	15.53	33.62	512.	1.18
20	1255.	69.	12.	1336.	22.74	16.14	34.68	539.	1.19
21	1294.	73.	12.	1379.	23.56	16.76	35.95	566.	1.19
22	1339.	75.	12.	1426.	24.42	17.37	37.20	593.	1.19
23	1380.	80.	12.	1472.	25.34	17.93	38.64	621.	1.19
24	1408.	82.	12.	1502.	26.02	18.05	39.28	649.	1.18
25	1449.	87.	12.	1548.	26.71	18.93	39.92	677.	1.19
26	1449.	89.	12.	1550.	27.46	19.37	41.17	705.	1.18
27	1477.	91.	12.	1580.	28.07	19.74	42.39	733.	1.19
28	1518.	95.	12.	1625.	28.96	20.21	43.43	760.	1.20
29	1546.	108.	12.	1666.	29.33	20.61	43.84	787.	1.20
30	1561.	118.	12.	1691.	29.95	20.98	44.69	814.	1.19
31	1588.	130.	12.	1730.	30.70	21.35	45.49	842.	1.19
32	1631.	143.	12.	1786.	24.31	21.67	46.09	870.	1.19
33	1631.	153.	12.	1796.	31.69	22.04	46.98	898.	1.19
34	1658.	165.	12.	1835.	32.41	22.34	47.62	925.	1.19
35	1670.	171.	12.	1853.	32.78	22.63	48.26	953.	1.19
36	1685.	174.	12.	1871.	33.13	22.91	48.88	975.	1.18
37	1713.	176.	12.	1901.	33.74	23.22	49.55	1003.	1.19
38	1727.	179.	12.	1918.	34.42	23.47	50.16	1030.	1.19
39	1741.	181.	12.	1934.	34.76	23.72	50.74	1057.	1.19
40	1755.	181.	12.	1948.	35.28	23.98	51.39	1084.	1.19
41	1769.	184.	12.	1965.	35.82	24.23	52.04	1111.	1.18
42	1797.	184.	12.	1993.	36.06	24.47	52.45	1139.	1.18
43	1812.	186.	12.	2010.	36.64	24.73	53.07	1167.	1.20
44	1826.	186.	12.	2024.	37.16	24.99	53.49	1195.	1.22
45	1841.	189.	12.	2042.	37.56	25.17	54.13	1223.	1.18
46	1855.	189.	12.	2056.	38.04	25.43	54.75	1251.	1.21
47	1884.	189.	12.	2085.	38.59	25.69	55.37	1279.	1.20
48	1912.	194.	12.	2118.	38.76	25.88	55.37	1307.	1.19
49	1912.	194.	12.	2118.	39.27	26.14	56.42	1335.	1.07
50	1912.	194.	12.	2118.	39.78	26.33	57.45	1363.	1.12
51	1912.	196.	12.	2120.	40.19	26.51	57.74	1390.	1.15
52	1912.	196.	12.	2120.	40.67	26.61	58.53	1418.	1.15
53	1912.	196.	12.	2120.	41.08	26.66	58.74	1446.	1.09
54	1912.	196.	12.	2120.	41.49	26.68	59.12	1475.	1.09
55	1912.	199.	12.	2123.	41.70	26.70	59.57	1503.	1.01
56	1912.	199.	12.	2123.	42.00	26.77	60.13	1531.	1.13
57	1912.	199.	12.	2123.	42.28	26.82	60.57	1559.	1.24
58	1912.	199.	12.	2123.	42.59	26.88	60.78	1587.	1.24
59	1912.	199.	12.	2123.	42.72	26.91	61.00	1615.	1.24
60	1912.	199.	12.	2123.	42.93	26.92	61.21	1643.	1.24
61	1912.	199.	12.	2123.	43.13	26.94	61.64	1671.	1.23
62	1912.	199.	12.	2123.	43.37	26.95	61.86	1699.	1.23
63	1912.	199.	12.	2123.	43.58	26.95	62.26	1727.	1.23
64	1912.	199.	12.	2123.	43.85	26.95	62.48	1755.	1.21
65	1912.	199.	12.	2123.	44.12	26.95	62.69	1783.	1.21
66	1912.	199.	12.	2123.	44.16	26.95	63.11	1811.	1.21
67	1912.	199.	12.	2123.	44.43	26.95	63.33	1839.	1.21
68	1912.	199.	12.	2123.	44.60	26.95	63.54	1867.	1.21
69	1912.	199.	12.	2123.	44.84	26.95	63.75	1895.	1.21
70	1912.	199.	12.	2123.	45.01	26.95	64.17	1923.	1.20
71	1912.	199.	12.	2123.	45.28	26.95	64.37	1951.	1.20
72	1912.	199.	12.	2123.	45.45	26.95	64.37	1951.	1.00

Table 1.A. (Cont'd)

HOURLY SYSTEM VARIABLES AND PARAMETERS - PART A

TEST NO R-73 FEED TYPE - PUREX OPERATION MODE - CONTINUOUS

RUN TIME HOURS	FEED LITERS	WATER LITERS	CALCINER ADDITIVE LITERS	EVAP. COND. LITERS	CALCINER FURNACE (HUNDRED-THOUSANDS OF BTUS)	CALCINER COND.	EVAP. COND.	SYSTEM OFF-GAS CU FT	EVAP. DENSITY GM/CC
1	135.	30.	0.	165.	0.	0.54	4.21	28.	1.12
2	225.	70.	0.	295.	1.37	1.54	7.91	56.	1.22
3	370.	91.	0.	461.	2.83	2.69	11.81	84.	1.24
4	560.	93.	0.	653.	4.30	3.96	16.12	113.	1.24
5	705.	94.	0.	799.	5.94	5.19	20.00	141.	1.25
6	851.	95.	0.	946.	7.31	6.35	23.71	169.	1.26
7	991.	96.	0.	1087.	8.67	7.42	27.30	197.	1.27
8	1135.	99.	0.	1234.	9.77	8.38	30.05	225.	1.27
9	1285.	129.	0.	1414.	11.06	9.12	34.06	225.	1.26
10	1396.	132.	0.	1528.	12.40	9.74	36.40	254.	1.35
11	1458.	132.	3.	1593.	13.15	10.24	36.84	283.	1.34
12	1458.	134.	5.	1597.	13.90	10.42	37.05	312.	1.32
13	1458.	136.	5.	1599.	14.41	10.65	37.28	341.	1.28
14	1458.	139.	7.	1604.	21.89	10.85	37.74	370.	1.26
15	1458.	142.	7.	1607.	15.40	10.99	38.12	399.	1.26
16	1458.	144.	10.	1612.	15.78	11.13	38.32	428.	1.26
17	1458.	147.	13.	1618.	16.22	11.26	38.74	457.	1.26
18	1458.	149.	13.	1620.	16.53	11.39	38.95	487.	1.26
19	1458.	152.	13.	1623.	16.90	11.49	39.38	516.	1.25
20	1458.	153.	13.	1624.	17.18	11.60	39.38	546.	1.25
21	1460.	157.	13.	1630.	17.52	11.72	39.81	575.	1.26
22	1460.	159.	13.	1632.	17.96	11.82	40.24	604.	1.27
23	1487.	159.	13.	1659.	18.34	11.94	40.87	633.	1.26
24	1505.	162.	13.	1680.	18.65	12.07	41.57	662.	1.27
25	1513.	164.	13.	1690.	18.92	12.18	41.99	691.	1.26
26	1527.	166.	13.	1706.	19.26	12.33	42.59	719.	1.25
27	1569.	169.	13.	1751.	19.64	12.46	43.67	747.	1.29
28	1606.	171.	13.	1790.	19.81	12.61	44.30	775.	1.31
29	1629.	173.	13.	1815.	20.15	12.73	44.92	803.	1.30
30	1638.	175.	13.	1826.	20.59	12.84	45.33	831.	1.32
31	1652.	177.	13.	1842.	20.93	12.97	45.33	859.	1.33
32	1666.	179.	13.	1858.	21.14	13.07	45.73	888.	1.25
33	1666.	182.	13.	1861.	21.48	13.16	45.95	917.	1.27
34	1680.	184.	13.	1877.	158.42	13.27	46.36	946.	1.27
35	1680.	186.	13.	1879.	22.23	13.36	46.78	975.	1.25
36	1680.	189.	13.	1882.	22.57	13.46	47.22	1004.	1.26
37	1694.	189.	13.	1896.	22.88	13.63	47.69	1033.	1.26
38	1694.	192.	13.	1899.	0.68	13.66	48.08	1062.	1.26
39	1694.	194.	13.	1901.	0.44	13.81	48.49	1091.	1.25
40	1708.	196.	13.	1917.	0.14	13.84	48.90	1120.	1.27
41	1708.	225.	13.	1946.	24.14	13.93	49.33	1149.	1.27
42	1708.	228.	13.	1949.	24.55	14.03	109.79	1178.	1.25
43	1708.	230.	13.	1951.	24.72	14.12	50.18	1207.	1.27
44	1721.	232.	13.	1966.	24.93	14.22	50.59	1236.	1.26
45	1721.	232.	13.	1976.	25.20	14.32	51.01	1265.	1.26
46	1735.	234.	13.	1992.	25.65	14.41	51.43	1294.	1.27
47	1735.	237.	13.	1995.	25.99	14.50	51.85	1323.	1.28
48	1735.	240.	13.	1998.	26.26	14.61	52.31	1352.	1.28
49	1749.	245.	13.	2017.	26.47	14.75	52.72	1381.	1.26
50	1749.	247.	13.	2019.	26.77	14.77	53.13	1410.	1.27
51	1763.	249.	13.	2035.	27.01	14.93	53.55	1438.	1.28
52	1777.	251.	13.	2051.	27.49	14.95	53.96	1467.	1.29
53	1777.	253.	13.	2053.	27.76	15.04	54.37	1496.	1.29
54	1777.	256.	13.	2056.	28.14	15.13	54.77	1525.	1.27
55	1791.	259.	13.	2073.	28.45	15.23	55.18	1554.	1.28
56	1805.	259.	13.	2087.	28.69	15.33	55.80	1583.	1.27
57	1805.	260.	13.	2088.	29.06	15.40	55.99	1612.	1.27
58	1818.	263.	13.	2104.	29.44	15.49	56.40	1641.	1.27
59	1838.	265.	13.	2126.	29.64	15.58	56.83	1670.	1.25
60	0.	265.	13.	2126.	29.95	15.66	57.24	1699.	1.21
61	0.	292.	13.	2153.	30.26	15.68	57.86	1729.	1.23
62	0.	292.	13.	2153.	30.50	15.69	58.28	1758.	1.23
63	0.	292.	13.	2153.	30.80	15.72	58.71	1787.	1.25
64	0.	292.	13.	2153.	34.49	15.75	58.71	1817.	1.23
65	0.	349.	13.	2210.	34.73	15.77	59.11	1847.	1.25
66	0.	375.	13.	2236.	35.04	15.78	59.77	1876.	1.25
67	0.	375.	13.	2236.	35.28	15.78	60.16	1906.	1.22
68	0.	375.	13.	2236.	35.48	15.78	60.79	1936.	1.21

Table 1.A. (Cont'd)

HOURLY SYSTEM VARIABLES AND PARAMETERS - PART A

TEST NO R-74 FEED TYPE - PUREX OPERATION MODE - CONTINUOUS

RUN TIME HOURS	FEED LITERS	WATER LITERS	CALCINER ADDITIVE LITERS	EVAP. COND. LITERS	CALCINER FURNACE (HUNDRED-THOUSANDS OF BTUS)	CALCINER COND.	EVAP. COND.	SYSTEM OFF-GAS CU FT	EVAP. DENSITY GM/CC
1	158	-	7	165	-.00	.04	1.60	-	1.20
2	290	-	8	298	.89	.69	5.36	37	1.22
3	413	-	9	422	2.25	1.55	8.75	77	1.23
4	528	3	11	542	3.59	2.57	12.41	115	1.23
5	640	3	11	654	4.88	3.37	15.46	152	1.24
6	737	24	11	772	6.22	4.19	18.58	189	1.24
7	846	24	11	881	7.44	5.01	21.59	224	1.24
8	946	35	11	992	8.64	5.95	24.85	258	1.24
9	1048	38	11	1097	9.77	6.94	26.13	287	1.27
10	1104	40	11	1155	10.89	7.48	27.67	306	1.27
11	1167	43	11	1221	11.78	7.90	29.00	321	1.28
12	1207	43	11	1261	12.53	8.25	30.28	340	1.28
13	1248	45	11	1304	13.11	8.62	31.88	354	1.28
14	1304	48	11	1363	13.83	8.97	33.19	370	1.28
15	1345	48	11	1404	14.38	9.30	34.24	389	1.28
16	1406	48	11	1465	14.96	9.60	34.90	394	1.29
17	1432	51	11	1494	15.74	9.87	35.80	411	1.29
18	1476	51	11	1538	16.26	10.14	36.89	422	1.27
19	1518	53	11	1582	16.73	10.41	38.26	432	1.28
20	1565	53	11	1629	17.28	10.65	39.33	448	1.29
21	1593	53	11	1657	17.89	10.89	40.41	459	1.28
22	1620	56	11	1687	18.20	11.14	41.54	469	1.27
23	1658	56	11	1725	18.71	11.35	42.39	477	1.26
24	1676	86	11	1773	19.29	11.56	43.32	484	1.29
25	1690	86	11	1787	19.91	11.76	44.17	492	1.30
26	1704	86	11	1801	20.32	11.95	44.61	499	1.30
27	1718	86	11	1815	20.83	12.12	45.05	507	1.30
28	1732	86	11	1829	21.48	12.27	45.88	515	1.30
29	1746	86	11	1843	21.86	12.42	46.71	525	1.31
30	1787	86	11	1884	22.40	12.59	48.03	540	1.29
31	1815	86	11	1912	22.85	12.75	48.87	551	1.28
32	1843	90	11	1944	23.22	12.90	49.76	564	1.28
33	1875	90	11	1966	23.70	13.03	50.40	572	1.29
34	1908	90	11	1999	24.14	13.12	51.05	578	1.25
35	1927	90	11	2018	24.66	13.20	51.70	581	1.19
36	1954	90	11	2045	24.93	13.22	51.92	582	1.04
37	1954	90	11	2045	25.34	13.22	52.58	582	1.05
38	1954	124	11	2079	25.75	13.22	53.24	582	1.00
39	1954	150	11	2105	26.06	13.22	53.88	582	1.00
40	1968	218	11	2187	26.40	13.22	54.78	582	1.04
41		244	11	2213	26.71	13.22	55.41	582	1.02
42		244	11	2213	27.01	13.22	56.11	582	1.01
43		263	11	2232	27.29	13.22	57.00	582	1.01
44		327	11	2296	27.63	13.22	57.65	582	1.01
45		353	11	2322	27.93	13.22	58.30	582	1.01
46		383	11	2352	28.14	13.22	58.96	582	1.01
47		409	11	2378	28.34	13.22	59.60	582	1.01
48		409	11	2378	28.55	13.22	60.25	582	1.02
49		428	11	2397	28.82	13.22	60.85	582	1.03
50		454	11	2423	29.10	13.22	61.51	582	1.04
51		480	11	2449	29.20	13.22	62.38	582	1.05
52		510	11	2479	29.47	13.22	63.01	582	1.05
53		510	11	2479	29.61	13.22	63.65	582	1.06
54		536	11	2505	29.78	13.22	64.26	582	1.07
55		536	11	2505	29.92	13.22	64.69	582	1.07
56		562	11	2531	30.15	13.22	65.36	582	1.08
57		588	11	2557	30.43	13.22	65.98	582	1.08
58		588	11	2557	30.67	13.22	66.43	582	1.08
59		614	11	2583	30.84	13.22	67.06	582	1.08
60		644	11	2613	30.97	13.22	67.50	582	1.09
61		644	11	2613	31.18	13.22	68.16	582	1.09
62		670	11	2639	31.52	13.22	68.59	582	1.09
63		670	11	2639	31.76	13.22	69.22	582	1.10

Table 1.B. Operating Conditions for Evaporator-Calcination Tests

HOURLY SYSTEM VARIABLES AND PARAMETERS - PART B

TEST NO R-72 FEED TYPE - PUREX OPERATION MODE - CONTINUOUS

RUN TIME HOURS	EVAP. LIQUID NITRATE MOLAR	EVAP.MAJOR CATION FE OR AL GM/LITER	CALCINER COND. NITRATE MOLAR	EVAP COND. H+ MOLAR	EVAP.COND. MAJOR ION FE OR AL GM/LITER	EVAP. COND. RUTHENIUM GM/LITER	EVAP. LIQUID TEMP. DEG.C	EVAP. VAPOR TEMP. DEG.C	CALCINER FEED TEMP. DEG.C	CALCINER OFF-GAS TEMP. DEG.C
1	1.57	14.0	0.15	0.03	0.001	0.	100.	99.	92.	400.
2	2.22	18.0	0.32	0.07	0.001	0.	100.	100.	95.	460.
3	5.84	48.0	1.59	0.49	0.001	0.	108.	106.	100.	475.
4	4.73	39.0	7.02	0.44	0.001	0.	106.	98.	97.	320.
5	4.48	36.0	3.35	0.30	0.001	0.	104.	101.	97.	480.
6	4.57	33.0	2.10	0.59	0.001	0.	105.	106.	94.	370.
7	3.70	20.0	2.67	0.16	0.001	0.	100.	101.	89.	230.
8	4.70	25.0	3.59	0.41	0.001	0.	101.	105.	99.	230.
9	4.90	26.0	3.57	0.25	0.001	0.	103.	107.	94.	201.
10	5.17	19.0	4.05	0.76	0.001	0.	102.	97.	91.	217.
11	4.06	17.0	4.95	0.83	0.001	0.	104.	107.	85.	170.
12	4.27	21.0	3.81	0.67	0.001	0.	106.	102.	86.	176.
13	4.37	18.0	3.95	0.75	0.001	0.	106.	106.	86.	185.
14	5.46	23.0	4.00	0.71	0.001	0.	106.	103.	90.	181.
15	6.00	22.0	3.62	0.70	0.001	0.	106.	106.	90.	178.
16	6.02	25.0	4.22	0.73	0.001	0.	106.	105.	91.	196.
17	6.19	23.0	4.37	0.78	0.001	0.	107.	106.	91.	183.
18	6.37	24.0	4.44	0.76	0.001	0.	107.	106.	91.	172.
19	6.65	24.0	4.49	0.75	0.001	0.	108.	107.	91.	160.
20	6.40	24.0	4.49	0.84	0.001	0.	107.	106.	91.	159.
21	6.33	22.0	4.67	0.78	0.001	0.	102.	106.	95.	163.
22	6.41	23.0	4.60	0.79	0.001	0.	107.	106.	95.	162.
23	6.63	21.0	5.03	0.89	0.001	0.	107.	106.	93.	167.
24	6.44	24.0	4.81	0.84	0.001	0.	108.	105.	92.	158.
25	6.70	19.0	4.92	0.79	0.001	0.	108.	105.	91.	167.
26	6.75	23.0	5.16	0.98	0.001	0.	107.	106.	92.	177.
27	6.38	29.0	4.71	0.75	0.001	0.	107.	106.	92.	173.
28	6.63	24.0	4.33	0.86	0.001	0.	108.	106.	88.	147.
29	6.44	26.0	4.16	0.67	0.001	0.	107.	104.	87.	154.
30	6.70	28.0	4.16	0.87	0.001	0.	120.	106.	86.	151.
31	6.63	27.0	3.73	0.83	0.001	0.	108.	106.	84.	152.
32	6.48	29.0	3.51	0.65	0.001	0.	108.	105.	84.	149.
33	6.46	30.0	3.40	0.75	0.001	0.	108.	105.	82.	154.
34	6.44	30.0	3.29	0.65	0.001	0.	108.	105.	81.	133.
35	6.49	30.0	3.37	0.60	0.001	0.	108.	105.	81.	133.
36	6.44	28.0	3.30	0.57	0.001	0.	107.	104.	81.	133.
37	6.49	29.0	3.22	0.67	0.001	0.	107.	105.	82.	126.
38	6.48	30.0	3.19	0.63	0.001	0.	108.	105.	81.	118.
39	6.63	30.0	3.25	0.67	0.001	0.	108.	105.	80.	121.
40	6.57	31.0	3.17	0.65	0.001	0.	108.	105.	80.	121.
41	6.73	31.0	3.57	0.65	0.001	0.	109.	106.	84.	122.
42	6.38	27.0	3.84	0.48	0.001	0.	107.	104.	85.	117.
43	6.46	28.0	3.98	0.75	0.001	0.	106.	105.	87.	124.
44	5.75	26.0	4.48	0.94	0.001	0.	106.	103.	80.	116.
45	6.44	29.0	3.94	0.52	0.001	0.	108.	105.	86.	118.
46	7.21	35.0	3.94	1.27	0.001	0.	110.	108.	87.	118.
47	7.32	41.0	3.41	1.35	0.001	0.	108.	109.	85.	116.
48	5.52	30.0	3.13	0.86	0.001	0.	104.	102.	84.	115.
49	4.27	19.0	3.81	0.30	0.001	0.	104.	100.	45.	113.
50	5.40	25.0	3.62	0.29	0.001	0.	106.	102.	56.	109.
51	5.32	23.0	2.95	0.24	0.001	0.	105.	102.	52.	113.
52	5.54	20.0	9.11	0.37	0.001	0.	105.	102.	80.	167.
53	4.81	16.0	9.32	0.87	0.001	0.	104.	98.	63.	185.
54	5.08	16.0	8.30	0.56	0.001	0.	104.	100.	65.	202.
55	4.38	14.0	0.	0.25	0.001	0.	104.	100.	23.	198.
56	5.44	18.0	0.	0.22	0.001	0.	106.	102.	26.	206.
57	6.02	21.0	0.	0.37	0.001	0.	106.	101.	25.	230.
58	5.76	21.0	0.	0.27	0.001	0.	106.	101.	25.	241.
59	5.62	21.0	0.	0.24	0.001	0.	106.	100.	25.	238.
60	5.44	21.0	0.	0.22	0.001	0.	105.	100.	25.	223.
61	5.37	21.0	0.	0.17	0.001	0.	105.	100.	23.	240.
62	5.17	21.0	0.	0.17	0.001	0.	104.	100.	23.	226.
63	5.14	21.0	0.	0.14	0.001	0.	104.	99.	24.	202.
64	4.89	20.0	0.	0.14	0.001	0.	104.	98.	23.	195.
65	4.79	20.0	0.	0.11	0.001	0.	103.	98.	23.	175.
66	4.65	19.0	0.	0.10	0.001	0.	104.	98.	23.	160.
67	4.54	19.0	0.	0.09	0.001	0.	104.	99.	23.	150.
68	4.46	19.0	0.	0.08	0.001	0.	104.	99.	23.	140.
69	4.41	19.0	0.	0.09	0.001	0.	103.	98.	23.	120.
70	4.33	19.0	0.	0.07	0.001	0.	103.	98.	22.	103.
71	4.25	18.0	0.	0.10	0.001	0.	103.	98.	22.	95.
72	0.	0.	0.	0.	0.	0.	0.	0.	0.	0.

Table 1.B. (Cont'd)

HOURLY SYSTEM VARIABLES AND PARAMETERS - PART B

TEST NO R-73 FEED TYPE - PUREX OPERATION MODE - CONTINUOUS

RUN TIME HOURS	EVAP. LIQUID NITRATE MOLAR	EVAP.MAJOR CATION FE OR AL GM/LITER	CALCINER COND. NITRATE MOLAR	EVAP COND. H+ MOLAR	EVAP.COND. MAJOR ION FE OR AL GM/LITER	EVAP. COND. CALCIUM GM/LITER	EVAP. LIQUID TEMP. DEG.C	EVAP. VAPOR TEMP. DEG.C	CALCINER FEED TEMP. DEG.C	CALCINER OFF-GAS TEMP. DEG.C
1	2.59	23.0	0.54	0.05	0.001	0.	98.	99.	91.	150.
2	4.95	35.0	2.62	0.41	0.001	0.	102.	104.	101.	330.
3	5.94	40.0	4.27	0.76	0.001	0.	104.	106.	102.	252.
4	6.38	40.0	5.33	0.94	0.001	0.	104.	106.	103.	228.
5	6.43	39.0	5.87	1.08	0.001	0.	104.	107.	103.	250.
6	6.43	39.0	5.75	0.97	0.001	0.	104.	106.	104.	226.
7	6.43	43.0	5.86	1.08	0.001	0.	105.	107.	103.	231.
8	6.86	47.0	7.03	1.24	0.001	0.	106.	107.	102.	206.
9	7.03	46.0	9.22	1.48	0.001	0.	107.	108.	102.	173.
10	6.81	63.0	7.52	1.21	0.001	0.	107.	107.	102.	164.
11	6.65	61.0	6.43	1.27	0.001	0.	109.	106.	101.	160.
12	6.68	53.0	5.22	1.05	0.001	0.	109.	104.	102.	179.
13	6.25	43.0	4.75	0.94	0.001	0.	108.	102.	101.	163.
14	6.37	41.0	4.44	0.73	0.001	0.	108.	105.	101.	143.
15	6.52	38.0	3.78	0.73	0.001	0.	108.	105.	101.	135.
16	6.52	38.0	2.11	0.83	0.001	0.	108.	104.	98.	137.
17	6.32	36.0	1.89	0.90	0.001	0.	108.	104.	95.	135.
18	6.57	38.0	4.25	0.87	0.001	0.	109.	105.	96.	123.
19	6.37	35.0	3.19	0.76	0.001	0.	109.	106.	95.	134.
20	6.37	33.0	4.44	1.03	0.001	0.	108.	99.	95.	188.
21	6.62	34.0	3.76	1.03	0.001	0.	108.	105.	92.	145.
22	6.51	36.0	3.62	0.98	0.001	0.	108.	106.	95.	150.
23	6.29	38.0	2.78	0.86	0.001	0.	108.	106.	95.	149.
24	6.02	39.0	2.94	0.73	0.001	0.	108.	105.	95.	151.
25	6.00	38.0	2.84	0.92	0.001	0.	109.	104.	95.	152.
26	5.10	32.0	2.44	0.84	0.001	0.	108.	106.	87.	143.
27	5.30	48.0	2.57	0.94	0.001	0.	109.	107.	87.	142.
28	5.54	45.0	2.46	0.81	0.001	0.	110.	106.	89.	138.
29	5.13	54.0	2.44	0.89	0.001	0.	110.	106.	83.	140.
30	5.24	57.0	2.22	0.71	0.001	0.	110.	106.	83.	135.
31	5.40	60.0	2.33	0.75	0.001	0.	110.	104.	85.	126.
32	4.06	44.0	2.14	0.32	0.001	0.	106.	100.	84.	131.
33	3.25	33.0	2.49	0.30	0.001	0.	108.	101.	83.	133.
34	4.19	43.0	2.08	0.86	0.001	0.	111.	106.	73.	134.
35	3.95	40.0	1.87	0.48	0.001	0.	109.	104.	75.	133.
36	4.11	44.0	1.76	0.49	0.001	0.	109.	104.	74.	136.
37	4.21	42.0	1.67	0.46	0.001	0.	109.	103.	75.	135.
38	4.13	41.0	1.57	0.41	0.001	0.	109.	114.	77.	132.
39	4.03	41.0	1.41	0.48	0.001	0.	110.	105.	75.	131.
40	4.92	50.0	1.49	0.52	0.001	0.	109.	103.	79.	135.
41	4.86	47.0	1.83	0.51	0.001	0.	108.	102.	80.	115.
42	4.62	44.0	2.33	0.46	0.001	0.	108.	103.	79.	124.
43	5.25	48.0	2.27	0.46	0.001	0.	108.	103.	84.	119.
44	5.00	46.0	2.49	0.46	0.001	0.	108.	103.	84.	116.
45	5.00	44.0	2.03	0.38	0.001	0.	107.	103.	84.	118.
46	5.33	44.0	1.57	0.48	0.001	0.	108.	104.	86.	115.
47	5.46	43.0	1.62	0.49	0.001	0.	107.	102.	87.	114.
48	4.90	43.0	1.89	0.48	0.001	0.	108.	103.	85.	112.
49	4.71	41.0	2.14	0.48	0.001	0.	107.	103.	84.	109.
50	4.86	41.0	2.00	0.44	0.001	0.	107.	104.	85.	109.
51	5.21	44.0	1.92	0.48	0.001	0.	108.	104.	87.	110.
52	5.49	46.0	1.86	0.52	0.001	0.	108.	104.	88.	111.
53	5.59	47.0	1.84	0.52	0.001	0.	108.	104.	89.	110.
54	5.35	45.0	1.79	0.56	0.001	0.	108.	104.	85.	105.
55	5.37	32.0	1.76	0.51	0.001	0.	108.	104.	87.	105.
56	5.02	34.0	1.78	0.57	0.001	0.	108.	104.	85.	106.
57	4.94	30.0	1.76	0.56	0.001	0.	107.	103.	85.	106.
58	4.78	41.0	1.81	0.52	0.001	0.	108.	104.	85.	106.
59	4.62	39.0	2.97	0.40	0.001	0.	106.	102.	84.	109.
60	4.14	34.0	5.65	0.35	0.001	0.	108.	104.	77.	117.
61	4.25	34.0	12.11	0.79	0.001	0.	108.	104.	76.	113.
62	4.38	35.0	13.92	1.00	0.001	0.	108.	104.	76.	119.
63	4.33	36.0	13.87	0.63	0.001	0.	109.	104.	77.	530.
64	4.67	41.0	12.43	0.44	0.001	0.	106.	102.	76.	510.
65	4.67	44.0	0.	0.29	0.001	0.	105.	101.	84.	530.
66	4.65	43.0	0.	0.24	0.001	0.	105.	100.	84.	530.
67	4.29	43.0	0.	0.24	0.001	0.	105.	100.	78.	530.
68	4.10	39.0	0.	0.24	0.001	0.	105.	100.	75.	505.

Table 1.B. (Cont'd)

HOURLY SYSTEM VARIABLES AND PARAMETERS - PART B

TEST NO R-74 FEED TYPE - PUREX OPERATION MODE - CONTINUOUS

RUN TIME HOURS	EVAP. LIQUID NITRATE MOLAR	EVAP.MAJOR CATION FE OR AL GM/LITER	CALCINER COND. NITRATE MOLAR	EVAP COND. H+ MOLAR	EVAP.COND. MAJOR ION FE OR AL GM/LITER	EVAP. COND. CALCIUM GM/LITER	EVAP. LIQUID TEMP. DEG.C	EVAP. VAPOR TEMP. DEG.C	CALCINER FEED TEMP. DEG.C	CALCINER OFF-GAS TEMP. DEG.C
1	5.13	40.0	1.95	.33	.001	.000	103	100	101	113
2	5.73	39.0	3.46	.68	.001	.000	102	102	101	221
3	6.22	36.0	4.29	.87	.001	.000	104	104	102	228
4	6.54	35.0	4.89	.97	.001	.000	104	105	103	220
5	6.73	34.0	5.11	1.05	.001	.000	106	104	104	215
6	6.59	26.0	5.08	.97	.001	.000	105	104	103	208
7	6.65	34.0	5.13	1.00	.001	.000	105	104	103	203
8	7.54	39.0	6.70	1.84	.001	.000	105	105	104	196
9	7.05	42.0	5.25	1.27	.001	.000	108	106	107	196
10	6.83	44.0	4.56	1.03	.001	.000	107	105	105	168
11	6.59	44.0	4.17	.92	.001	.000	107	105	105	160
12	6.48	44.0	4.06	.84	.001	.000	106	105	104	154
13	6.48	43.0	4.11	.87	.001	.000	106	104	102	138
14	6.49	42.0	4.08	.90	.001	.000	106	104	102	129
15	6.81	46.0	4.78	1.13	.001	.000	107	105	101	126
16	6.46	39.0	4.83	1.16	.001	.000	108	105	99	123
17	5.98	39.0	4.10	.98	.001	.000	106	105	98	139
18	5.57	39.0	3.68	.84	.001	.000	106	105	94	118
19	5.79	42.0	3.59	.90	.001	.000	106	104	92	135
20	5.62	41.0	3.41	.95	.001	.000	106	104	93	118
21	3.49	26.0	2.67	.97	.001	.000	106	105	90	112
22	3.06	26.0	1.92	1.06	.001	.000	107	105	75	110
23	4.48	43.0	2.06	.76	.001	.000	108	105	69	111
24	4.33	42.0	2.14	.86	.001	.000	106	104	85	120
25	5.14	51.0	2.02	1.11	.001	.000	107	102	82	107
26	4.98	50.0	2.03	.84	.001	.000	108	104	82	108
27	5.48	51.0	2.06	.76	.001	.000	107	102	84	108
28	5.62	55.0	2.73	.76	.001	.000	107	103	90	107
29	5.48	46.0	3.10	.76	.001	.000	107	103	90	108
30	5.21	50.0	3.05	.81	.001	.000	106	103	91	108
31	5.41	57.0	2.63	.89	.001	.000	106	104	87	107
32	5.41	58.0	2.90	.89	.001	.000	108	103	83	105
33	4.71	54.0	2.86	1.14	.001	.000	108	103	85	104
34	3.30	42.0	2.29	1.49	.001	.000	110	104	77	100
35	1.38	13.0	2.22	1.35	.001	.000	117	106	67	98
36	.22	5.0	3.41	.16	.001	.000	59	100	53	97
37	.16	11.0	4.35	.06	.001	.000	107	100	52	95
38	.02	8.0	9.11	.13	.001	.000	99	95	48	120
39	.00	.0	10.89	.14	.001	.000	98	95	49	137
40	.00	.0	.00	.10	.001	.000	99	95	38	148
41	.00	.0	.00	.02	.001	.000	99	96	40	510
42	.00	.0	.00	.02	.001	.000	99	96	35	530
43	.00	.0	.00	.02	.001	.000	99	96	39	515
44	.00	.0	.00	.02	.001	.000	99	96	40	525
45	.00	.0	.00	.02	.001	.000	99	96	37	500
46	.00	.0	.00	.00	.001	.000	99	96	33	490
47	.00	5.0	.00	.00	.001	.000	99	96	35	535
48	.00	21.0	.00	.00	.001	.000	98	96	26	530
49	.00	10.0	.00	.00	.001	.000	99	96	26	530
50	.00	21.0	.00	.00	.001	.000	99	96	25	500
51	.00	20.0	.00	.00	.001	.000	98	96	25	520
52	.00	11.0	.00	.00	.001	.000	99	96	25	530
53	.00	7.0	.00	.00	.001	.000	98	96	25	500
54	.00	11.0	.00	.00	.001	.000	98	96	25	500
55	.00	6.0	.00	.00	.001	.000	99	96	25	500
56	.00	6.0	.00	.00	.001	.000	98	96	25	510
57	.00	4.0	.00	.00	.001	.000	99	96	25	530
58	.00	4.0	.00	.00	.001	.000	99	96	25	525
59	.00	4.0	.00	.00	.001	.000	99	96	25	520
60	.00	5.0	.00	.00	.001	.000	98	95	24	520
61	.00	7.0	.00	.00	.001	.000	98	95	24	510
62	.00	23.0	.00	.00	.001	.000	99	96	25	525
63	.00	.0	.00	.00	.000	.000	99	96	25	520

Table 2. Material Balance for Tests R-72, R-73 and R-74

Run No.	Constituent				
	NO_3	Fe	Na	Hg	SO_4
R-72	58.5	95.9	69.4	55.2	89.6
R-73	83.8	106.6	85.7	146	85.9
R-74	77.9	102.3	76.0	73.7	76.1

Table 3. Compositions (wt %) of Calcined Solids

Run No.	Constituent				
	NO_3	Fe	Na	Hg	SO_4
R-72	0.01	27.0	12.7	0.01	32.0
R-73	0.04	28.06	14.38	0.02	28.53
R-74	0.015	27.7	12.5	0.08	28.3

Table 4. Properties of Calcined Solids

Run No.	Solid Nitrate (ppm)	Calcining Time		Bulk Density (g/cc)
		Total Time (hr)	Above 600°C (hr)	
R-72	100	25	16	1.3
R-73	400	9	3	1.23
R-74	150	24	10	1.30

calcined solids held above 600°C from 10 to 16 hr should have a nitrate composition of 100 to 150 ppm. The bulk density of the calcined solids varied from 1.23 to 1.30 and was proportional to the concentration of the feed to the calciner and the rate at which the calcined solids were deposited.

Release of sulfate from the calciner vessel during operation causes two problems: (1) The sulfate concentration in the evaporator increases, causing increased corrosion in the evaporator and the calciner off-gas lines, and (2) the sulfate must be recycled to the calciner pot or allowed to accumulate in the evaporator and thus become a secondary disposal problem. Consequently, calcium nitrate was adopted as a standard additive to the feed to the calciner. A 10% stoichiometric excess of calcium plus sodium over the concentrations of SO_4^{2-} plus F^- plus PO_4^{3-} is maintained. The insoluble calcium sulfate formed in the calciner is thermally stable. Sulfate content of the calciner condensate for these tests is tabulated in Table 5.

Table 5. Sulfate Volatility and Entrainment

	Calciner Condensate (% of Total in Feed)			Calcium Added: Molar Fraction, Ca/SO_4
	Sulfate	Iron	Sodium	
R-72	2.0%	2.0%	0.5%	0.33
R-73	1.2%	1.0%	0.5%	0.41
R-74	0.3%	0.2%	0.1%	0.28

It was concluded that the sulfate in the calciner condensate was the result of entrainment because the ratio of nonvolatile to volatile ions is about the same.

Addition of Calcium Nitrate. Calcium nitrate was added to the calciner vessel at such a rate as to maintain a fixed molar ratio of calcium to sulfate in R-74. In previous tests the calcium nitrate was added at the beginning (R-72) or middle (R-73) of the test but was never added in a controlled molar ratio to the sulfate ion. Since these procedures allowed segregation, controlled addition system was developed and tested.

The controlled addition system consisted of a calibrated fuel tank equipped with a differential pressure (DP) cell liquid-level sensing device. The DP cell in the calcium nitrate feed tank was calibrated so that it would give an identical signal with the DP cell monitoring the liquid level in the waste feed tank and therefore ensure proportional feeding of the two solutions. For automatic control a remote set point controller was used (Fig. 1). This system maintained satisfactory control (Fig. 2).

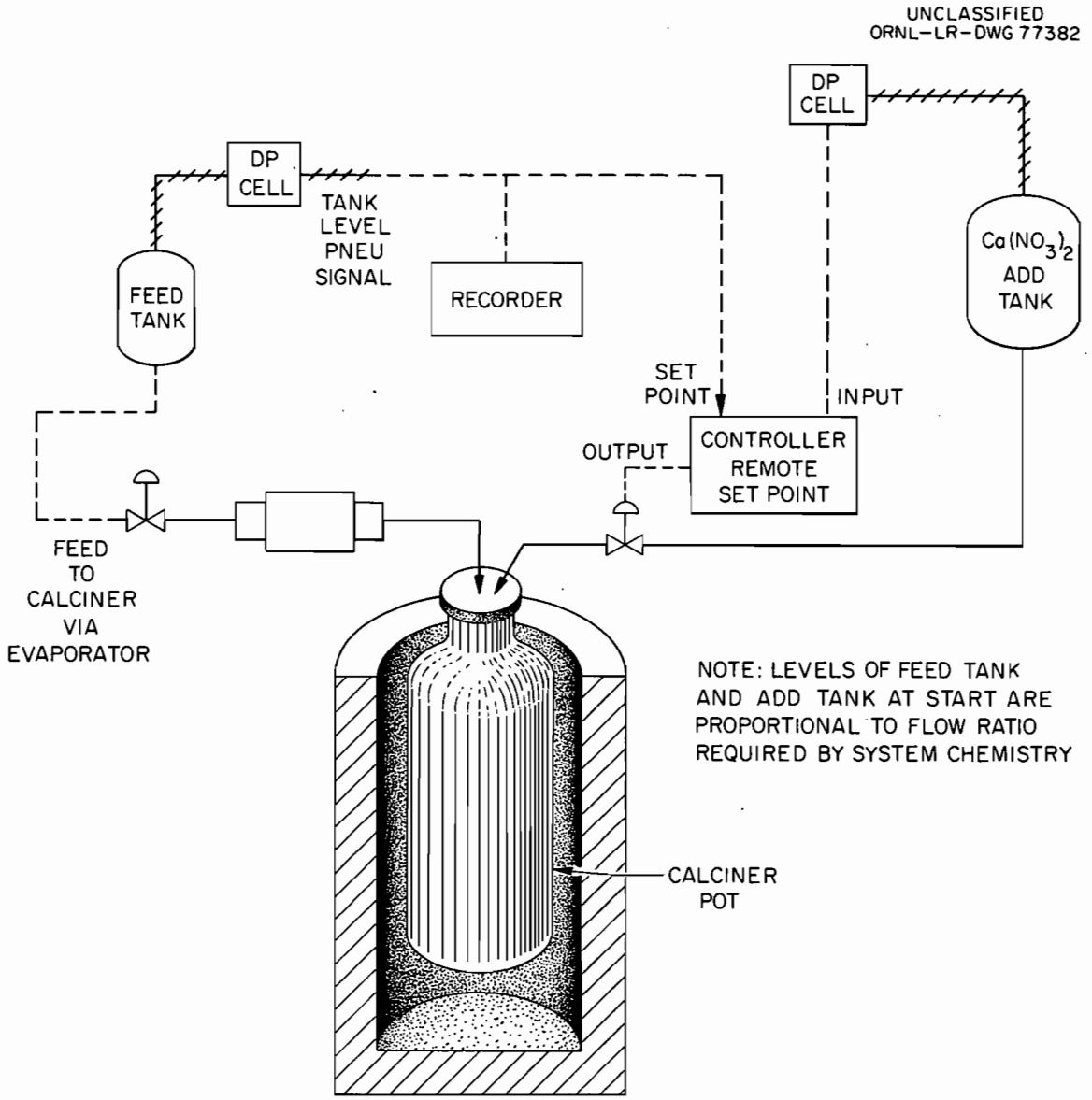

Fig. 1. Control System for Adding $Ca(NO_3)_2$ to the Calciner Pot in Proportion to the Waste Solution.

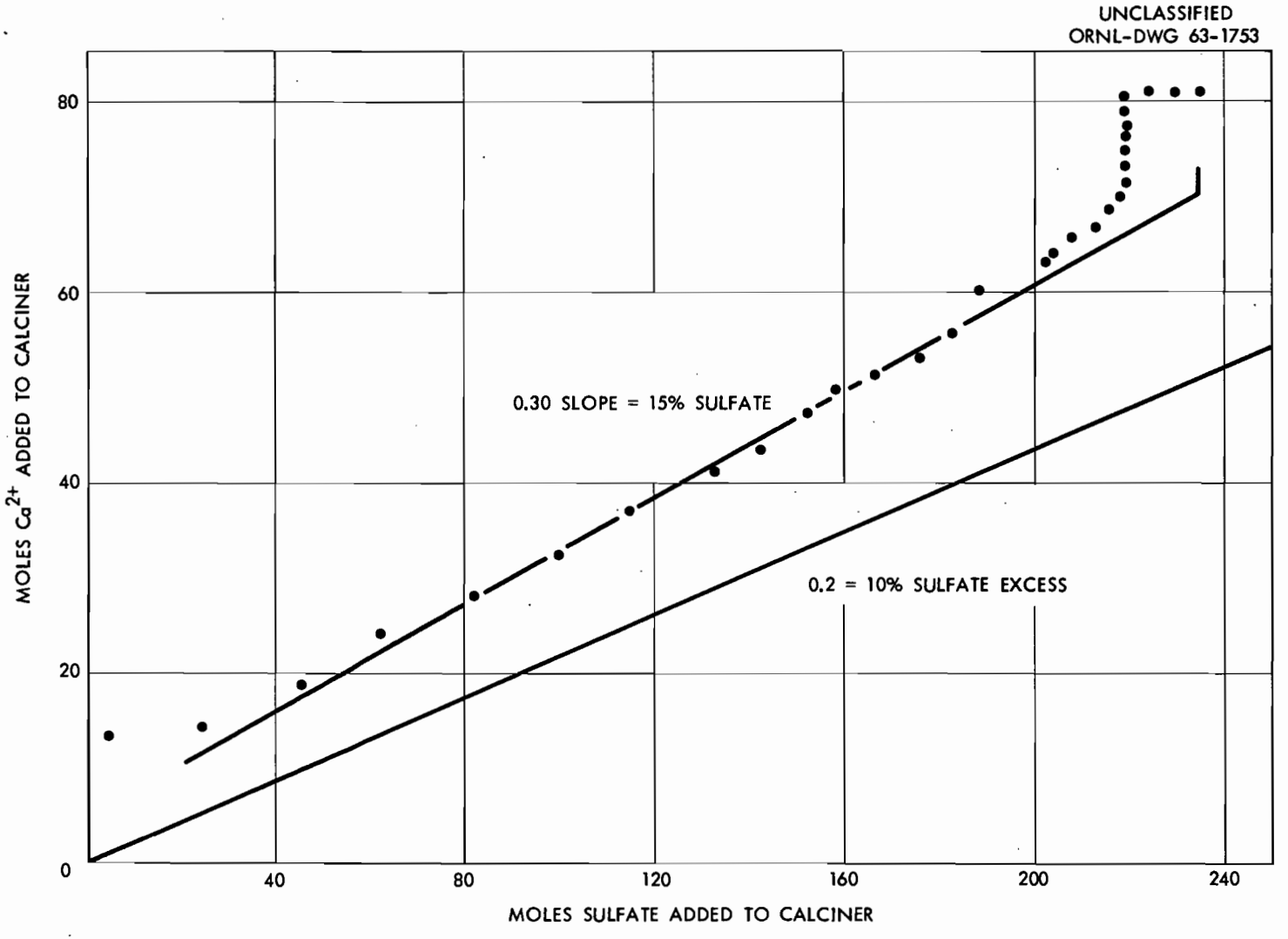

Fig. 2. Proportional Addition of $Ca(NO_3)_2$ and Waste Feed in Test R-74.

Ruthenium Distribution. The waste feed contained 170 g of inert ruthenium in test R-72 (0.0009 M), and 137 g were accounted for. The remainder probably plated on the calciner and evaporator metal surfaces. During cleanup operations, a black, flaking solid was noted. One-hundred-twenty-six grams of ruthenium (90%) was found in the solid calcined product. The decontamination factor across an impingement plate de-entrainer, used in the upper section of the evaporator, was 3300 (Fig. 3) over the entire test. The cause of the peaks showing high ruthenium entrainment from the evaporator is unknown.

Mercury Catch Tank. When the in-line mercury trap, which was tested previously,[4] failed to give the desired results, a mercury catch tank was installed. The principle of the mercury catch tank is to catch the last portion of calciner condensate which contains most of the mercury volatilized from the calciner. The percentage of mercury caught in the catch tank for the three tests was 8, 54, and 27%, respectively. In the first test, the valve to the mercury catch tank was opened when the feed to the calciner was stopped. Therefore, only a small amount of condensate was retained. For tests R-73 and R-74, the valve was opened about 2 hr before the feed to the calciner was stopped, thus producing a larger amount of condensate. The difference between the percentage caught in runs R-73 and R-74 cannot be explained. However, the off-gas lines in test R-73 were operated at about 500°C, compared with 400°C for test R-74.

Corrosion. When the calciner vessel was examined after tests R-72 and R-73, considerable corrosion was evident. In those tests, the feed was 0.005 M in fluoride. The corrosion may have been due to the fluoride in the feed or due to an excess or deficiency of calcium deposited in the solid near the calciner wall. In test R-74 there was no fluoride in the feed, the calcium was added uniformly throughout the test, and there was no corrosion evident when the calciner vessel was examined. The maximum fluoride concentration expected is 0.0005 M (see Table 6). Satisfactory corrosion control is expected at this concentration. (See Sec 2.3 for corrosion tests.)

2.2 Laboratory Scale Development

W. E. Clark H. W. Godbee J. F. Easterly

Work was directed primarily toward the fixation of Hanford Formaldehyde-Treated Waste, 1965 (FTW-65) in insoluble glassy solids that will retain sulfate during the fixation process. Work continued on the removal of mercury from FTW-65, determining the thermal conductivity of calcined powders, and studying the corrosion of materials of construction for waste-processing equipment during both fixation and storage in salt. Nonradioactive synthetic wastes were used in all experiments.

2.2.1 Fixation of Hanford Formaldehyde Treated 1965 Waste

Past experience with this waste and the high-sulfate waste previously studied indicated the feasibility of fixation in solid, nonglassy products which retain >95% of sulfate during fixation[4] or in glassy solids which lose more sulfate. In general, an excess of the cations Na^+, Ca^{2+}, Mg^{2+} and probably Pb^{2+} over the total nonvolatile

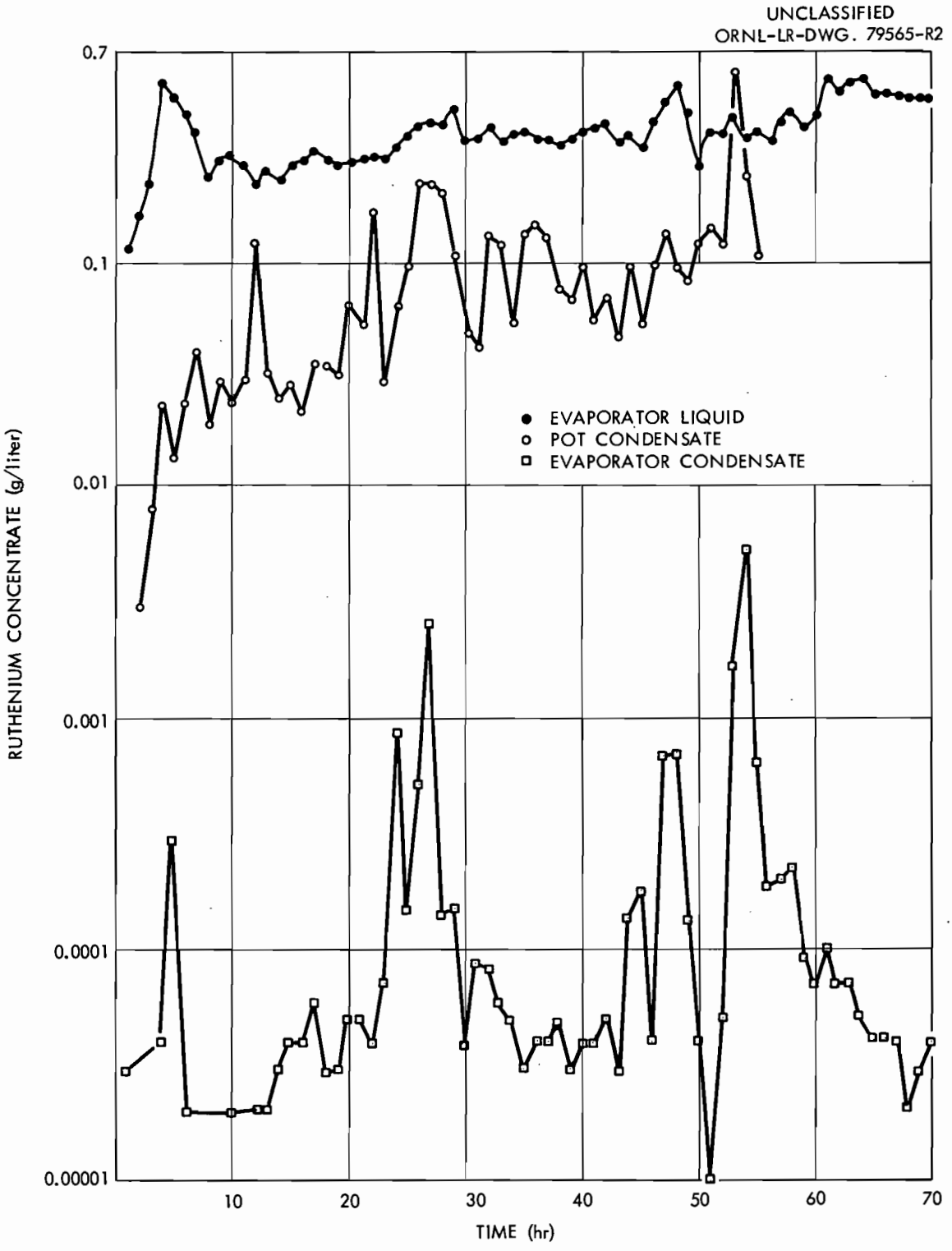

Fig. 3. Ruthenium Volatility in Test R-72.

anions in the melt favors retention of sulfate but destroys the glassy nature of the solid. Relatively small changes in melt composition can result in large changes in the appearance and behavior of the final product, indicating the existence of a complex phase system. Efforts were made to improve the physical characteristics of the solid product without loss of gross amounts of sulfate.

Simulated FTW-65 wastes were evaporated to a fourth of their volume, with visible precipitation of solids,[4] but make-up of a synthetic FTW-65 waste concentrate of this composition for use in experimental glass-making was impractical. A solution corresponding to volume reduction by a factor of 3, was practical and the latter will be adopted as a standard feed for fixation experiments with FTW-65 (Table 6).

Formation of melts similar to that prepared on a semiengineering scale from high sulfate Purex waste[5] resulted in the formation of a non-glassy melt which lost 23% of its SO_3 when heated for 100 minutes at 100°C above its softening temperature and two glassy melts, one of which lost 65.3% of its SO_3 when heated 155° above its softening temperature (Table 7).

Another series of melts was prepared from FTW-65 waste by adding varying amounts of sodium, lead, phosphate, and borate to a fixed volume of waste containing fixed amounts of calcium and aluminum. Percentages of waste oxides varied from 43.0 to 53.5 and initial softening temperatures varied from 725° to 850°C. Although the (Na + Ca)/anion ratio was less than unity, in most cases the loss of SO_3 varied from 5.9 to 21.4% on heating ~100° above the initial softening temperature for 100 minutes. Most of the low-melting materials were excessively soluble in water (Table 7).

A series of sodium-calcium-aluminum phosphate melts incorporating 30-44% waste oxides was prepared by adding lead oxide, aluminum nitrate and sodium borate to the concentrated waste, to give melts whose compositions were variations of one of the better melts obtained in a previous experiment (see ref 6, Table 7, melt A-1). The three lead melts were excessively soluble. The melting point of the melts containing added aluminum increased with aluminum content and the melts became progressively less glassy. The addition of borate resulted in insoluble glassy melts with softening points increasing from 775° to 850°C as the sodium tetraborate content increased from 0.2 to 0.6 gram moles per liter of concentrated waste solution (Table 8). Sulfate losses for the borate melts increased from 10.7% to 60.8% as the percentage of B_2O_3 increased from 10.8 to 28.7% and the ratio:

$$\frac{\text{Chem. eqs } (Na^{+} + Ca^{++})}{\text{Chem. eqs nonvolatile anions}} \quad \text{from 0.865 to 0.566.}$$

Use of stainless steel fixation pots imposes a maximum operating temperature of about 1050°C for the fixation process. However, lower operating temperatures are desirable both to reduce corrosion and because of furnace limitations. The resistance furnaces used in both semiengineering and engineering- scale tests (see Sec 2.1) have a maximum operating temperature of 1050°C and maintain the pot walls at a maximum temperature of 900-970°C. Consequently, attempts were made to produce lower melting

Table 6. Compositions of Simulated Hanford Formaldehyde Treated 1965 Waste Solution (FTW-65) Used in ORNL Laboratory Fixation Experiments

Constituent (gm moles/liter waste)	FTW-65 Waste	FTW-65 Waste Concentrated to 1/3 Volume
H^+	0.5	1.5[a]
Na^+	0.30	0.90
Al^{+3}	0.05	0.15
Fe^{+3}	0.10	0.30
Cr^{+3}	0.02	0.06
Ni^{+2}	0.01	0.03
Hg^{+2}	0.0035[b]	0.0105[b]
Ru	0.002	0.006
SO_4^{-2}	0.15	0.45
PO_4^{-3}	0.005	0.015
SiO_3^{-2}	0.01	0.03
F^-	0.02[c]	0.06[c]
NO_3^-	balance	balance
gallons waste/ton U	82	27.3

[a]Material balances from concentration by distillation give values between 1.3 and 1.4 M. The value of 1.5 M is well within the probable variation of waste solution composition.

[b]Values listed represent the maximum concentrations of Hg^{+2} expected.

[c]Values listed based on private communication A. M. Platt, HAPO, to W. E. Clark, ORNL. Later information from Hanford lists 0.0005 M F^- as more nearly correct for the unconcentrated waste.

Table 7. Fixation Experiments on Concentrated Hanford FTW-65 Waste Solution

Boro-phosphate Melts.

Additive (g moles/liter waste conc'd x 3)	Melt Designation: R-Series				F-Series									
	Reference[a] (High Sulfate Waste)	R-1	R-2	R-3	F-1	F-2	F-3	F-4	F-5	F-6	F-7	F-8	F-9	F-10
NaH_2PO_2	---	1.0	1.0	1.0	---	---	---	---	---	1.0	1.0	1.0	1.0	1.0
NaH_2PO_4	---	---	---	---	0.81	0.81	0.81	0.81	0.81	---	---	---	---	---
H_3PO_3	1.52	---	0.37	0.175	0.175	0.175	0.175	0.175	0.175	0.175	0.175	0.175	0.175	0.175
$Ca(OH)_2$	0.8	---	---	---	0.144	0.144	0.144	0.144	0.144	0.144	0.144	0.144	0.144	0.144
CaO	---	0.144	0.144	0.144	---	---	---	---	---	---	---	---	---	---
$Al(NO_3)_3$	---	0.153	0.153	0.153	0.153	0.153	0.153	0.153	0.153	0.153	0.153	0.153	0.153	0.153
$Na_2B_4O_7$	0.34	---	---	---	---	---	---	---	---	---	0.123	0.25	---	0.123
B_2O_3	---	0.123	0.123	0.123	0.123	0.123	0.123	0.123	0.123	0.123	---	---	0.123	---
NaOH	1.34	---	---	---	0.123	0.25	---	---	0.123	0.123	0.123	0.25	0.123	0.123
$Pb(NO_3)_2$	---	---	---	---	---	---	0.13	0.25	---	---	---	---	0.13	0.13
Wt % Waste Oxides Composition of Melt (Wt % Theoretical)	35.7	46.4	41.6	43.9	53.5	52.6	47.8	43.0	51.6	47.1	48.4	44.3	44.5	43.2
Na_2O	19.9	25.9	23.1	24.4	16.4	17,8	12.9	11.6	15.8	14.4	14.9	15.1	13.6	13.2
CaO	11.0	3.5	3.2	3.4	3.8	3.7	3.4	3.0	3.2	3.3	3.4	3.1	3.2	3.0
PbO	---	---	---	---	---	---	12.4	21.3	---	---	---	---	11.5	11.2
Al_2O_3	1.2	5.1	4.6	4.8	7.1	6.9	6.3	5.7	10.1	12.6	6.4	5.9	5.9	5.7
Fe_2O_3	9.8	10.5	9.4	9.9	11.9	11.6	10.6	9.5	11.5	10.4	10.7	9.8	9.8	9.5
Cr_2O_3	0.2	2.0	1.8	1.9	2.2	2.2	2.0	1.8	2.2	2.0	2.0	1.9	1.9	1.8
NiO	0.2	1.1	0.9	1.0	0.6	0.6	0.6	0.5	0.6	0.6	0.6	0.5	0.5	0.5
RuO_2	0.1	0.3	0.3	0.3	0.4	0.4	0.4	0.3	0.4	0.4	0.4	0.4	0.4	0.3
SO_3	19.6	15.7	14.1	14.9	18.6	18.4	16.7	15.1	18.2	16.4	16.9	15.5	15.5	15.1
P_2O_5	26.4	31.5	38.5	35.2	34.3	33.8	30.7	27.6	33.3	35.8	36.8	33.8	33.9	32.8
B_2O_3	11.7	3.8	3.4	3.6	4.1	4.0	3.6	3.3	3.9	3.6	7.5	13.7	3.4	6.6
SiO_2	---	0.8	0.7	0.7	0.2	0.2	0.2	0.2	0.2	0.2	0.2	0.2	0.2	0.2
F^-	---	---	---	---	0.2	0.2	0.2	0.1	0.2	0.2	0.2	0.1	0.1	0.1
	100.0	100.0	100.0	100.0	99.9	99.9	100.0	100.0	99.9	99.9	100.0	100.0	99.9	100.0
Approx. Softening Temp (°C)	850	950	850	<850	825	775	850	775	800	825	725	750	725	750
Approx. Melting Temp (°C)	---	1050	950	900-950	875	850	900	850	925	900	800	825	825	825
Max. TGA Temp (°C)	---	1048	---	1005	925	875	---	875	925	925	825	---	---	---
% SO_3 Lost (100 min)	15-20[b]	23.0	---	65.3	12.7	7.2	---	15.1	11.9	21.4	5.9	---	---	---
Ratio[c]	0.826	0.959	0.825	0.891	0.936	0.992	0.997	0.891	0.936	0.941	0.946	0.915	1.05	1.04
Description (Small sample, annealed)	Glassy, some segregation.	Highly segregated, some voids.	Homogeneous, glassy.	Homogeneous, glassy.	Dense black rock. Soluble; surface segregation.	Dense black rock. Soluble; surface segregation.	Fine-grained black rock. Insoluble; surface segregation.	Dense gray rock. Soluble; surface segregation.	Dense black rock. Insoluble, very little segregation.	Dense black rock. Insoluble.	Gray-green rock. Dense, soluble.	Gray-green rock. Soluble; surface segregation.	Gray-green rock. Dense, soluble; surface segregation.	Dark green rock. Dense, soluble; surface segregation.

[a] See Reference 1.

[b] From semi-engineering scale experiment (Ref. 1). Other values are from thermogravimetric data.

[c] $$\text{Ratio} = \frac{\text{Gm. eqs } (Na^+ + Ca^{2+} + Pb^{2+})}{\text{Gm. eqs } (SO_4^{2-} + PO_3^- + BO_2^- + SiO_3^{2-} + F^-)}$$

Table 8. Fixation Experiments on Concentrated FTW-65 Waste

The Effects of Adding Varying Amounts of Lead, Aluminum, and Boron to a Sodium-Aluminum-Calcium-Phosphate Melt

Additives (moles/liter)	Melt Designation								
	Al-Pb-(1)	Al-Pb-(2)	Al-Pb-(3)	Al-Al-(1)	Al-Al-(2)	Al-Al-(3)	Al-B-(1)	Al-B-(2)	Al-B-(3)
H_3PO_3	1.02	1.02	1.02	1.02	1.02	1.02	1.02	1.02	1.02
NaOH	1.14	1.14	1.14	1.14	1.14	1.14	0.75	0.35	---
$Ca(OH)_2$	0.21	0.21	0.21	0.21	0.21	0.21	0.21	0.21	0.21
$Al(NO_3)_3 \cdot 9H_2O$	0.24	0.24	0.24	0.50	0.80	1.0	0.24	0.24	0.24
$Pb(NO_3)_2$	0.20	0.40	0.60	---	---	---	---	---	---
$Na_2B_4O_7 \cdot 10H_2O$	---	---	---	---	---	---	0.20	0.40	0.60
% Waste Oxides	39.0	33.8	29.8	43.8	41.2	39.8	43.3	40.9	38.5
% Theo. Oxides									
Al_2O_3	6.7	5.9	5.1	12.8	17.7	20.8	7.6	7.2	6.7
CaO	4.0	3.5	3.1	4.5	4.2	4.1	4.5	4.2	4.0
Na_2O	22.8	19.8	17.4	25.6	24.2	23.2	20.7	15.0	10.4
Fe_2O_3	8.6	7.5	6.6	9.7	9.1	8.8	9.6	9.0	8.5
Cr_2O_3	1.6	1.4	1.3	1.8	1.7	1.7	1.8	1.7	1.6
NiO	0.5	0.4	0.4	0.5	0.5	0.5	0.5	0.5	0.5
RuO_2	0.3	0.3	0.2	0.4	0.3	0.3	0.3	0.3	0.3
SO_3	13.7	11.8	10.4	15.3	14.4	13.9	15.1	14.3	13.4
P_2O_5	25.8	22.4	19.8	29.0	27.5	26.5	28.7	27.3	25.5
SiO_2	0.1	0.1	0.1	0.1	0.1	0.1	0.1	0.1	0.1
F^-	0.2	0.2	0.1	0.2	0.2	0.2	0.2	0.2	0.2
PbO	15.6	26.8	35.5	---	---	---	---	---	---
B_2O_3	---	---	---	---	---	---	10.8	20.3	28.7
	99.9	100.1	100.0	99.9	99.9	100.1	99.9	100.1	99.9
Approx. Softening Temp (°C)	925	950	>1000	800	900	>1000	775	825	850
Approx. Melting Temp (°C)	975	1050	---	950	1050	---	875	925	950
Max. TGA Temp (°C)	---	---	---	---	---	---	~900	~950	~950
% SO_3 Lost (100 min)	---	---	---	---	---	---	10.7	50.9	60.8
Ratio*	1.39	1.59	1.78	1.20	1.20	1.20	0.865	0.676	0.566
Description	Dense black rock. Soluble.	Dark brown rock. Soluble; segregated.	Very hard, dense, brown rock. Soluble.	Viscous melt, hard, glassy rock. Insoluble.	Very hard rock, slightly glassy. Soluble.	Did not melt. Insoluble.	Black, glassy rock. Insoluble; some segregation.	Glassy, brown, slightly segregated. Insoluble.	Good black glass. Insoluble.

*

$$\text{Ratio} = \frac{\text{Gm. eqs } (Na^+ + Ca^{2+} + Pb^{2+})}{\text{Gm. eqs } (SO_4^{2-} + PO_3^- + BO_2^- + SiO_3^{2-} + F^-)}$$

solids by lowering the percentage of waste oxide in the melt. Some of the melts prepared in this way had sufficiently low softening and melting temperatures (e.g., melts F-2, F-4, F-7, F-8, F-9, F-10, Table 7) but were excessively soluble in water.

Melts formed by lowering the waste oxide content below 25% and increasing P_2O_5 content to 45 to 55% softened at 800 to 850°C and were satisfactorily fluid at 850 to 950°C (Table 9). Three of the most promising were reproduced using the concentrated waste. The initial softening and melting points varied from 700 to 750 and from 750 to 825°C, respectively, 50 to 100°C lower than those with dilute waste (Table 9.A). Only one melt (melt FTW-3R) appeared to be reasonably insoluble in water, but this melt lost 16.8% of its sulfate when heated to 800°C for 100 minutes.

Varying the amounts of calcium and borax added to melts containing 45% waste oxides failed to improve the physical properties of the resulting solids (Table 10).

2.2.2 Semiengineering Scale Fixation of FTW-65 Waste

Two semiengineering scale fixation experiments were run on Hanford FTW-65 waste in 4-in. diam by 24-in. high stainless steel pots. The following materials were added per liter of concentrated waste (Table 6): 1.02 moles $NaHPO_2$, 0.24 moles $Al(NO_3)_3$, 0.21 moles $Ca(NO_3)_2$, and 1.14 moles NaOH. All additives except the calcium nitrate were added to the feed solution in the feed tank and the calcium nitrate was metered into the feed line just before the fixation pot. The solid product was a hard, dark brown rock-like substance with the nominal percentage composition by weight shown in Table 11 (melt A-1, Table 7, Quarterly Report for November 1962-January 1963).

Difficulty was experienced with plugging of the off-gas line during the early stages of both experiments. In the first case operation was resumed after unplugging of the line and subsequent operation was very smooth. The second semi-continuous experiment was run to test electrical resistance probes for determining the levels of solution, calcine and melt in the pot. The probe operated satisfactorily in this initial test and will be developed further in succeeding tests.

The resistance probe consisted of a bundle of seven quartz tubes 3 mm OD, 1.0 mm wall through which were threaded 30 mil nichrome wire. About 1/4-in. of the wire extended from the end of each tube. The lengths were arranged to place probes at about 3-in. intervals from the bottom to the top of the pot (Fig.4). The tube bundle was sealed into a threaded fitting with Sauereisen cement, the tube ends sealed with lead phosphate glass, and the bundle inserted into the center tube of the pot, one-half of which had been cut away longitudinally to allow access of solution and melt to the probes.

The probe readings were compared with those of the pot and furnace thermocouples. Plots of resistance for probes and thermocouple readings at the same level of the pot indicated the feasibility of the method (Fig.4).

Table 9.A. Fixation of Simulated FTW-65 Waste in Phosphate and Silico-Phosphate Melts

(Re-runs of three promising melts from Table 4; concentrated waste used)

Additives (gm moles/liter conc'd waste)	Melt Description		
	FTW-3R	FTW-7R	FTW-8R
H_3PO_3	2.88	5.76	2.88
NaOH	2.16	2.40	1.47
$Ca(OH)_2$	1.20	1.32	0.82
SiO_2	---	1.32	0.76
Weight % Waste Oxides	25.0	15.0	25.0
Melt Composition (wt % oxides, theo.)			
Na_2O	21.8	14.1	16.8
CaO	15.0	10.0	10.0
Al_2O_3	1.6	1.0	1.6
Fe_2O_3	5.5	3.3	5.5
Cr_2O_3	1.1	0.6	1.1
NiO	0.3	0.2	0.3
RuO_2	0.2	0.1	0.2
SO_3	8.7	5.2	8.7
P_2O_5	45.5	55.3	45.5
SiO_2	0.1	10.0	10.1
F^-	0.3	0.2	0.3
Softening Temp (°C)	700	750	750
Melting Temp (°C)	750	800	825
Maximum TGA Temp	800	---	---
% Theo. SO_3 lost	16.8	---	---
Ratio $\frac{\text{gm eqs } (Na^+ + Ca^{2+})}{\text{gm eqs } (SO_4^{2-} + PO_3^- + SiO_3^{2-} + F^-)}$	1.4	0.63	0.74
Description	Insoluble, dark green, glassy rock	Soluble, shiny light green rock	Soluble, hard gray rock with voids

Table 10. Fixation of Simulated FTW-65 Waste Solution in Boro-Phosphate Melts

FTW-C Series

Additives (g moles/liter conc'd waste)	FTW-CI	FTW-CII	FTW-CIII	FTW-CIV	FTW-CV	FTW-CVI
H_3PO_3	0.352	0.352	0.352	0.352	0.352	0.352
$Ca(OH)_2$	0.074	---	0.112	---	0.06	0.037
NaOH	0.41	0.41	0.41	0.41	0.41	0.41
$Na_2B_4O_7$	0.03	0.03	0.016	0.015	0.015	0.03
MgO	---	0.103	---	0.155	0.072	0.052
PbO	---	---	---	---	---	---
Wt % Waste Oxides	45.0	45.0	45.0	45.0	45.0	45.0
Composition of Melt (Wt % oxides, theoretical)						
Na_2O	27.2	27.2	27.2	27.2	27.2	27.2
CaO	5.0	---	7.5	---	4.0	2.5
Al_2O_3	2.9	2.9	2.9	2.9	2.9	2.9
Fe_2O_3	9.9	9.9	9.9	9.9	9.9	9.9
Cr_2O_3	1.9	1.9	1.9	1.9	1.9	1.9
NiO	0.5	0.5	0.5	0.5	0.5	0.5
RuO_2	0.4	0.4	0.4	0.4	0.4	0.4
SO_3	15.7	15.7	15.7	15.7	15.7	15.7
P_2O_5	30.9	30.9	30.9	30.9	30.9	30.9
SiO_2	0.1	0.1	0.1	0.1	0.1	0.1
F^-	0.5	0.5	0.5	0.5	0.5	0.5
B_2O_3	5.0	5.0	2.5	2.5	2.5	5.0
PbO	---	---	---	---	---	---
MgO	---	5.0	---	7.5	3.5	2.5
Approx. Softening Temp (°C)	800	850	850	900	900	900
Approx. Melting Temp (°C)	850	900	900	950	950	950
Ratio*	1.02	1.09	1.15	1.25	1.20	1.06
Description	Segregated, porous, rocky	Very porous, segregated	Dark, rocky, some segregation	Dark, porous, badly segregated	Dark, porous, some segregation	Dark, porous, some segregation

* $$\text{Ratio} = \frac{\text{gm eqs } (Na^+ + Ca^{2+} + Mg^{2+} + Pb^{2+})}{\text{gm eqs } (SO_4^{2-}\ PO_3^- + SiO_3^{2-} + F^-)}.$$

Table 11. Semiengineering Scale Fixation Test

	wt %		wt %		wt %
Al_2O_3	7.9	Cr_2O_3	1.9	SO_3	15.7
CaO	5.0	NiO	0.5	SiO_2	0.1
Na_2O	27.2	RuO_2	0.4	F^-	0.5
Fe_2O_3	10.0	P_2O_5	30.9	---	---

Waste oxide content ... 45%
Softening temperature ... 850°C
Ruthenium volatilized ... 24%
Bulk density ... 2.6 g/cc
Volume reduction ... 30
Sulfate volatilized ... 1.8%*

*9% predicted from thermogravimetric tests.

2.2.3 Fixation Experiments on Non-Sulfate Purex Waste

Six phosphate melts were made in scouting tests on fixation of non-sulfate bearing Purex waste. Waste oxide contents varied between 27 and 45%. No completely satisfactory material was obtained, but two products were glasses (Table 12).

2.2.4 Removal of Mercury from FTW-65 Waste Solution

A series of experiments were run in which FTW-65 waste solution was passed through a bed of copper shot at 5 bed volumes per hour. Simultaneously a small cathodic current was imposed on the bed between an anodic platinum screen above the copper pellets and a cathodic platinum screen around the lower portion of the pellets. Residence time of the solution was 12 minutes. Without current a residence time of at least 25 minutes was necessary to remove >99% of the mercury by displacement by the copper. With a current, which varied from 1/3 to 1.1 times the theoretical required to remove the Hg^{2+} without chemical displacement, more than 99% of the mercury was removed in 12 minutes. In the absence of current or when the current was less than the theoretical required for complete removal of mercury, the amount of copper which dissolved was roughly three times that required for stoichiometric displacement of Hg(II) by Cu(II).

2.3 Corrosion Studies

W. E. Clark

2.3.1 Fixation Container Corrosion (W. E. Clark)

A series of rapid and approximate corrosion tests were run in simulated stainless steel fixation pots. Three to 3.5 liters of synthetic waste solutions, with and without added calcium and with 0, 0.02 M, or 0.0005 M fluoride added, were evaporated to

UNCLASSIFIED
ORNL-DWG 63-1755

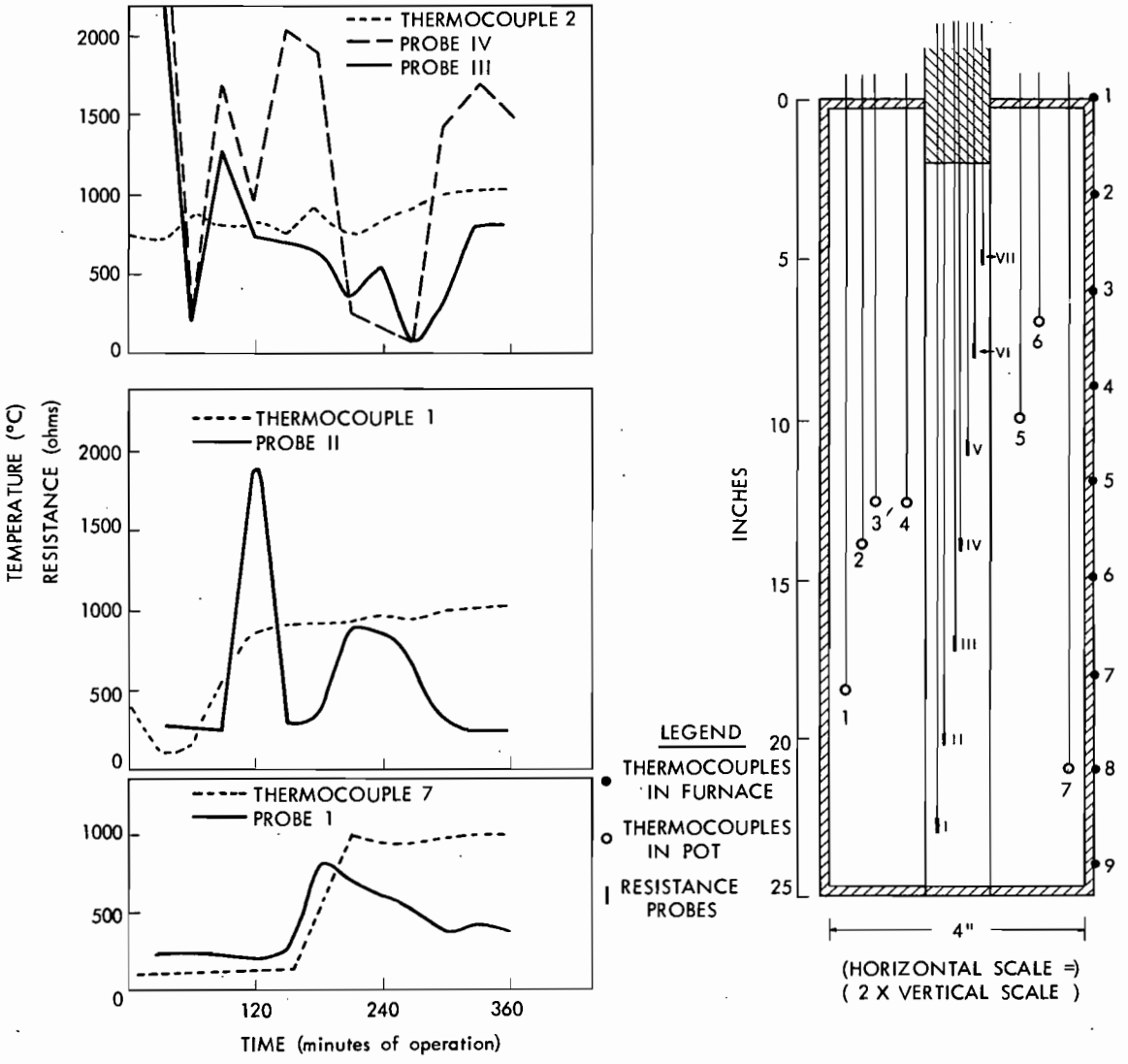

Fig. 4. Comparison of Thermocouple and Resistance Probe Readings During Pot Fixation of Simulated Hanford FTW-65 Waste.

Table 12. Fixation Experiments on Simulated Non-Sulfate Purex Waste

Additives (moles/liter waste sol'n)	Melt Designation NS-1	NS-2	NS-3	NS-4	NS-5	NS-6
H_3PO_3	0.6	0.7	0.7	0.7	0.7	0.8
$Al(NO_3)_3$	---	---	0.5	---	0.3	0.2
$Pb(NO_3)_2$	---	---	---	0.2	0.1	---
$Ca(OH)_2$	---	0.1	---	---	---	---
Weight % waste oxides	45.4	38.9	31.2	27.2	28.4	34.1
Composition of Melt (Wt % theo. oxides)						
Al_2O_3	13.2	11.3	33.9	7.9	22.0	20.8
Cr_2O_3	0.6	0.5	0.4	0.4	0.4	0.4
Fe_2O_3	5.2	4.4	3.5	3.1	3.2	3.9
Na_2O	24.0	20.6	16.5	14.4	15.0	18.1
NiO	0.6	0.5	0.4	0.3	0.4	0.4
P_2O_5	56.4	56.5	45.3	39.4	41.2	56.4
PbO	---	---	---	34.6	18.1	---
CaO	---	6.2	---	---	---	---
Softening Temp (°C)	750	725	850	700	750	800
Melting Temp (°C)	800	800	*	750	800	**
Bulk Density (g/ml)	1.7	2.0	~1.3	3.1	~1.9	2.5
Volume Reduction (ml sol'n/ml solid)	26	25	~14	28	~19	28
Description	Rough green rock; crumbled in water	Insoluble, green rock	Insoluble, brown glass, some voids	Insoluble, 2-phase; lower glassy, upper rocky	Insoluble, brown glass; some voids and segregation	Green, crumbly rock

*Too viscous to pour at 1050°C.

**Too viscous to pour at 1000°C.

dryness at <600°C. The solids were then packed loosely around 304L stainless steel coupons in a stainless steel cup (1.9-in. OD x 8-in. high, 0.020 in. wall). The pipe was enclosed in a stainless steel pot (1.75-in. OD x 9-in. high, 1/8-in. wall) equipped with an off-gas system and a condenser. Temperature was measured and controlled by a stainless steel-clad chromel-alumel thermocouple located in the cup near the specimen. Reagent grade sodium nitrate or sodium sulfate decahydrate were also tested. In this case a volume of water equal to the condensates from the waste tests was added to the cup with the salts.

The results (Table 13) indicate that the presence of fluoride and of excess water accelerate corrosion and that the addition of excess calcium suppresses the effect of both fluoride and sulfate. This is consistent with the belief that the corrosion mechanism involves the reaction of superheated steam with the steel as indicated by the presence of magnetite in the corrosion products. The attack is accelerated and may be initiated by HF and H_2SO_4 resulting from hydrolysis of the fluoride and sulfate salts by the steam. The odor of SO_2, which was observed in some cases, indicated that oxidation of the metal by the sulfate occurred.

Sodium sulfate decahydrate was the most corrosive material tested. There was no magnetism associated with the corrosion products formed in this case nor was the odor of SO_2 detected. Therefore, the attack was probably caused by bisulfate, HSO_4^-.

The sodium nitrate experiment was abandoned before the temperature reached 900°C due to blockage of the off-gas line by sublimed and/or entrained solids.

2.3.2 Condenser and Salt Storage (P. D. Neumann, Reactor Chemistry Division)

Welded specimens of Type 304L stainless steel were exposed for 672 hours in salt (NaCl) at 300°C in a sealed container with and without additives (Table 14) to evaluate the resistance of the fixation pots stored in natural salt formations. Average corrosion rates were quite low ($\leq$ 0.03 mils/mo maximum) in all cases. As expected, the rates were slightly higher in the presence of impurities (e.g. H_2O, $CaSO_4$, $MgCl_2$) than in pure salt. Some pitting was observed. Specimens exposed to salt with added water developed a heavy blue-black film. Those exposed to dry salt had straw-colored films.

This indicates that corrosion during storage in salt formations will be acceptable provided the salt is not too impure and that the temperature of the pot wall in contact with the salt does not exceed 300°C. Increasing the temperature of the pot wall would result in accelerated corrosion.

Welded specimens of Hastelloy F, Type 304L stainless steel, titanium 45A and couples of 304L stainless steel with titanium 45A showed satisfactory resistance during long-term exposures in vapor and solution phases of boiling FTW-65 waste. After 1584 hours of testing, uncoupled specimens of 304L and titanium showed weight gains of 1 to 2 mg/cm^2 in the vapor and 8 mg/cm^2 in the solution. Titanium, from Ti-304L couples disassembled after 1368 hours of exposure, gained 2 and 6 mg/cm^2 in the solution and vapor phases, respectively, while the stainless steel specimens corroded at rates of 0.1

Table 13. The Corrosion of Stainless Steel by Partially Calcined Waste Solids, Na_2SO_4 and $NaNO_3$ at ~900°C.[a]
304L Stainless Steel Corrosion Coupons

Feed	Additives	Max. Pot Temp. (°C)	Temp. °C Furnace	Total Cond. ml	Time at Max. Temp. hours	Thermocouple	Observations
FTW-65 (3.5L) (0.02 M F^-)	None	925	Lost Thermo. at 625	24.5	11	Lost after 9-1/2 hours	Cup and specimen heavily corroded.
FTW-65 (3.5L) (0.02 M F^-)	10.16 g/l $Ca(NO_3)_2$	970	950	25	11	Lost after 25 min at temperature	Cup scaled on the outside; specimen heavily corroded; SO_2 odor.
FTW-65 (No HF) (3.5L)	None	925	900	21	11	Lost after 45 min at temperature	Specimen heavily corroded; little corrosion on cup.
FTW-65 (No HF) (3.5L)	10.16 g/l $Ca(NO_3)_2$	925	900	31	11	Intact	Little corrosion on cup or specimen.
$NaNO_3$ 342.9 g	25 ml H_2O	875	875	24.5	Shut Down at 875°C	Lost at 740°C	Little corrosion on cup or specimen; solid collected on outside and at top of cup; danger of off gas line plugging.
Na_2SO_4 263.0 g	25 ml H_2O	925	900	156	11	Lost at 825°C	Cup heavily corroded; holes formed; little corrosion on pot.
FTW-65 (3.5L) (0.02 M F^-)	50.80 g/l $Ca(NO_3)_2$	925	900	18	11	Intact	Outside of the cup heavily scaled; inside of cup slightly corroded; slight corrosion of the specimen; corroded spots slightly magnetic.
FTW-65 (3.5L) (0.02 M F^-)	10.16 g/l $Ca(NO_3)_2$	925	900	29.5	11	Lost after ~45 min at temperature	Specimen heavily corroded; some corrosion on cup; strong odor of SO_2.
FTW-65 (0.0005 M F^-) (3.0L)	10.16 g/l $Ca(NO_3)_2$	925	900	16	11	Intact	Cup and specimen lightly corroded; slightly magnetic.
FTW-65 (0.0005 M F^-) (3.5L)	None	925	900	17.0	11	Intact	Cup and specimen slightly corroded; cup slightly magnetic; specimen slightly magnetic.
Purex (High Sulfate)	0.003 M F^-	925	900	68	11	Intact	Neg. corrosion on cup; slight corrosion on specimen; specimen slightly magnetic.
Purex (High Sulfate)	0.003 M F^- 181.84 g/l $Ca(NO_3)_2$	925	900	21	11	Intact	Neg. corrosion on cup or specimen.

[a] Composition of FTW-65 waste solution: 0.5 M H^+, 0.30 M Na^+, 0.05 M Al^{+3}, 0.10 M Fe^{+3}, 0.02 M Cr^{+3}, 0.01 M Ni^{+2}, 0.0035 M Hg^{+2}, 0.002 M Ru, 0.15 M SO_4^{-2}, 0.005 M PO_4^{-3}, 0.01 M SiO_3^{-2}, NO_3^- to balance.

Composition of high sulfate purex waste solution: 5.6 M H^+, 0.6 M Na^+, 0.1 M Al^{+3}, 0.5 M Fe^{+3}, 0.01 M Cr^{+3}, 0.01 M Ni^{+2}, 1.0 M SO_4^{-2}, NO_3^- to balance.

Table 14. Corrosion of Type 304L Stainless Steel in Simulated Salt Mine Storage, 300°C

(Reagent grade NaCl plus additives as shown)

Test No.	Additives	Corrosion Rate (mpm)
1	None	0.01
2	2% H_2O	Gain ~0.1 mg/cm^2
3	5% $CaSO_4$	0.01
4	0.25% $MgCl_2$	0.01
5	2% H_2O, 5% $CaSO_4$, 0.25% $MgCl_2$	0.03

and 0.3 mil/mo in similar phase positions. There was no localized attack. The Hastelloy F specimens showed weight gains of about 7 to 10 mg/cm^2 after 1296 hours exposure.

2.4 Thermal Conductivity

H. W. Godbee

Effective thermal conductivities were measured for several magnesia, alumina, and zirconia powders in air at atmospheric pressure at temperatures from 200°F to 1500°F. Volume fraction solid in the heterogeneous systems varied from 0.49 to 0.65. Measurements were made using a steady-state method based on radial heat flow in a hollow cylinder. A few measurements were made using an unsteady-state method to corroborate the steady-state measurements. The unsteady-state method is based on the heating of a cylinder of a perfect conductor surrounded by an infinite amount of the material whose conductivity is being measured.

The powders had mean particle sizes ranging from about 255 microns to 895 microns as determined by screening. There was little or no internal pore volume as would be expected for powders prepared from fused and crushed oxides. The surface area (BET nitrogen adsorption) ranged from 0.03 to 0.12 m^2/g.

In the range of temperatures studied, the effective thermal conductivity of all the powders increased with increasing temperature (Figs. 5 and 6). The variation of effective thermal conductivity was approximately quadratic with temperature. Since the thermal conductivity of both theoretically dense zirconia and of air increase with temperature, the effective thermal conductivity of a zirconia powder would be expected to increase with increasing temperature. However, the thermal conductivities of theoretically dense magnesia and alumina both decrease with increasing temperature (over the range of temperature studied), and a priori argument would not necessarily predict that the effective thermal conductivities of these powders would increase with increasing temperature. The fact that their conductivities do increase with increasing

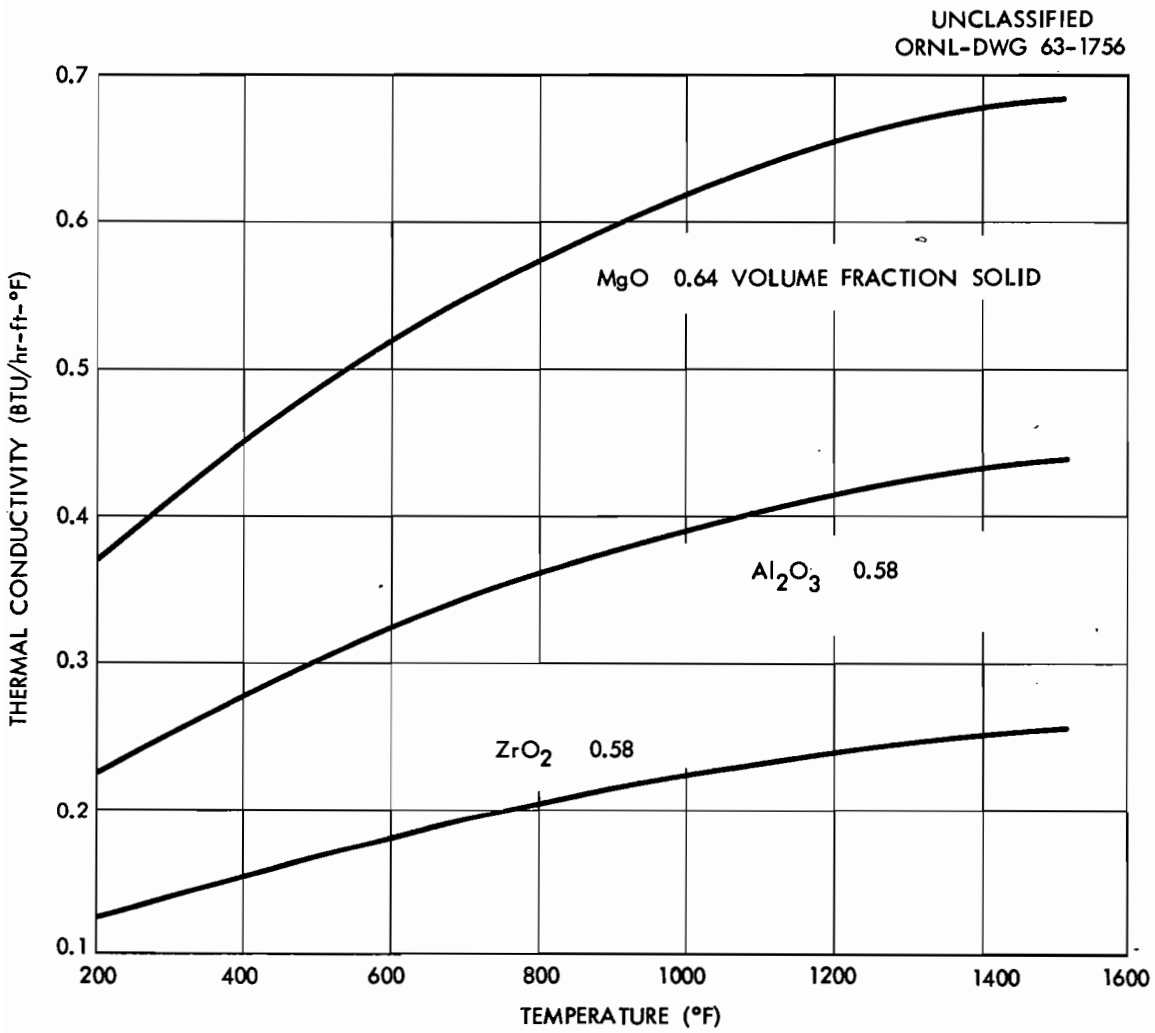

Fig. 5. Variation of Thermal Conductivity with Temperature for MgO, Al_2O_3, and ZrO_2 Powders in Air at Atmospheric Pressure.

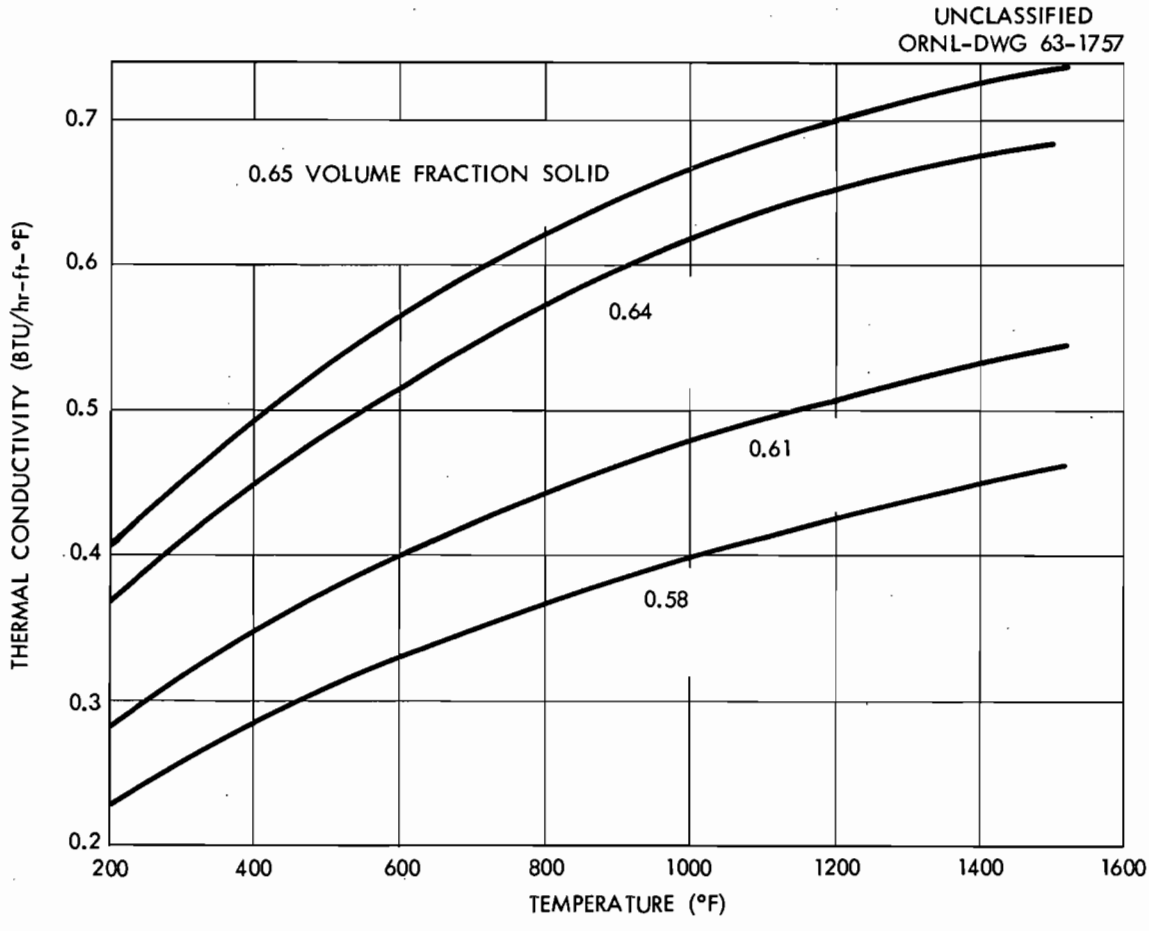

Fig. 6. Variation of Thermal Conductivity with Temperature with Volume Fraction Solid as a Parameter for a MgO Powder in Air at Atmospheric Pressure.

temperature means that the gas conductivity has more influence on the conductivity of the composite body than does the solid conductivity. This is an important qualitative observation, and has been recognized by numerous investigators in the past.

3. LOW-LEVEL-WASTE TREATMENT

Scavenging-precipitation-ion exchange and foam processes are being developed in both laboratory and pilot plant programs for decontaminating the large volumes of slightly contaminated water produced in nuclear installations. ORNL low-activity waste is used for this study. The ion-exchange process uses phenolic resins, as opposed to polystyrene resins, since the phenolic resins are much more selective for cesium in the presence of sodium at high pH; the cesium-sodium separation factor is 160 for phenolic groups and 1.5 for sulfonic groups. Other cations, for example, strontium and the rare earths, are also sorbed efficiently. Other ion exchangers, such as alumina, vermiculite, clinoptilolite, and organic anion resins are being studied as alternatives. The waste solution must be clarified prior to ion exchange because the resins do not remove colloids efficiently. Foam separation is being studied as an alternative to ion exchange after the clarification step and also as a method for both clarification and decontamination.

3.1 Pilot Plant Tests

Topical reports describing laboratory[6,7] and pilot plant[8] demonstration of the ORNL Scavenging-Precipitation Ion-Exchange process for decontamination of low level wastes have been issued. The pilot plant is being modified[4] to test (1) improved precipitation-flocculation equipment, (2) continuous ion exchange equipment with a strong acid cation resin, (3) batch ion exchange with a carboxylic acid cation resin column followed by a strong acid resin column, (4) alumina adsorption column for phosphate and ruthenium removal, and (5) foam separation equipment (see Sec 3.2.2).

3.2 Laboratory Development

R. R. Holcomb W. E. Clark

The scavenging-precipitation ion-exchange process[6-8] employs precipitation of calcium carbonate with sodium hydroxide at pH 11.7 as the headend treatment. Unless special precautions are taken,[9] the water becomes supersaturated with hardness salts and poor softening is obtained. The presence of phosphates in the waste stream hinders complete precipitation and tends to stabilize the supersaturation. Laboratory studies have been designed to describe and counteract the supersaturation effect and the detrimental effect of phosphates.

Treatment of the low-level waste stream with alumina, Al_2O_3, prior to precipitation softening with caustic (~0.01 $\underline{M}$ NaOH) reduced the phosphate concentration enough to allow nearly complete precipitation of hardness. Residual hardness exiting

the lab-model clarification system at the pilot plant increased from < 10 to 73 ppm within 24 hours after changing from tap water to low-level waste feed. Use of an anthracite filter on the discharge stream had no effect on residual hardness, indicating high phosphate (> 3 ppm) in the original waste. Pretreatment of the near neutral waste with alumina, upflow through a column of fluidized particles (80-200 mesh F-20 grade), reduced the hardness of the waste from 128 to 0 ppm for about one hour in addition to removing phosphate. After breakthrough of hardness on the alumina and recovery to 128 ppm hardness, the precipitation-softening step with caustic produced a steady state residual hardness of < 10 ppm rather than the 73 ppm experienced without the alumina pretreatment. In addition, the appearance of the floc was similar to that obtained with tap water. The alumina column containing about 400 g of Al_2O_3 was used for 260 hours of operation and treated 3900 liters of waste (8,666 column volumes). The residual hardness of the clarifier overflow stream fluctuated between 8 and 15 ppm during this period. The phosphate concentration of the untreated waste feed varied between 0.8 and 3 ppm and the effluent from the alumina column 0.2-0.5 ppm.

Elution of the alumina column with 1 M NaOH yielded a dark brown concentrate containing 4 μc of Ru^{106}. The efficiency of ruthenium removal is unknown since the experiment was optimized for phosphate removal. The alumina eluate also contained small amounts of cobalt, cerium, and protactinium. The combination of alumina pretreatment, caustic precipitation, and cation exchange may produce near complete decontamination for ruthenium, cobalt, and other anionic or complexed activities which were less efficiently removed previously.

In the laboratory, an anion-exchange resin, TAD-1, sorbed phosphate from 22 bed volumes of a 1000 ppm orthophosphate solution at pH 7 (Fig. 7), as compared to 10 bed volumes obtained on alumina with the same solution. More than 90% of the phosphate was eluted from the anion resin with about one bed volume of 1 M NaOH. Because of its superior loading and elution characteristics over the alumina, the anion resin is now being tested for sorption of activities from the ORNL waste stream.

3.3 Foam Separation

3.3.1 Chemical Development (W. Davis, Jr. E. Rubin,* E. Schonfeld,** A. H. Kibbey)

Two-Step Decontamination Process. Preliminary runs were conducted to test the 2-step process to decontaminate low-radioactivity-level process waste water. These steps involve (Fig. 8 removal of most of the calcium and magnesium in a sludge column followed by a foam separation column for removal of strontium. ORNL tap water, containing total hardness of about 100 ppm (as $CaCO_3$) and Sr^{85} tracer, was used as feed (Fig. 8). Calcium carbonate and magnesium hydroxide were precipitated by making the water 0.005 M in NaOH and Na_2CO_3 (pH = 11.3); iron (5 ppm Fe^{+3}) was used as coagulant. Flow rates in the sludge and foam columns were 20 and 60 gal ft^{-2} hr^{-1}, respectively. The foaming agent sodium dodecylbenzenesulfonate (NaDBS) was added to both the effluent from the sludge column (50 ppm) which was used as foam column feed, and to the bottom of the foam column (12 ppm).

*Radiation Applications, Inc., New York, N. Y.
**On loan to ORNL from Radiation Applications, Inc.

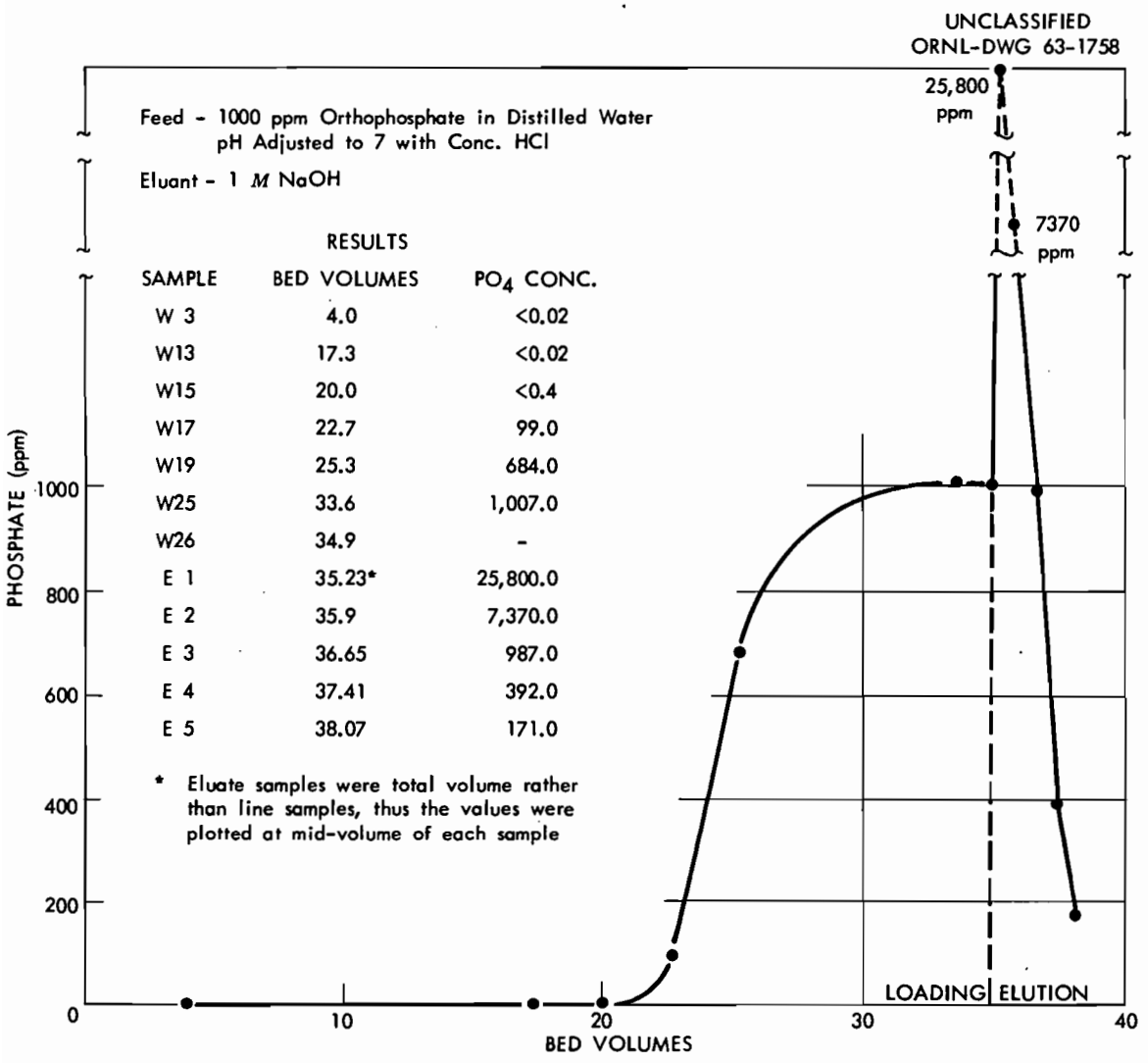

Fig. 7. Loading and Elution of Phosphate with TAD-1 Resin.

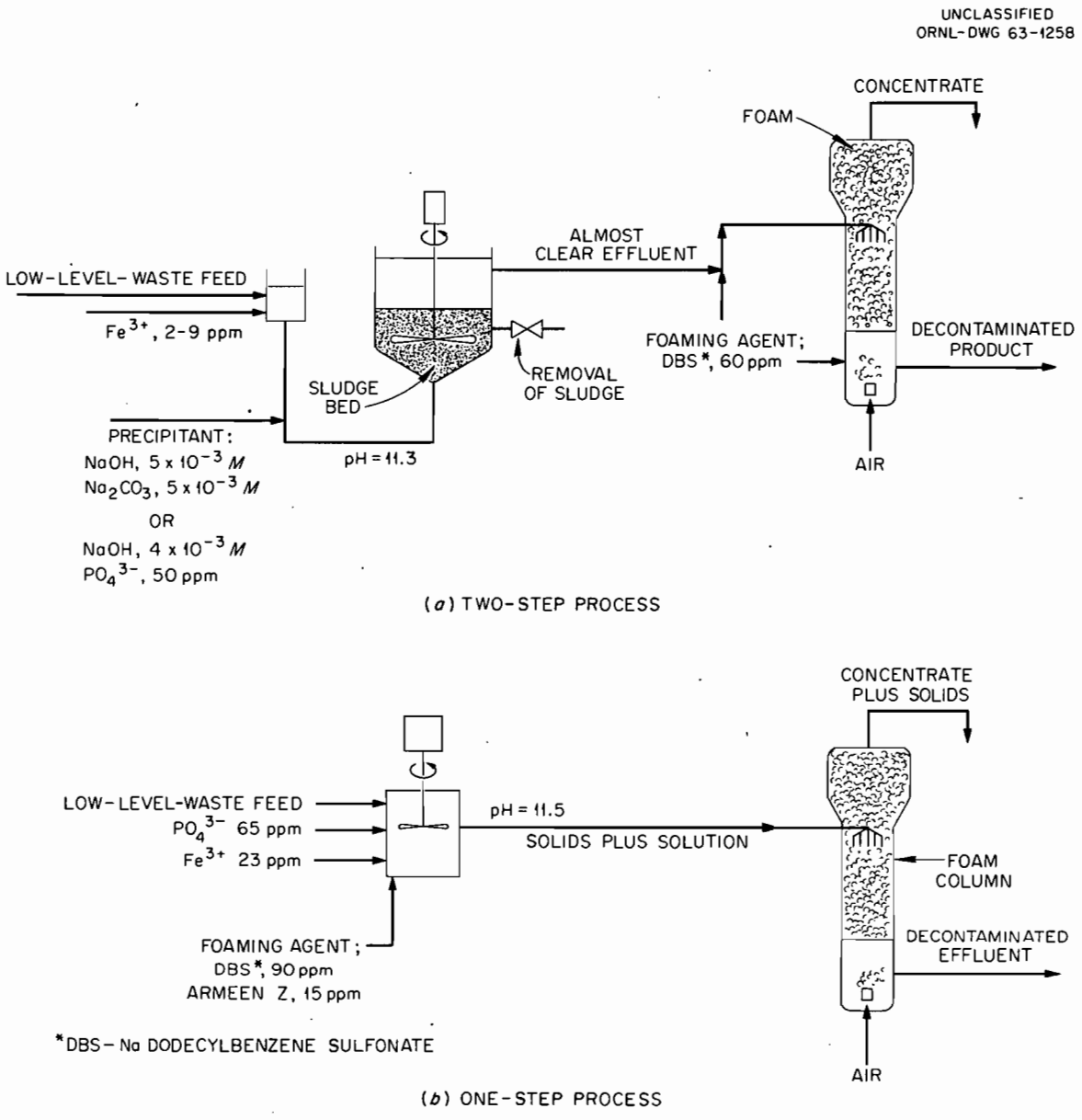

Fig. 8. The (A) Two-Step, Precipitation-Foam Separation and (B) One-Step Flotation-Foam Separation Processes.

Two 50-gallon batches of ORNL low-radioactivity-level process waste water were also used as feed to the 2-step decontamination unit. Neither of these batches was representative of normal waste water since they contained 2 to 5 ppm PO_4^{3-}. Values of $V_FL^{-1}D^{-1}$ were in the range 110 to 130 cm^{-1} and strontium decontamination factors in the foam column were 11 to 16. These two quantities are similar to those obtained with tap water (Table 15). Overall strontium decontamination factors were about 250. In addition, total phosphate was reduced in the sludge column from 2 to 5 in the feed to about 0.3 ppm in the effluent. No phosphate removal occurred in the foam column.

Future experiments will be performed at higher values of E', or $V_FL^{-1}D^{-1}$, to obtain higher decontamination of strontium in the foam column. This can be achieved by reducing the bubble diameter, which was in the range of 1.3 to 1.4 mm in the experiments summarized above, to about 0.8 mm.

One-Step Process.[11] Calcium phosphate precipitation is fast and is not inhibited by the polyphosphates or other phosphates and hence a simpler one-step process may be practical. Instead of using a large holdup up-flow sludge column as a precipitator, a small premixer-precipitator is used, and the feed to the foam column consists of solution containing suspended solids (Fig. 8). Experiments with this process were conducted using a synthetic waste water of the following composition:

$MgCl_2 \cdot 6H_2O$	58.5 ppm
$NaHCO_3$	28.5 ppm
$CaCl_2 \cdot 2H_2O$	98.5 ppm
Sr^{2+}	10^{-6} M
pH	7
Sr^{85} tracer	$\sim 10^{-10}$ M

Approximately 67 ppm of PO_4^{3-}, 23 ppm of Fe^{2+}, 90 ppm of foaming agent Siponate DS-10, 15 ppm of the flotation agent Armeen Z were added and the pH adjusted to 11.5 with sodium hydroxide. The solution and the precipitate that was formed after the pH adjustment and during the holdup of 10 to 20 min in the premixer, were fed continuously into a 2-in.-diam multistage foam separation column. The liquid feed throughput was 30 gal ft^{-2} hr^{-1}, and the gas to liquid feed ratio for the best decontamination factor for strontium was 12.4. Under these conditions, a strontium decontamination factor in excess of 1000 was achieved. The decontamination factor increased as the gas-to-liquid ratio and as the height of the foam column below the feed distributor were increased. Initial tests of the one-step process with ORNL process waste water gave strontium decontamination factors of 200 to 300.

Bacterial Degradation of Dodecylbenzenesulfonate. No degradation of a dodecylbenzenesulfonate (DBS added as Trepolate F-98) by bacteria existing in ORNL low-radioactivity-level process waste water was noted after 9 days, but 60 to 65% degradation

occurred after 2 to 3 weeks. On the other hand, the alkylbenzenesulfonate (ABS, primarily from Fab) originally present in the pond water, 0.30 to 0.35 ppm, showed only 20% and the ABS in Fab added to the waste water in special experiments, only 25 to 30% degradation during the same period, indicating considerable stability against bacterial attack. In a control solution made with demineralized water containing only DBS, no degradation occurred after 3 weeks. Trepolate F-95, a branched-chain DBS compound, was used to adjust the test solutions to 1.5 mg DBS per liter, except for one sample in which 5 ppm of commercial Fab detergent (about 34% ABS) was used. The waste water itself, as sampled from the pond, showed no significant difference in ABS concentration between filtered and unfiltered specimens. The presence of 1.5 ppm of sodium hexametaphosphate had no effect on either ABS or DBS degradation. The phosphate, however, was completely converted from soluble to insoluble form, presumably due to algae in the process waste water specimen.

3.3.2 Engineering Development (P. A. Haas)

Engineering problems studied included scaleup of liquid feed distributors and foam breakers, and studies of foam drainage and surfactant recovery.

Liquid Feed Distributors. A 24-in.-diam foam column was operated with feed introduced through 19 tubes in a 5-in. triangular spacing. The approximately 0.21-in.-ID tubes were fed from a common liquid reservoir through 3-in. lengths of 0.083-in.-ID tubes as flow control orifices. Visible channeling was observed for tubes positioned at distances up to 2-1/2 inches from the column wall. Channeling persisted for 18 to 30 inches below the tube ends for 40 gal hr^{-1} ft^{-2} and 10 to 22 in. for 15 gal hr^{-1} ft^{-2}. The flow appeared to be uniformly divided among the 19 tubes except when siphoning caused a complete loss of liquid and flow from some tubes at low flow rates. Smaller orifices would have prevented this difficulty.

The use of screens across the column cross section below the liquid distributor was considered as a means of obtaining better feed distribution. First a 40 mesh screen was supported about 8 in. below the liquid feed point in the 24-in.-diam column. Nearly all the liquid flow and much of the foam flow appeared to bypass the screen through the small gap (0 to 1/16 in.) between the screen and the column wall. A 20 mesh screen was then installed with a rubber ring to seal the screen to the wall. No channeling was visible below the screen while 10 to 30 inches of channeling below the feed point was visible at the same flows without the screen. Large bubbles or small voids appeared in the foam during passage through the screen and some accumulation of liquid on the screen was observed. A 20 mesh screen sealed between two gaskets at a joint were then used below the single tube liquid distributor in the 6-in.-diam column. Liquid accumulated on the screen and "dumped" through at irregular intervals (10 to 40 seconds were common) to cause very severe channeling. It is probable that the same type of "dumping" occurred in the interior of the 24-in. column where the screen had several slight depressions. The only visual evidence of "dumping" in the 24-in. column was slight variations in the levels of accumulated liquid on the screen at the column walls.

The important factor in the evaluation of the foam column is the extraction factor, E', defined, as in solvent extraction, by the relation

$$E' = \frac{\text{mass of component in the extracting phase (foam)}}{\text{mass of component in the extracted phase (foam column raffinate)}} .$$

The larger the value of E', the higher the decontamination obtained. Since the exact value of E' was not known, a value proportional to it was used, namely, $V_F L^{-1} D^{-1}$ where V_F is the foam rate in ml min^{-1}, L is the feed rate in ml min^{-1} and D is the bubble diameter in cm. Results of the present experiments in terms of this flow group and decontamination factors are given in Table 15.

Table 15. Results of Preliminary Tests of the 2-Step Decontamination Process

$V_F L^{-1} D^{-1}$ (cm^{-1})	Strontium DF Across Foam Column	Strontium DF Overall
108	2	320
110	6	1000
135	12	3700
135	20	1200
175	>100	>15000
178	>400	>15000

Based on a value of Γ/x for strontium of about 2×10^{-3} cm^{-1} from single stage experiments, the rapid increase of decontamination factor (Table 15) with $V_F L^{-1} D^{-1}$ can be used to show that there were about 10 stages in the 12 inches of foam height of these experiments. The strontium decontamination factor in the precipitation step was in excess of 10^2.

Removal of calcium and magnesium in the sludge column was checked closely, since these elements can interfere in the strontium removal.[10] The feed contained about 65 ppm of calcium and 35 ppm of magnesium as $CaCO_3$. The total hardness was 2 to 5 ppm after the precipitation step, with approximately equal amounts of calcium and magnesium. Raffinate from the foam column contained no detectable calcium, whereas the magnesium content of the raffinate was approximately equal to that of the feed to the foam column.

Drainage with Horizontal Foam Flow. A low density is desirable for the foam discharged from a foam separation column to obtain a high volume reduction, i.e., to obtain the separated surface active materials in a minimum volume of condensed foam. The usual procedure for increasing the volume reduction is to reduce the vertical foam velocity. Since high foam velocities tend to reduce channeling and reduce the column size, a countercurrent column is usually topped by a "drainage section" of larger diameter. Drainage appears to approach equilibrium after several feet of vertical "drainage section" and additional drainage at the same foam velocity occurs only because of loss of surface due to foam condensation. An equilibrium foam density would be expected from foam drainage models at the density where the downward liquid velocity with respect to the foam equals the bulk foam velocity upward.

Drainage in a channel with horizontal flow of foam would not be limited by this liquid-foam velocity equilibrium since the two flows would be at right angles to each other. Liquid would collect at the bottom of the horizontal channel where it could be drained off and returned to the column. The use of a larger diameter would not be necessary for such a horizontal drainage section. Since the maximum liquid drainage distance would be the channel diameter, a larger diameter might actually be less effective than the same volume of a smaller diameter.

Drainage with horizontal foam flow was measured experimentally in a 48-in. length of 6-in.-diam horizontal glass pipe as the drainage section for a short 6-in.-diam foam column (Fig. 9). The pipe was at about a 2° angle to the horizontal (with the foam exit at the low end) to insure collection of the drained liquid by a cross in the middle. The gas rate was set at a selected value and the pump set to recycle all the condensed foam and drained liquid.

The amount of drained liquid and condensed foam were measured under equilibrium conditions for gas rates of 1100 to 18,400 cc/min and for two surfactant concentrations. Good drainage was obtained and foam densities were below 6 mg/ml even at very high foam rates (Fig. 10). The lower curve shows the densities of the exit foam as determined by the condensed foam rate. The upper curve shows the foam densities into the horizontal section as indicated by the sum of the condensed foam and drained liquid rates. For comparison, the exit foam densities for about the same volumes of vertical drainage were 5 to 8 mg/ml for about 7 cm/min velocities in either a 6-in.-diam or 10.5-in.-diam drainage sections.

The foam densities entering and leaving the horizontal drainage section may be used to check foam drainage models. Either a capillary foam drainage or packed bed models as described in the literature adapted for capillary flow in the Plateau borders of foam indicate the following form of correlation where ϵ is small.*

$$L = k_1 d^2 \epsilon^2,$$

*Unpublished derivations of P. A. Haas.

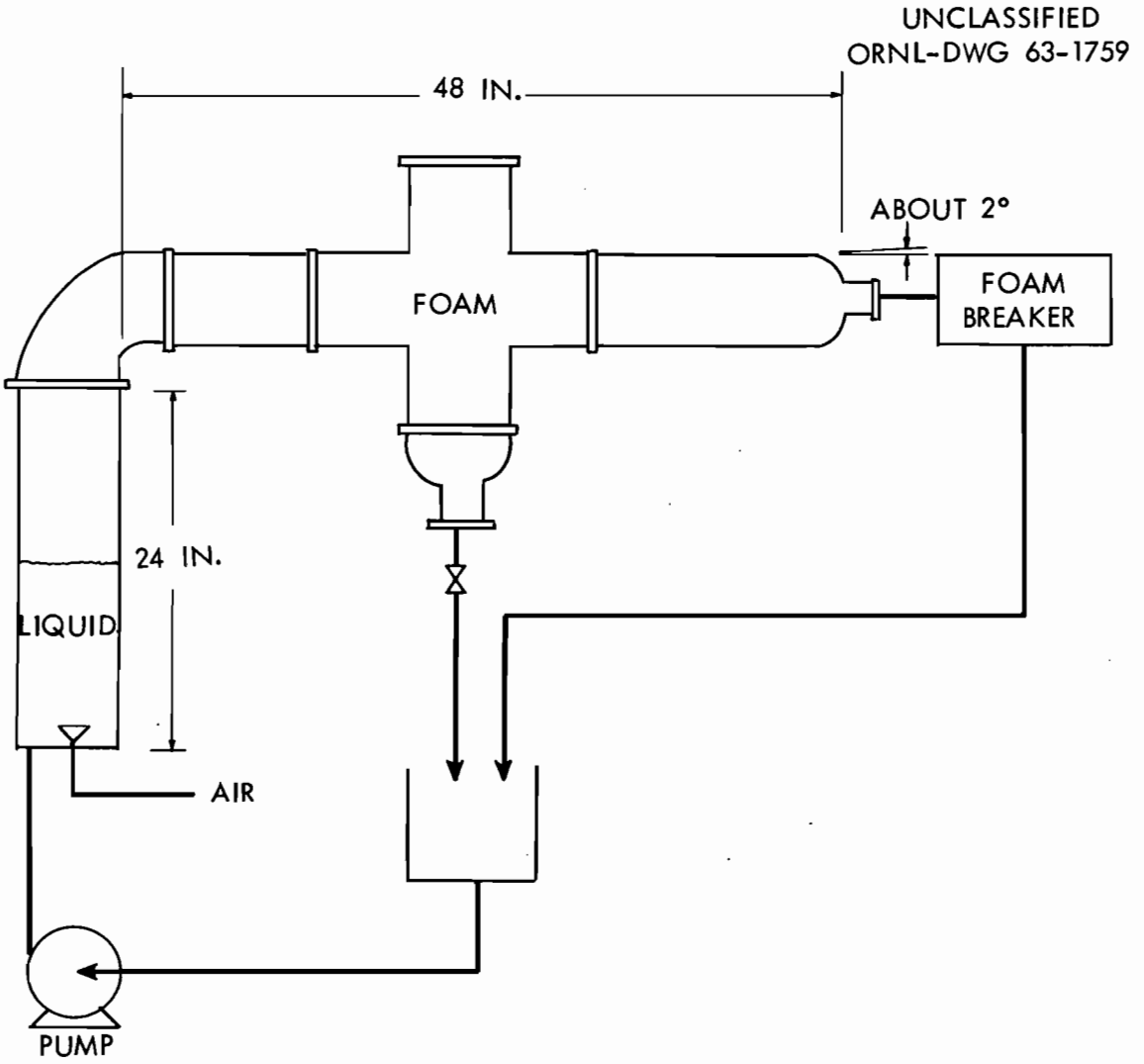

Fig. 9. Drainage Test Apparatus with Horizontal Foam Flow.

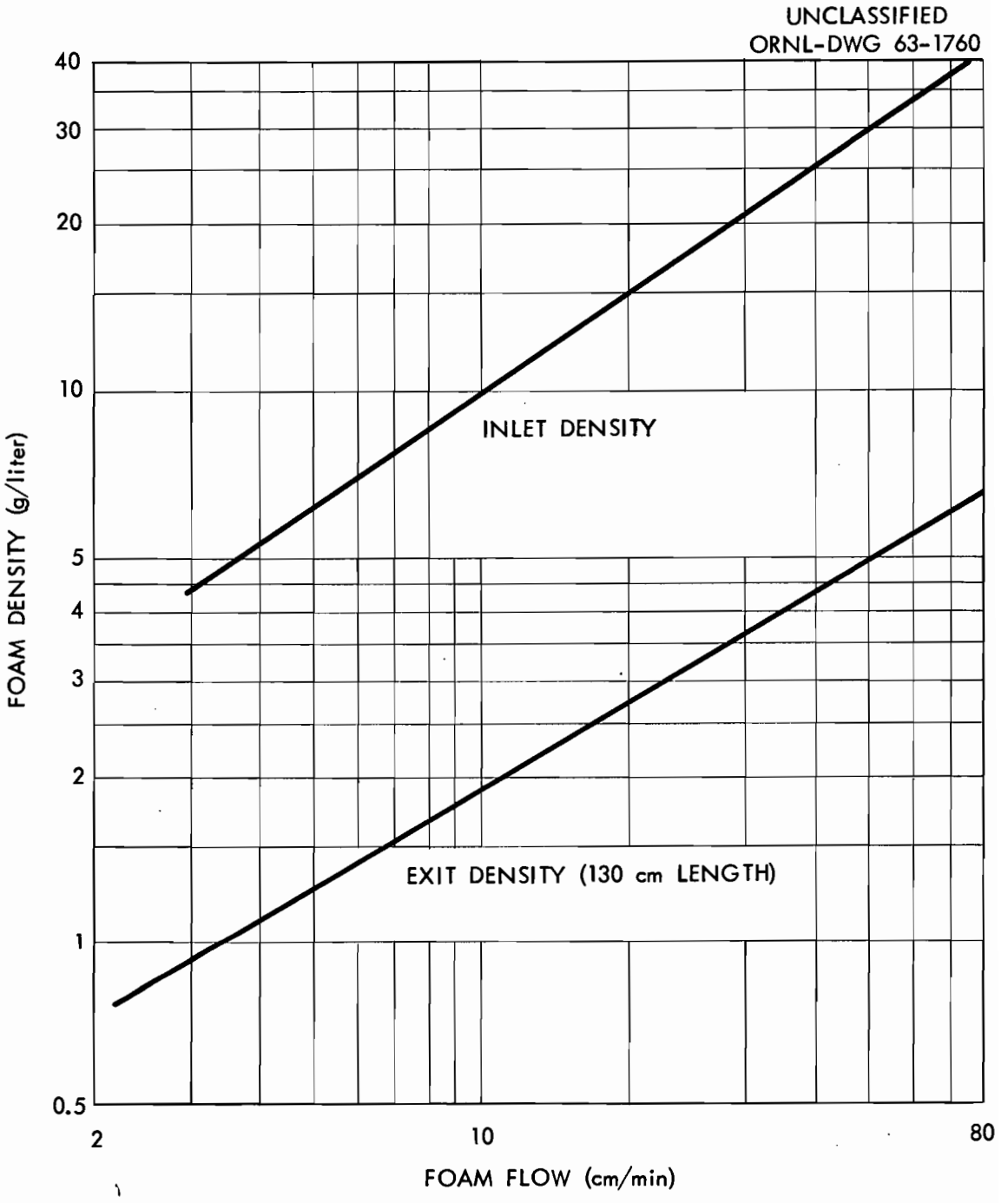

Fig. 10. Foam Densities for an Extra Coarse Fritted Glass Gas Sparger in a Horizontal Drainage Section.

where

L is the superficial liquid velocity,

d is the bubble diameter,

ϵ is the "void volume" or g liquid/cc foam,

k_1 is a constant.

In the horizontal drainage section the vertical foam velocity is zero and does not appear in the drainage correlation. The superficial liquid velocity, L, is a drainage velocity proportional to the rate of foam density change with time, t. Using a proportionality constant, k_2, which has the units cc foam/cm^2,

$$L = k_2 \frac{d\epsilon}{dt}.$$

Combining equations and constants $k_1/k_2 = k_3$, then

$$\frac{d}{dt} = k_3 d^2 \epsilon^2.$$

Integrating for a foam of specified bubble diameter and for $\epsilon = \epsilon_o$ at t = 0

$$\frac{1}{\epsilon} - \frac{1}{\epsilon_o} = k_3 d^2 t$$

The experimental data were used to calculate values for the constant, k_3 (Table 16). Values for ϵ_o and ϵ versus foam flow rates in cm/min were read from Fig. 10. The drainage time was calculated by dividing the 120-cm length by the foam velocity. The bubble diameters were the surface area average diameters, d_s, measured photographically as previously reported.* The values of k_3 were calculated from

$$k_3 = \frac{1}{td^2}\left(\frac{1}{\epsilon} - \frac{1}{\epsilon_o}\right)$$

The calculated values of 163 to 196 for k_3 with times of 72 to 1200 seconds, bubble diameters of 0.054 to 0.117 cm and densities of 0.032 to 0.0014 g/cc appear to provide a good check of the drainage model. The capillary flow models for foam drainage indicate that k_3 should be on the order of 50 for the 6-in.-ID drainage section. The bubble diameters are the same for 250, 275 or 400 ppm DBS at low gas flow rates. The bubble diameters were measured for only the 400 ppm concentration at rates above 50 cm/min. The breaks in the density versus foam flow rate curves at 60 to 80 cm/min (Fig. 10 appeared to be due to merging of bubbles at the gas sparger at these high flow rates. For the lower (250 ppm) concentration, this merging probably started at a lower

*Unit Operations Monthly Report, July 1962, ORNL-TM-343.

flow rate and was more pronounced. Therefore the true bubble diameter was probably larger than the 0.117 cm measured for 400 ppm; a value of 0.145 cm for d would have given k_3 in the range of the other values.

This model indicates several results of importance to applications of horizontal foam drainage. The wetness of the foam entering such a drainage section is of small importance for good drainage since $1/\epsilon_o$ becomes of little significance when $\epsilon_o >> \epsilon$. The total time in the horizontal drainage section is controlling while the foam velocity, which is the controlling variable in a vertical drainage section, does not appear directly. Since the surface area per cubic centimeter of foam is proportional to 1/d, the amount of liquid per square centimeter of area is given by

$$\frac{\epsilon}{a} \infty \frac{d}{d^2 t} = \frac{1}{dt} .$$

For a specified constant area rate, the volume rate is proportional to d and the time in the drainage section is proportional to 1/d. Thus the weight of liquid per unit of surface area is a constant independent of bubble diameter for a given horizontal drainage section volume and given surface area flow rate.

Sonic Foam Breakers. The generation of intense sound and its application in the destruction of foams have been described in technical literature.[12-14] Several mechanisms of foam breakage are involved. Intensities of 143-155 decibels are effective with a unidirectional radiation pressure effect predominant for frequencies above 2000 cycles/sec and acoustic pressure and bubble resonance phenomena are important at low frequencies. Air-operated sound generators of several types were used to destroy foam at rates of 0.20-0.36 cfm of foam per cfm of operating air supplied at 40 to 60 psi.[13]

Two air operated whistles were purchased* and used for foam condensation. The first unit was a Teknika Airjet Sonic Defoamer recommended for destroying foam over a 6- to 24-in-diam area. An air supply to deliver up to 15 scfm at 40 psig was specified to produce "highly intense sound at a frequency of 12,000 cycles per sec." This unit was used as the foam breaker for all the runs with Sr^{89} tracer. The unit was operated inside a 6-in.-ID Pyrex pipe vented to the hot off-gas system.

This unit condensed the foam for all flow rates used (0-12 liters/min, spinnerette and extra coarse fritted glass gas spargers). The foam came to within one inch of the whistle for some of the higher flow rates and small scraps of foam were carried out with the operating air. The foam from the fritted glass was more difficult to condense than foam at the same volume flow rates from the spinnerettes. Water or dilute acid discharged at 10 ml/min immediately below the whistle seem to cause more efficient foam breakage. This discharge of acid was necessary during runs with Sr^{89} in order to obtain reproducible condensed foam rates and gross β material balances. Evaporation of water from this added stream was 2.8 to 3.5 g/min. This evaporation rate was greater than the condensed foam rate for some conditions and the sonic foam breaker completely evaporated the water in the foam for some initial tests.

*From Teknika, Inc., Hartford 5, Conn.

The second unit was described as a Sonic Vortex Transducer of increased efficiency requiring 10 scfm of operating air at 40 psig. This unit, purchased as a package in a 6-in.-diam stainless steel tank, was tested with foam from extra coarse fritted glass gas spargers in the 24-in.-diam column. The capacity was about 24 liters/min for foam from 250 ppm Trepolate F-95, 0.01 N NaOH solution and 20 liters/min for foam from 500 ppm Trepolate F-95, 0.01 N NaOH solution.

Separation of the foam breaker and operating air from the foam by thin (0.001-0.002 in.) rubber or aluminum sheets was tested. The foam rose to the sheet surface (1/2 to 2 inches below the whistle) at flow rates where it would have been condensed at much lower positions if the sheets were absent. Most of the foam condensed near the sheets; some foam passed through the vent hole located at the sheet level. Thin plastic membranes are reported to decrease the sound outputs as much as 50%.[13]

If sonic foam breakers were used for low level waste decontamination, the cost of the operating air would be significant. The foam volume would be about 1000 cu ft/1000 gal of waste. Thus the operating air would be about 2×10^4 cu ft/1000 gal. Since the cost of 40 psig air would be on the order of 1¢/1000 cu ft, the foam breaker air operating cost would be about 20¢ per 1000 gal.

Recovery of Surfactant. A three-stage continuous surfactant recovery system (Fig. 11) was operated to verify the dependability of calculations and the advantages of multistage recovery. Liquid flowed in series through the three 2-in.-diam stages. The air flow was in parallel, one-third to each stage, and the foam streams were combined and condensed in a single centrifugal foam breaker. The air rate and liquid rate were set at selected values; then the pump rate and the vertical positions of the stages were adjusted to maintain the desired liquid levels. The initial surfactant concentrations were usually in the ratios 1:1:0.5:0.2 for the reservoir, first stage, second stage, and third stage, respectively. About two hours were allowed to reach equilibrium. The condensed foam rate was measured and the condensed foam and each stage were sampled.

The observed concentrations agree well with those calculated for $(\Gamma/x)_{DBS}$ equal to 7×10^{-4} cm (Table 17). The flow rates and the value of $(\Gamma/x)_{DBS}$ were used to calculate the ratios of the concentrations in each stage to those in the reservoir. The fractions of the total condensed foam from each stage was assumed from observations of the foam flows. The calculated concentrations tabulated are from these ratios with the total amount in agreement with the total amount indicated by analyses. For example, test C samples showed 99, 55, 17 and 158 ppm Trepolate F-95 in the 1st stage, 2nd stage, 3rd stage, and condensed foam, respectively. For a volume of 1 liter per stage and in the reservoir, these analyses show 308 mg present while 338 were added to the system by rough volume measurements. The calculated concentration ratios assuming theoretical stages are 1.0:0.75:0.45:0.16 for the reservoir, 1st stage, 2nd stage, and 3rd stage solutions. If 308 mg is present, these ratios indicate concentrations of 98, 58, 21 and 150 ppm for the 1st stage, 2nd stage, 3rd stage, and condensed foam solutions.

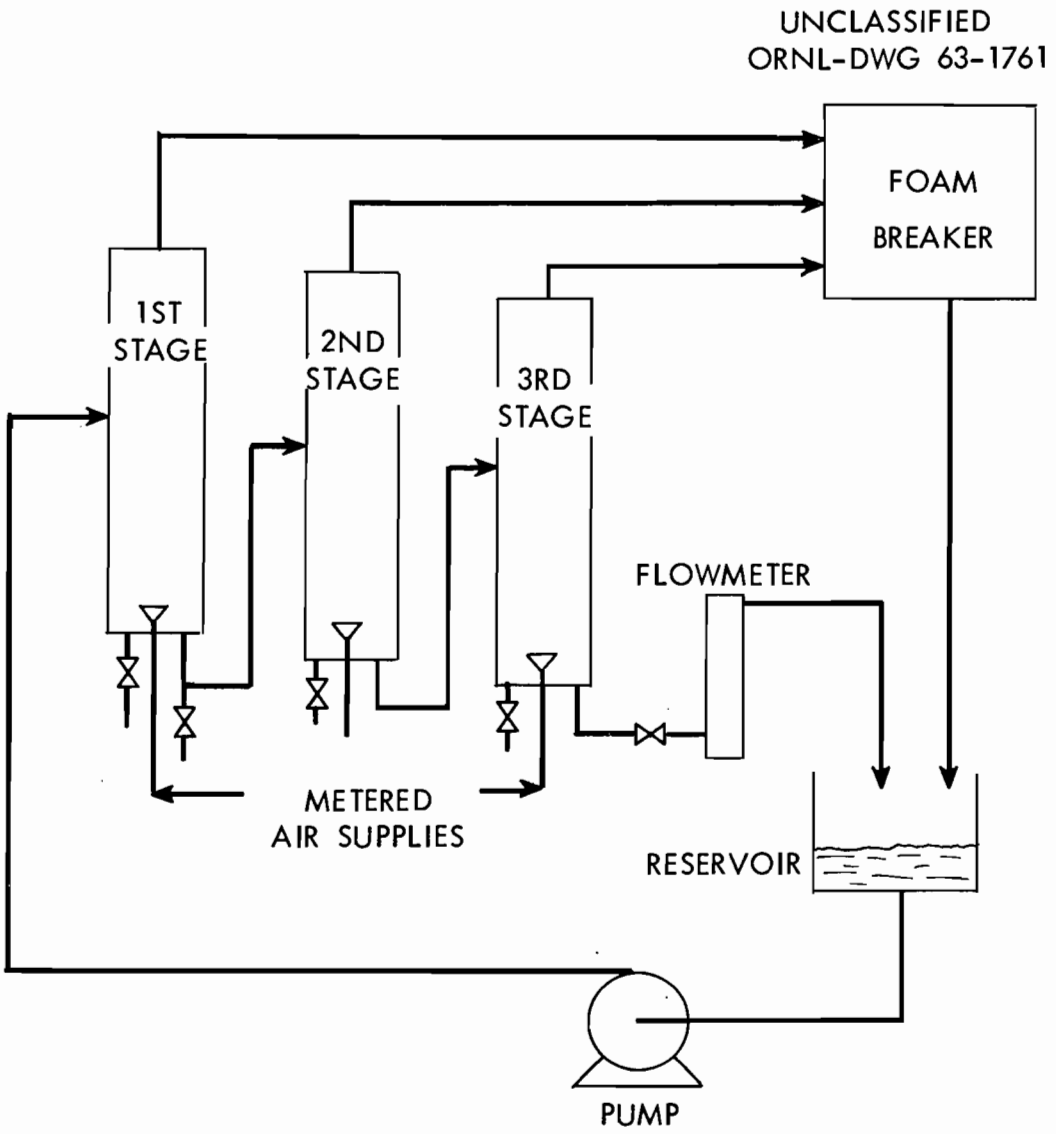

Fig. 11. Multistage Surfactant Recovery Test Apparatus.

Table 16. Comparison of a Foam Drainage Model and Experimental Results for a Horizontal Drainage Section

Drainage Section: 120 cm length, 6 in. ID horizontal pipe.
Gas Sparge: Extra coarse porosity fritted glass disc.

Foam Flow (cm/min)	Time, t (seconds)	t_o (g/cc)	t (g/cc)	Bubble diam;d (cm)	k_3
6	1200	.007	.0014	.054	163.
10	720	.010	.0019	.056	188.
20	360	.016	.0029	.063	196.
40	180	.026	.0043	0.76	186.
55	131	.032	.0052	.086	166.
100 (400 ppm)	72	.031	.0053	.117	170.
100 (250 ppm)	72	.018	.0029	.117*	290.

*Value experimentally measured for 400 ppm DBS only.

Proposed Design of Foam Columns for Decontamination of Low Level Waste. An equipment-process flowsheet was recommended for an ORNL low level waste (LLW) pilot plant (Fig. 12). Selection of the flowsheet represents a compromise between several partly conflicting requirements as follows:

(1) A high strontium decontamination factor should be obtained by use of the equivalent of multiple stage countercurrent contact and a favorable (high surface/liquid) flow ratio.

(2) A high volume reduction should be obtained by use of a low surface/liquid ratio and drainage to give a dry foam.

(3) The amounts of surfactant used should be minimized to minimize both the effluent and condensed foam disposal problems. A significant economic saving is also possible.

The surfactant concentration used will be the minimum which gives a stable foam throughout the column since reducing the surfactant concentration favors all three requirements. The concentrations must be high enough to avoid an unstable foam in the countercurrent region since the latter decreases strontium decontamination.

The conflicts between the listed requirements are best reconciled by using a two step flowsheet. The countercurrent column would be operated with a high enough surfactant concentration (30-125 ppm DBS) and the minimum surface/liquid ratio to

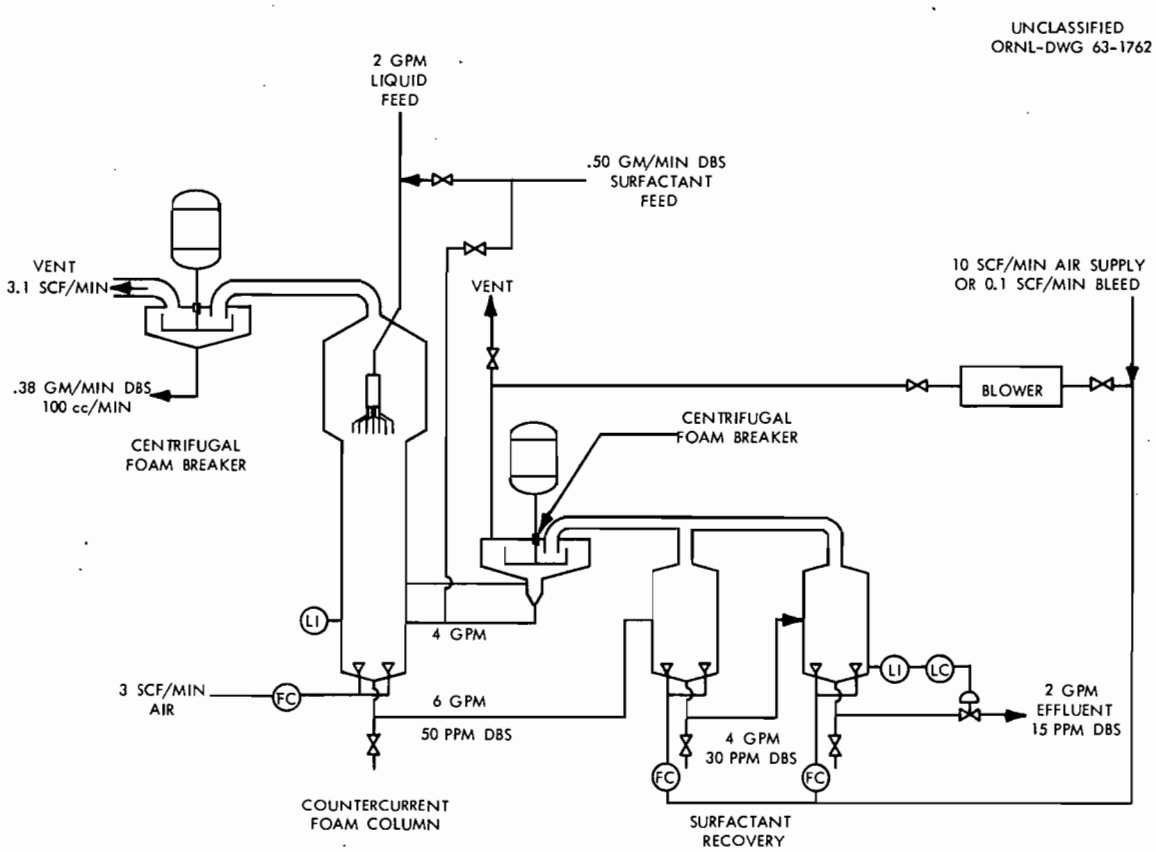

Fig. 12. Design of Foam Columns for Decontamination of Low Level Waste.

Table 17. Multistage Surfactant Recovery Tests

Volumes: 1 liter each stage and liquid reservoir

Quantity	Units	Test A	Test B	Test C	Test D	Test E
Liquid effluent, 3rd stage	cc/min	75	75	50	25	75
Gas rate per stage	cc/min	730	730	1400	1400	1000
Surface rate per stage	10^5 sq cm/min	1.1	1.1	1.6	1.6	1.35
Initial conc., 1st stage	ppm	250	125	125	125	125
2nd stage	ppm	125	63	63	63	63
3rd stage	ppm	50	25	25	25	25
reservoir	ppm	50	125	125	125	125
Total initial amount	mg	475	338	338	338	338
Condensed foam rate	g/min	60*	40	285	230	165
Measured conc., 1st stage	ppm	141	103	99	106	111
Measured conc., 2nd stage	ppm	92	32	55	46	79
Measured conc., 3rd stage	ppm	61	14	17	6	34
Measured conc., cond. foam	ppm	350*	340	158	125	171
Reservoir concentration	ppm	190	128	137	114	128
Total final amount	mg	484	277	308	272	352
Calculated conc., 1st stage	ppm	140	80	98	88	105
Calculated conc., 2nd stage	ppm	81	43	58	45	67
Calculated conc., 3rd stage	ppm	44	21	21	11	35
Calculated cond., cond. foam	ppm	435	343	150	139	196
Assumed cond. foam flow split**		50-30-20	60-35-5	60-35-5	60-35-5	50-30-20

*Estimated, not measured.

**Percent of total volume from each stage, based on appearance.

ensure good countercurrent stripping of strontium. Conservative gas/liquid volume ratios would be ~10 to give $(\Gamma/x)_{Sr}(V/L) = \sim 3$ depending on the average bubble size and the solution concentrations. The second step would be foaming with a very high surface/liquid ratio to favor the stripping of strontium and DBS with conditions which give low volume reduction and unstable foams. Since this second step would be without countercurrent flow and the condensed foam would be returned to the countercurrent column liquid pot, the poor foam stability and the low volume reduction are acceptable in this step.

The flow rates and concentrations listed are probable operating conditions; maximum flow rates for design purposes should probably be twice those shown in order to permit operation over a range of flows. The column diameter is limited to 24 in. to be certain that the clarifier capacity will be adequate to test the foam column fully. A six-foot countercurrent length and a two-foot liquid depth are recommended to give an eight foot total length of the 24-in.-diam for the countercurrent column. Two surfactant recovery stages of cross section area equal to 24-in. diameter and of about 36-in. total height appear desirable. The surfactant may be introduced with the liquid feed or into the countercurrent column liquid pot depending on the operating conditions.

The usual procedure for obtaining a large volume reduction is to use a large column cross section as a drainage section to give a low vertical foam velocity. A 24-in. height of 48-in. diameter would be suitable for the LLW pilot plant foam column. A horizontal drainage section, as previously described, of 24-in. diameter and 96-in. length is recommended as an alternative.

Good distribution of the liquid feed in large columns has been obtained only by using orifices or capillary tubes to split the flow into equal streams which are introduced separately over the column cross section. One stream in columns of 2-in. diameter or smaller and seven streams in a 6-in.-diam column have been adequate at all flow rates. One tube in the 6-in.-diam column or 19 in a 24 in. diameter column have required about two feet of the countercurrent length before a uniform distribution is obtained at low flow rates (20 to 80 $gal/ft^{-2}/hr^{-1}$ and have not given acceptable distributions at higher flow rates. Therefore it appears that at least 30 and perhaps as many as 100 streams are needed for the 24-in.-diam column. A screen in the feed line should be provided to protect the orifices from plugging. The orifices and lines into the column should be arranged so the pressure drop through them exceeds the gravity head possible at all flows planned. This is necessary to avoid siphoning with flow through only part of the lines.

Either the equivalent of micrometallic porosity D sintered stainless steel or extra coarse porosity fritted glass should be good gas spargers for the second, or surfactant, recovery step. Since there is no countercurrent flow, uniform bubble size and good foam stability are not essential and the larger surface per unit volume of foam from these spargers is desirable. From present information, we should use spinnerettes for the countercurrent column. The spargers should be installed as a number of units distributed uniformly over the column cross section area. The sparger surfaces should be at an angle so that the liquid convection from the rising bubbles sweeps the bubbles away from the sparger surface.

Commercial centrifuges with screen-lined perforated bowls and a Teflon sheet lining the centrifuge case appear to be the most reasonable choices for the foam breakers. The literature on sonic defoaming report about 0.2 cu ft of foam condensed per cu ft of operating air and UNOP experimental results for the stable DBS foams have been more nearly 0.05 cu ft/cu ft. The sonic foam breakers for the 24-in. diam column and surfactant recovery system would cost several thousand dollars and require ~300 scf/min of air at 40 psig. The cyclone foam breaker did not work well for inlet/outlet pressure ratios of two or less. Therefore use of cyclones would require operation of a hot vacuum pump with the condensed foam collector at 5 psia or operation of the column at 30 psig.

Relatively small and low-speed commercial centrifuges should be completely satisfactory. Flow rates through a 120-mesh screen in a 4-in.-diam bowl were about 1 cu ft/sq ft min at 150 g's and 2.5 cu ft/sq ft min at 230 g's. From this, it appears that 12-in.- or 8-in.-diam centrifuges at 3500 rpm should have the required capacity. Centrifugal foam breaker capacities at higher centrifugal fields will be tested in the near future. The lines carrying foam to the foam breakers should be at least 3 in. ID.

4. ENGINEERING, ECONOMICS, AND SAFETY EVALUATION

4.1 Safety of Tank Storage of High-Level Liquid Wastes

L. C. Emerson

The atmospheric contamination problem resulting from an assumed accidental release of fission products from the hypothetical storage-tank site at ORNL has been completed. The results of this study will be used to estimate the radiation dose to the neighboring population, which may be expected under typical meteorological conditions following the assumed accidental release. The events leading to the release, as well as the type and magnitude of the release, are being considered in a separate phase of this study.

The results of this phase of the study are incorporated in machine programs which accept as input the meteorological parameters and the coordinates of the downwind positions of interest and produce, from this, the downwind ground concentrations. The programs are flexible in that they allow for a wide range of input parameters. The two general cases studied were: continuous release and an instantaneous release.

Although the radiation doses cannot be obtained until some data is available regarding the magnitude and conditions of the assumed release, some features of the study may be seen by assuming a release of a unit amount of activity. For the continuous-release accident, 1 curie/sec was assumed to be released to the atmosphere. The resulting downwind concentrations in microcuries per cubic centimeter at ground level are shown in Fig. 13. For this case typical daytime meteorological conditions were assumed. The wind direction chosen corresponds to the most frequent daytime

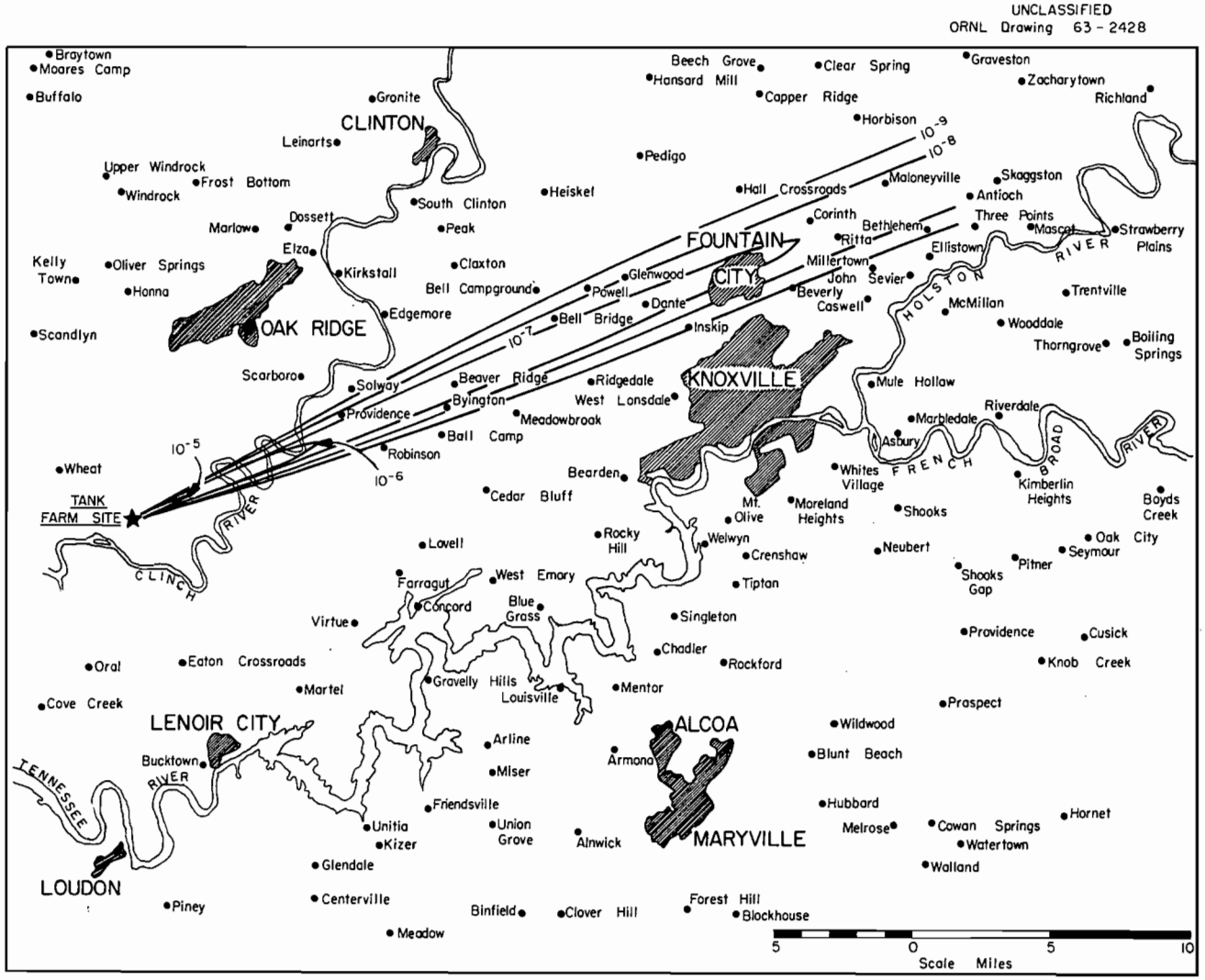

Fig. 13. Downwind Ground Concentration, Assuming a Continuous Unit Release Per Unit Time Under Typical Daytime Conditions.

direction for surface winds within the Southern Appalachian area. These concentrations do not take into account the removal of activity from the cloud by fallout or surface impaction. The patterns, in any real release, undoubtedly would be modified by the presence of the hill and valley type of terrain in the general vicinity of the hypothetical tank-farm site.

Typical results for the instantaneous release of one curie of activity at two downwind positions under daytime and nighttime weather conditions are presented in Figs. 14 and 15, respectively. The effects of a relatively stable atmosphere are seen in Fig. 15 in the form of a small, but more highly concentrated, radioactive cloud.

5. DISPOSAL IN DEEP WELLS

5.1 Mix Development for Hydrofracture

T. Tamura

5.1.1 Mix Evaluation at Halliburton Company

A waste-mix formulation for use with normal ORNL waste was developed by Westco Research of Dallas, Texas; this formulation appears to be usable over a wider range of waste concentrations than several earlier mixes. This mix was evaluated by the Halliburton Company, which is under subcontract to ORNL to aid in the planned waste injections. Their evaluation consisted of tests to establish the pumping time of the mix (which in recent tests at Westco Research had varied considerably from results obtained earlier), to measure the fluid loss under 1000-psi pressure (as well as 100 psi), and to measure the pumping time of the mix with contaminants such as tributyl phosphate (TBP) and kerosene and with varying caustic content.

The thickening time of the mix originally formulated by Westco Research is shown in Table 18 (slurry 1) to be 18 hr 18 min. This thickening time is very close to the later values of 20 hr reported by Westco. Fluid loss of the mix is 48 cc/30 min at 100 psi, and 96 cc/30 min at 1000 psi. To maintain the fluid loss of 60 cc, or less, at 1000 psi, the CMHEC concentration was increased from 0.5% to 0.8%. With a concentration of 0.8% CMHEC, tests were made to determine the effect of a new sample of Volunteer Cement from Knoxville, Tennessee, a new waste solution prepared with technical grade chemicals, and a new waste solution prepared by neutralizing acid with caustic. These tests (slurries 3, 8, 9, and 10) show that thickening time and fluid-loss characteristics were nearly the same in all cases. The thickening time of about 50 hr is well in excess of the 8-hr-pumping-time requirement, and the fluid loss of less than 18 cc at 100 psi is less than that for most mixes reported in the oil-well industry.[15]

Although long thickening times retard the setting of the mix for about 120 hr, the set grout shows excellent strength after curing 7 days and has a strength of over 3000 psi after 28 days.

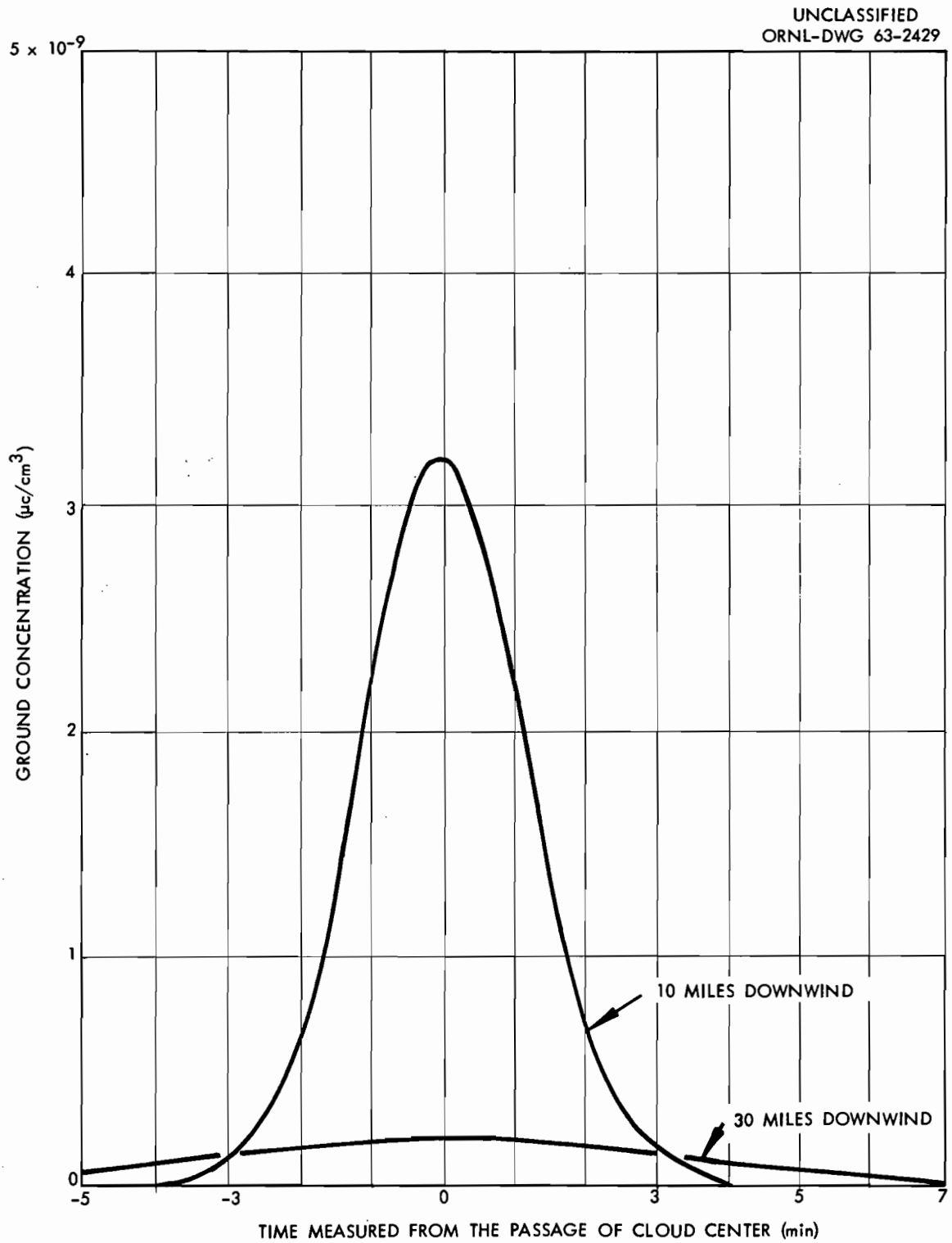

Fig. 14. Downwind Ground Concentration, Assuming an Instantaneous Release of Unit Amount under Typical Daytime Conditions.

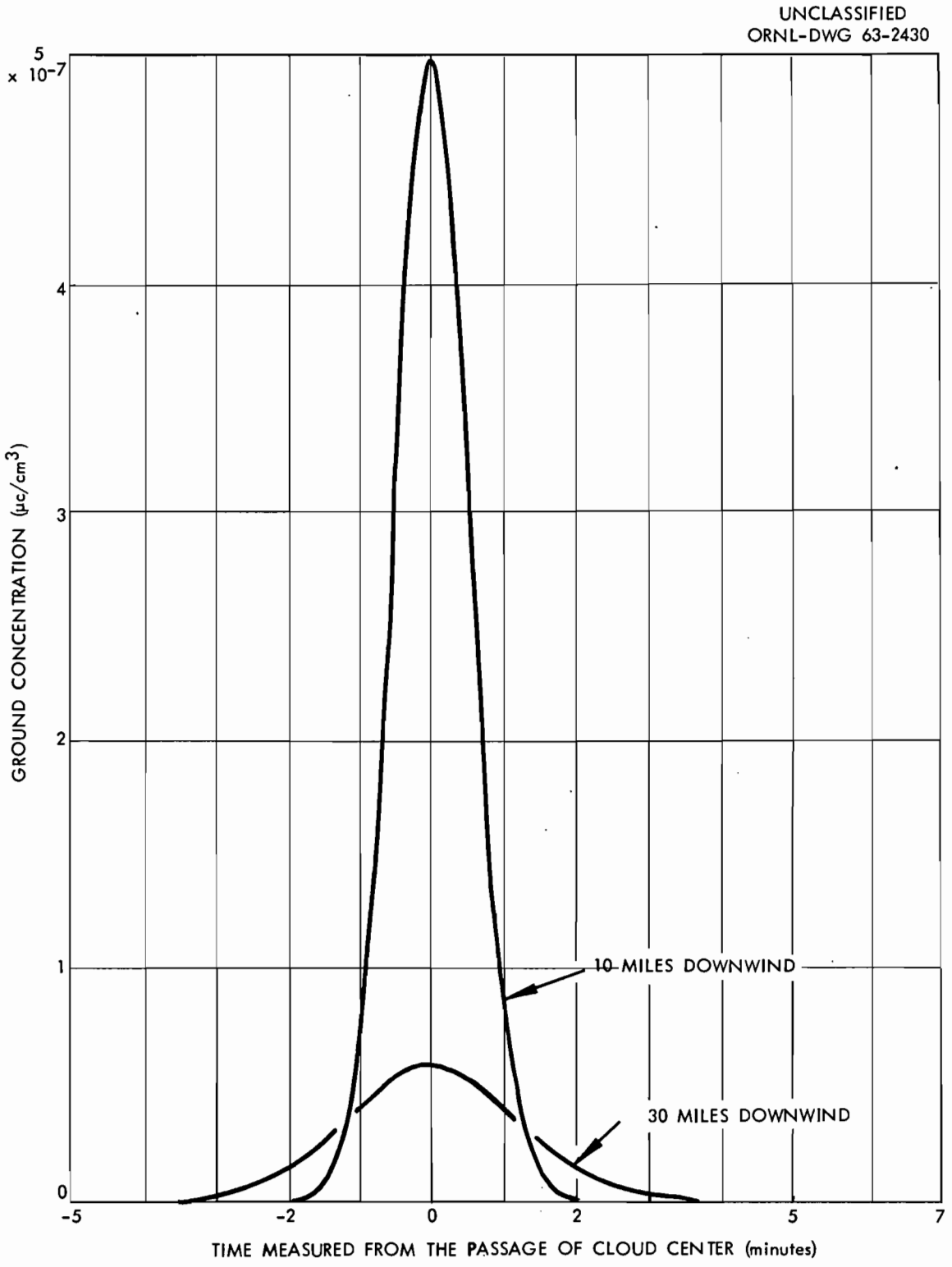

Fig. 15. Downwind Ground Concentration, Assuming an Instantaneous Release of Unit Amount under Typical Night Conditions.

Table 18. Characteristics of Waste-Cement Mixes Prepared with Normal Waste Composition and Various Additives

Basic Slurry Components
- Volunteer Cement, Knoxville, Tenn.
- Bentonite - 6% by weight of cement
- Silica Flour - 2% by weight of cement
- Calcium Lignosulfonate - 0.8% by weight of cement
- CMHEC - Variable - 0.5 and 0.8% by wt of cement

Normal Waste - 265 cc/pound of cement

Sodium Hydroxide	- Variable from basic	0.22 M
Sodium Nitrate	-	0.315 M
Sodium Sulfate	-	0.037 M
Sodium Chloride	-	0.006 M
Aluminum Nitrate	-	0.022 M
Ammonium Nitrate	-	0.025 M

Slurry No.	CMHEC (%)	NaOH (M)	Thickening Time 1000 ft (hr:min)	Fluid Loss (cc/30 min) psi 100	1000	Compressive Strength at 80°F (psi) 24 hr	48 hr	72 hr	96 hr	120 hr	7 Days		28 Days
1	0.5	0.22	18:18	48	96	n.s.[d]	n.s.	185	925	1565	2455	2835[a]	3700
2	0.5	0.55	9:46									1080[a]	
3	0.8	0.22	49:32[b]	16	56	n.s.	n.s.	n.s.	n.s.	120	1050	1275[a]	3440
			50:01[b]									2920[a]	
4	0.8	0.11	40:43[b]	17	48	n.s.	n.s.	15	125	520	1175	3630[a]	2400
5	0.8	0.33	31:49	12	48	n.s.	n.s.	195	805	1405	1790	2460[a]	2690
6	0.8	0.55	15:13	12	66	n.s.	75	690		1695	1810	2520[a]	2810
7	0.8	0.22+0.4% Na_2CO_3											
			30:15	12	44	n.s.	n.s.	n.s.	100	525	1795	3100[a]	3440
8	0.8	0.22 - Technical Grade Chemicals (Salts)											
			47:37	14	40	n.s.	n.s.	n.s.	75	320	1015	3635[a]	3590
9	0.8	0.22 - Acids Neutralized with NaOH - Technical Grade											
			57:08	14	56	n.s.	n.s.	n.s.	n.s.	40	540	3005[a]	3340
New Sample of Volunteer Cement													
10	0.8	0.22	49:15	18	54	n.s.	n.s.	n.s.	45	550	1345	3035[a]	3850
			48:43[b]									1555[a]	
11	0.8	0.55	14:36[b]									2265[a]	
12	0.8	0.55+0.4% Na_2CO_3											
			25:31[b]	12	48	n.s.	20	420		1755	2275	2915[a]	
			26:27[b]		32[c]							1410[a]	
13	0.8 CLS reduced to 0.5%												
		0.22	29:37[b]	16	56	n.s.	n.s.	32	110	305	1080	1290[a]	
14	0.8	0.22+0.1% of 85-15 Kerosene-Tributyl Phosphate											
			39:15[b]									2700[a]	
15	0.8	2.2 - 10X Concentration of Waste											
			14:57	6	30	10		795			1225		

[a]Strength of specimens prepared from slurry after thickening time test was completed.

[b]Synthetic waste solution prepared for each slurry sample. Other tests made using solution from common source.

[c]Fluid loss after slurry was stirred one hour at room temperature.

[d]n.s. = no set.

Earlier tests had indicated that variations in the sodium hydroxide content influenced thickening time considerably. Tests, therefore, were made with wastes having sodium hydroxide concentrations of 1/2 to 2-1/2 times the normal concentration. These test results are also shown in Table 18 (slurries 3, 4, 5, and 6). Reduced thickening times resulted when the caustic concentration was either increased or decreased from 0.22 M. The shortest thickening time of about 15 hr was observed with an 0.55 M NaOH concentration.

In general, compressive strength was related to thickening time. When thickening time was accelerated, by a variation in caustic content, compressive strength development started more quickly and strength remained higher at 7 days. The 28-day strength data indicate a lower ultimate strength potential, however.

It is anticipated that waste solutions may contain small quantities of organics, kerosene-TBP being the most likely contaminant. The addition of 0.1% of TBP (85% kerosene - 15% tributyl phosphate) to the waste reduced thickening time from about 50 to 39 hr (slurry 14). The effect of other contaminants in waste solutions was also studied. The addition of 0.4% Na_2CO_3 to a normal waste reduced thickening time to 30 hr (slurry 7). The presence of 0.4% Na_2CO_3 in a waste with 0.55 M NaOH resulted, however, in an increase in thickening time from 15 hr for the 0.55 M solution alone to 26 hr with the Na_2CO_3 present (slurries 11 and 12). Reduction in the calcium lignosulfonate (CLS) concentration from 0.8% to 0.5% also reduced the thickening time (slurry 13).

The thickening times were longer than the 8-hr minimum pumping time in all tests; even with waste solutions concentrated tenfold, the thickening time was 15 hr. At a concentration of 0.8% CMHEC, the fluid loss was below 60 cc/30 min at 1000 psi for all tests except when the sodium hydroxide was 0.55 M. All slurries lost their fluid properties within seven days and became solids with substantial strength.

5.1.2 Mix Evaluation at ORNL

A sample of ORNL's intermediate-level waste was obtained from the Operations Division. A portion of the sample was sent to the Analytical Chemistry Division for determination of the radionuclide and stable-element content. The results are shown in Table 19. The major sources of activity are Cs^{137} and Ru^{106}. The stable-element composition shows that the waste has a much lower $NaNO_3$ and NaOH content (by a factor of 5 to 10) than the synthetic waste that has been formulated for preparing mixes. Obviously, the composition of ORNL's intermediate-level waste changes considerably with time.

A slurry was prepared as follows: 1 lb of cement per 265 cc of the above waste, 6% (of weight of cement) bentonite, 0.5% CMHEC, 0.8% calcium lignosulfonate. The fluid loss was 30 cc/30 min at 100 psi, compared with 48 cc/30 min when synthetic waste with the previously accepted standard $NaNO_3$ and NaOH concentrations was used. The filtrate from the fluid-loss test of the actual waste was analyzed for its

Table 19. Composition of ORNL Waste and of the Filtrate from Fluid Loss Test

Radiochemical Components			Stable-Chemical Components			
Radionuclide	Waste Concentration (dis/min/ml)	Analysis of Fluid Lost from Slurry (dis/min/ml)	Ion	Concentration (N)	Ion	Concentration (ppm)
Sr^{90}	6.34×10^3	440	Na^+	0.10	Fe	<1.0
Cs^{137}	1.44×10^6	5.55×10^4	OH^-	0.04	Cu	<1
Ru^{106}	1.84×10^6	4.04×10^5	NO_3^-	0.029	Mg	<10
Ce^{144}	6.54×10^3	180	CO_3^{2-}	<0.001	Ca	<1
Co^{60}	1.3×10^3	1.0×10^3	SO_4^{2-}	0.001	K	15
$Zr\text{-}Nb^{95}$	780	206	SO_3^{2-}	0.0005		
Gross β[a]	3.0×10^5	2.06×10^4	Cl^-	<0.001		
Gross γ[a]	4.4×10^5	25.01×10^4	Al^{3+}	0.003		

[a]Counts/min/ml.

radionuclide content. The results are shown in Table 19. Gross gamma activity per milliliter in the filtrate is reduced by 89%. The concentration of Sr^{90}, Cs^{137}, and Ce^{144} in the fluid that separated from the grout was less than 10% of that in the original waste. Ruthenium-106 and Zr-Nb^{95} were not retained as well; and the concentration of Co^{60} was only about 20% lower in the separated liquid. The major contributor to the gross gamma activity was Ru^{106}.

After the fluid-loss test, the slurry was placed in a mold (2 x 2 x 2 in.) and cured for five days at 80°F. After curing, the cement specimen was placed on a Nichrome wire stand in a bottle and immersed in 500 cc of demineralized water. The water was stirred with a magnetic stirrer, and a 1-ml aliquot was periodically removed and counted in a well-type scintillation counter. The activity buildup in the water is shown in Fig. 16. After 408 hr of leaching, the solution was scanned with a 512-channel analyzer, and the radionuclides identified were Cs^{137} and Co^{60}. The highest count rate recorded corresponds to a loss of about 7% of the Cs^{137} from the original waste solution.

Ruthenium was the major nuclide detected in the filtrate from the fluid-loss test, but it was not detected in the water used to leach the set grout. Cobalt appears to be difficult to "tie-up" in this system, as evidenced by its presence in both the fluid-loss filtrate and the leaching solution. The amount of cesium detected in the leach water, assuming the activity to be due entirely to this element, is slightly higher than the observed activity noted when simulated waste tagged with cesium was used. A possible reason for the higher leachability of actual waste may be the presence of 15 ppm of potassium in the waste solution which competed with trace cesium for exchange sites on the bentonite. Further tests are being conducted on slurries prepared with ORNL waste.

5.2 Design of Hydrofracturing Pilot Plant

H. O. Weeren

5.2.1 Waste Transfer Line

The new waste line that will connect the existing Melton Valley waste-transfer system with the hydrofracturing pilot plant will have a run of a little over 1000 ft and a net change in elevation of 60 ft. The line crosses White Oak Creek above the gaging station at the mouth of the creek. There will be a low section of the line, about 500 ft long, where the line must cross White Oak Creek and an adjacent swampy lowland. It is not deemed practical to run the waste line over White Oak Creek, because the elevation of the adjacent area is so near that of the creek that the line would have to be run above ground across this area, and the problems of protection and support would become formidable. The waste line will, therefore, be run under the creek and ditched across the adjacent lowland. This section of the waste line will be made of welded carbon steel, welding being specified because of the greater strength of the welded joint and the likelihood that an underground line in the swampy area would be subjected to considerable stresses by local earth movement. The rest of the waste line will be cast iron, with mechanical joints. This type of construction is the same as

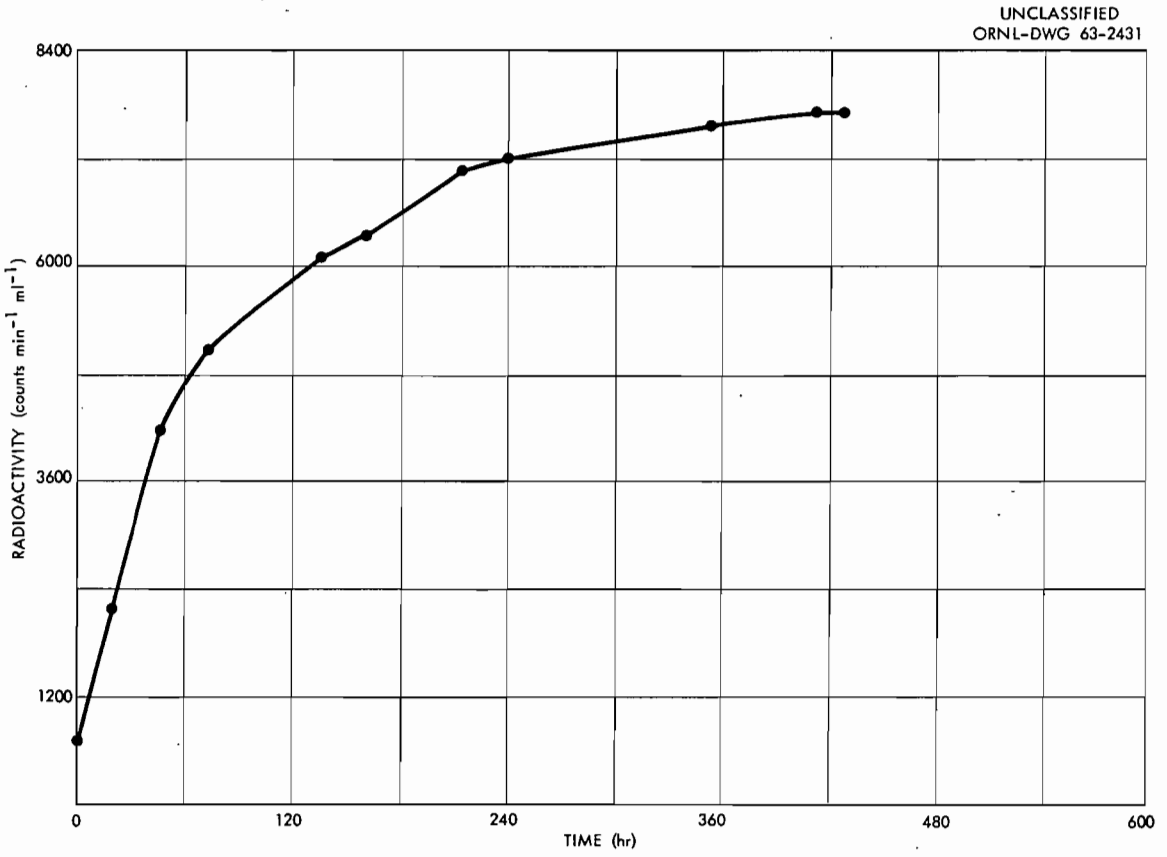

Fig. 16. Activity Build-up in Water by Leaching 5-Day-Cured Grout.

that used in most of the existing waste-transfer system; it has a working pressure rating of 150 psi and is regularly tested at 70 psi prior to use.

It is thought possible (but unlikely) that during a waste injection one of the waste storage tanks may develop a leak at a time when the other tanks are full. Should that happen, it would be desirable to empty the leaky tank as quickly as possible by using the waste-transfer pump in the hydrofracturing pilot plant to pump waste from the leaky tank back through the transfer line to waste trench 7. Valving at the pump is so arranged that this can be done readily. An 80-psi pressure-relief valve is installed at the pump so that the plastic section of the existing waste-transfer line will not be overpressurized if a valve is inadvertently left closed. This arrangement will also make possible the pressure testing of that part of the waste-transfer line that crosses White Oak Creek prior to each transfer.

5.2.2 Waste Storage Tanks

The three waste storage tanks have been installed underground in a pit partially filled with crushed rock. Concrete-block walls were used to segregate possible leakage from a tank. Dry wells were installed near each tank so that samples of the water (if any) in the crushed rock below each tank can be obtained. A drain for ground water is provided; this will empty on the ground at some point between the waste storage tanks and the bed of White Oak Creek. The level of ground water around the waste tanks indicates that this level is below that of the waste tanks.

Prior to each injection, the contents of the waste tanks will be stirred and sampled. The sample will be mixed with additives such as will be used in the injection so that pumping time and other pertinent characteristics of the waste-cement mix can be verified and adjusted if necessary. Agitation will be by means of air-lift spargers - four each in two of the tanks and two in the third tank, which is shorter. The calculated air flow rate for each sparger is 5 cfm. The air streams from each tank will be combined, passed through an absolute filter, and discharged to the atmosphere through a 3-in. pipe that extends 9 ft above ground level.

Mixing and Injection Facility. Detailed design of the mixing and injection equipment and the associated structure is well under way. Preliminary drawings of the mixer assembly, sump tub, valve rack, and air slide arrangement to the bulk storage tanks have been made.

5.3 Hydrofracture Well Construction

R. C. Sexton W. de Laguna

Drilling of the injection and observation wells was started in this quarter. The surface casing of the injection well was set and cemented; the 8-7/8-in. hole for the 5-1/2-in. casing was drilled to a depth of 668 ft. The surface casing of the observation well was set but not cemented; the 6-1/2-in. hole for the 2-7/8-in. tubing was drilled to a depth of 578 ft.

The well drillers arrived with a single drilling rig on March 11 and started drilling on March 12. Because of frequent cave-ins at shallow depths, they found it necessary to set a short string of 7-in. surface casing, drill a 6-1/4-in. hole to 150 ft, remove the surface casing and ream out the hole to a 12-in. diameter and a depth of 162 ft. They then installed 157 ft of 9-5/8-in. (36 lb/ft) surface casing.

The surface casing was cemented in by a Halliburton crew. They washed the hole (pumped water down the casing string and up the annulus between the casing and the hole), pumped in a grout of 80 sacks of Portland cement with 3% $CaCl_2$ and then displaced this grout with water. Although this quantity of grout was calculated to be 100% in excess of the amount needed, the grout failed to fill the annulus between the casing and the hole; the cement was filling voids in the formation somewhere. The level of the cement in the annulus was found to be 30 ft from the surface. The following day a 1-in. pipe was placed between the casing and the hole, and another 83 sacks of cement was pumped into the annulus. This closed off the hole.

After the grout had had time to set, drilling was recommenced and an 8-7/8-in. hole was drilled to 217 ft. The formation produced water at about 26 gpm, and it was decided that the water-bearing formation should be sealed off from the well before proceeding with the drilling.

The Halliburton crew pumped in a grout of 64 sacks of cement, 210 lb of bentonite, and 640 lb of gilsonite and then displaced this mixture with water. The pumping time was 9 min; shut-in pressure was 250 psi. Drilling was recommenced. At 260 ft another water-bearing formation was encountered; flow was greater than 30 gpm. A second "squeeze job" was performed. The Halliburton crew pumped in a grout of 64 sacks of cement, 105 lb of bentonite, and 400 lb of gilsonite, and followed this with a gilsonite-cement mixture, and then displaced the whole with water. Shut-in pressure was 700 psi.

It was decided at this point that the formation should be core drilled to 1080 ft to determine whether any more localized water pockets existed and to aid in interpreting the results of the waste injections. It was further decided, in view of the unexpected difficulties encountered with the injection well, that the surface casing of the observation well should be 200 ft long instead of the 100 ft originally planned.

The drilling rig was moved to the site of the observation well and drilling started there. A core drill was set up over the injection well, and two 20-ft cores were taken of the grout injected by Halliburton (which filled the bottom 130 ft of the hole). It was found at this point that the core hole was deviating from the path of the 8-7/8-in. hole. It was feared that the core hole would continue to deviate, that it could not be adequately plugged after completion, and that a channel to the surface would thus be provided for the escape of subsequent waste injections. Core drilling was, therefore, discontinued, it being decided that the desired information could be obtained subsequent to the waste injections by drilling one of the planned core holes close to the injection well. The heavy drilling rig was moved back to the injection well from the observation well, and drilling on the 8-7/8-in. hole was recommenced. A second rig was moved in to continue drilling the observation well.

In the observation well, a small flow of water (2 to 3 gpm) was noticed at 32 ft. A 10-in. hole was drilled to 297 ft, and the 7-in. surface casing was set (but not cemented). A gamma-ray log was made of both wells to check for possible seepage of radioactivity from the nearby burial grounds; no significant activity was found. Drilling was continued on the 6-1/4-in. hole.

5.3.1 Plant Construction (R. C. Sexton)

Installation of the waste tanks and waste pumps and their associated piping started April 1 and is about 80% complete. Construction on the waste transfer line was started April 22.

6. DISPOSAL IN NATURAL SALT FORMATIONS

6.1 Demonstration of the Disposal of Solid, High-Level Waste in Salt Mines

Work is underway on the design of a demonstration of the disposal of solid, high-level radioactive waste, solids to be carried out in the Lyons, Kansas, mine of the Carey Salt Company. Fourteen irradiated ETR fuel assemblies contained in seven cans will serve as a source of radiation in lieu of actual solidified wastes. The assemblies will be placed in a circular array of holes in the floor, with one can in the center and the other six cans located peripherally, with the cans spaced 5 ft on centers. The duration of the test will be two years, and, at the end of that time, all fuel assemblies will be returned to ICPP for recovery of the unfissioned fuel.

An identical array, with electrical heaters only, will be operated as a control to help determine the effect of radiation and heat on the salt.

The objectives are: (1) to demonstrate the handling equipment and procedure; (2) to determine the possible gross effects of radiation on hole closure, floor uplift, salt-shattering temperature, etc., in an area where salt temperatures are in the range of 100° to 200°C; and (3) to determine the possible radiolytic production of chlorine.

Information obtained on the creep and plastic flow of salt at these temperatures will be used later in the design of an actual disposal facility.

A schematic cross section of the demonstration is shown in Fig. 17. The plot plan of the demonstration site is shown in Fig. 18. As presently conceived, the assemblies, after canning in Idaho, would be shipped by rail in an existing cask, modified for the purpose. At Lyons, the cask would be removed from a rail car standing on an existing spur, and up-ended over a cased, vertical shaft extending to the mine working area, about 1000 ft below. The assemblies would be lowered, one at a time, through the shaft and into a shielded cask mounted on a fuel assembly transporter which permits vertical, as well as horizontal, movement of the cask on the transporter. The transporter would move to the experimental area where the cask would be positioned and lowered over the designated hole in the floor of the mine. The can would then be

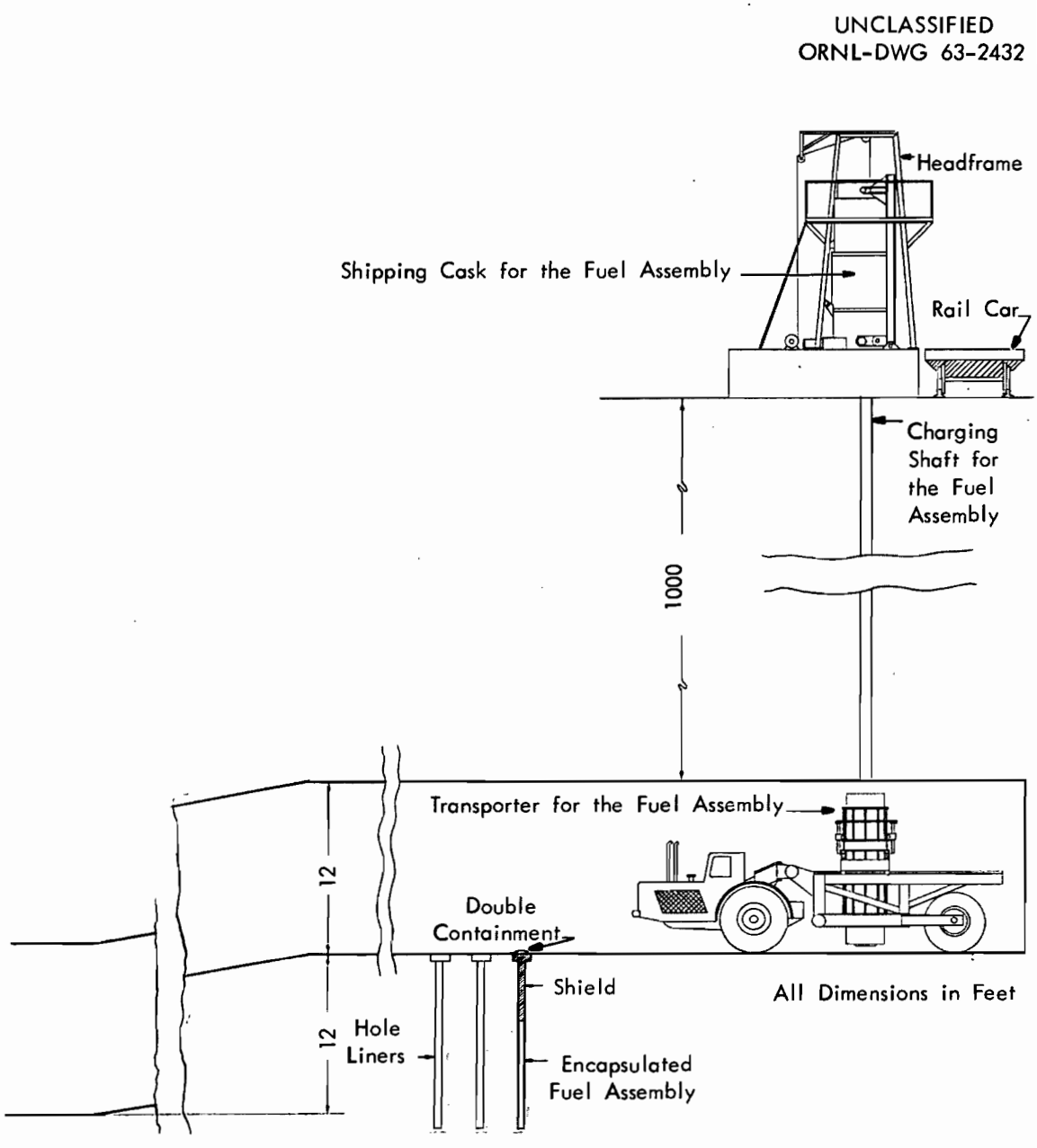

Fig. 17. Demonstration Site in Newly Mined Area, Lyons, Kansas.

UNCLASSIFIED
ORNL-DWG 63-2433

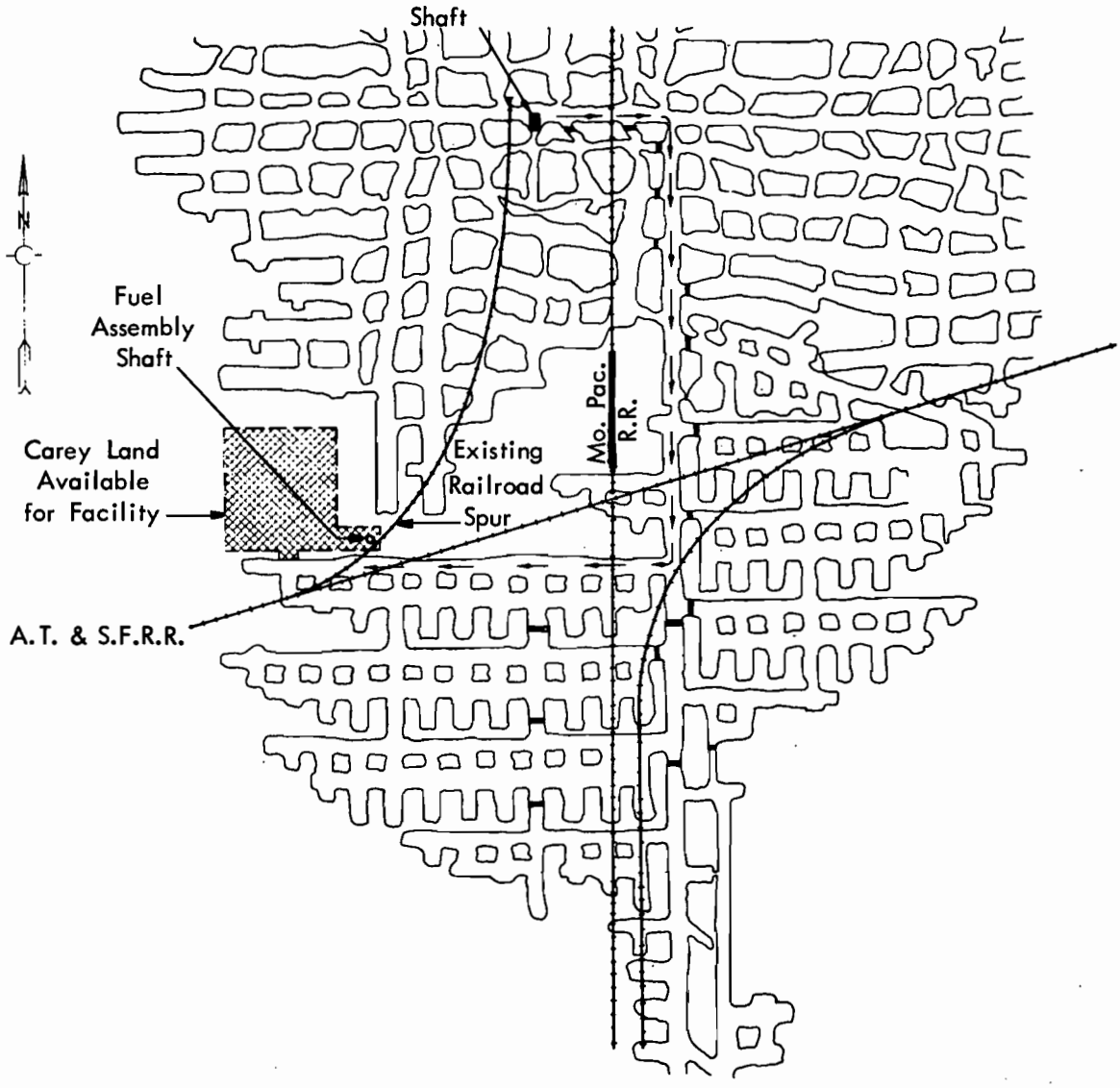

Fig. 18. Plot Plan of Demonstration Site.

lowered through the bottom of the cask into place. The holes, about 10 in. in diameter and 12 ft deep, would have stainless steel or aluminum liners. Lead shields placed in the top of each would serve as biological shielding while the cans were in place. The cans would be removed at the end of the experiment.

6.1.1 Fuel Element Selection (R. L. Bradshaw, J. J. Perona, and J. O. Blomeke)

The decision to use irradiated reactor fuel elements in this experiment, rather than actual calcined wastes or separated fission-product sources, was based on considerations of availability, cost, and radiation characteristics. The ETR fuel was selected after consideration of the operating cycle of the reactor, the number of elements required to charge seven holes in the demonstration, the dimensions of the elements, and their thermal properties. From the standpoint of thermal stability, power reactor elements would have been preferable; but uncertainties in availability led to the selection of the ETR fuel assembly as the best overall choice.

The ETR has an average thermal flux of about 2×10^{14} and a cycle time of about six weeks. A typical reactor cycle might average about 20 full-power days out of 23 operating days. The dimensions of the assembly are convenient, and the only major disadvantage (one which it shares with most test reactors) is that it is a relatively low-melting aluminum-base fuel.

The fact that the cladding is aluminum (m.p. 660°C) sets the minimum decay time at which the assembly can be canned for use in the hot demonstration. If the temperature of the assembly is to be kept below 475°C, the earliest it can be canned is about 60 days. This means that it will be 90-day decayed before it is placed in the salt mine.

The final salt-dose calculations have not yet been made, but, based on preliminary calculations, it appears that the peak salt dose with two 90-day-decayed ETR assemblies in a can will be about 3×10^8 rads. Since laboratory tests indicated little change in physical properties at 10^8 rads, but a significant (about 10%) drop in compressive strength at 5×10^8 rads, it is desirable to achieve doses near 10^9 rads in this experiment, if practical. Changing the assemblies three times during the course of the 2-year test (four sets of assemblies, total) should increase the peak dose to about 8×10^8 rads. At the same time, this will give additional experience with the operation of the handling equipment.

6.1.2 Experimental Layout in Mine (R. L. Bradshaw, J. J. Perona, and J. O. Blomeke)

Consideration of Use of Existing Mine Space. For an actual disposal operation in an abandoned mine, it would probably be cheaper to use existing mine space for the disposal of the waste rather than using it to store excess salt, provided that it could be shown that the use of existing space for disposal did not significantly reduce the safety of the operation. At present it is not possible to predict the structural safety of a mine in general or of the Lyons mine in particular, under temperature conditions that would prevail in a disposal operation. Further, in the Lyons mine, and in practically all bedded salt mines, there is considerable water-bearing shale in the floor. Corrosion data

indicate that stainless steel waste containers will corrode rapidly in the presence of salt and water, possibly to failure in a matter of a few months. (It would be possible to make calciner pots of a more resistant material, but this would result in prohibitive costs.) It is also reasonably certain, on the basis of experimental data, that water from the shale will migrate to the surface of the floor,[4] and that in all likelihood this water which has been in contact with the waste cans will contain some radioactivity.

In an actual operation it may be possible to cope with mine instability and water problems, but at this time it is not apparent what measures would have to be taken and thus what cost must be assessed for such measures.

If the fuel-assembly demonstration were run in the existing floor of the Lyons mine, some information could be obtained on the behavior of such an area if used for a disposal operation. However, to get any really meaningful information would require significant heating of at least one pillar, and, in view of the structural instabilities which have already manifested themselves in this mine, this could jeopardize the primary objectives of the demonstration. The water-induced corrosion could be handled by the use of highly corrosion-resistant materials for fuel-assembly containers, thermocouples, etc., but the additional cost would quite likely be as great as that involved in creating new space in the mine periphery where the fuel cans could be in pure salt. In theory it would be desirable to test the operation in the existing floor, but since it is felt that it would not be desirable to allow the fuel cans to corrode through (with the possible release of some fission-product gases even if no water vapor were to come in contact with the fuel assemblies), it does not appear that much additional information will be gained by operating in the existing floor. Some information would be gained, of course, on the migration of shale-borne water, but migration of such water to the floor surface has already been demonstrated in electrical-heater tests in the Hutchinson mine.

Another consideration involved is the choice of the particular mining pattern in the existing mine. The major portion of the mined area, while generally similar to the modified-checkerboard pattern in current use, really fits no repeating pattern, and, thus, it would be difficult to say that one had chosen a representative area in which to run the demonstration.

It was concluded by the salt-project staff that the hot demonstration should be run in the periphery of the mine, with the fuel cans being located in the relatively pure salt strata that had been mined originally, thus minimizing the water problem and also allowing the choice of a desirable experimental layout.

Alternative Layouts in Specially Mined Areas. Since the demonstration array of seven fuel-assembly cans is to be operated in the floor where stresses are minimized, the possibility of introducing stresses in the vicinity of the array by using flat jacks installed in the floor around the array or by jacking between floor and ceiling was considered. It was concluded that this method would not produce data that could be interpreted in terms of conditions that might prevail in an actual operation.

An experimental pattern was considered in which a central, square pillar would be surrounded by four arrays (the radioactive array, the nonradioactive array, and two simple heater arrays) and four additional square pillars (plan I). This pattern would yield information on both primary and secondary objectives but has the disadvantage that salt flows could be of such nature and magnitude to jeopardize the primary objectives by forcing the premature removal of the fuel assemblies.

A second pattern (plan II), consisting of a single rib-pillar with only the radioactive and the duplicate arrays, was considered. This pattern would minimize the possibility of interference with the changeout of the fuel assemblies but would not be likely to yield much information on salt flow.

Therefore, a third plan, incorporating the best features of the two was chosen and is shown in Fig. 19. If the 30-ft rooms and pillars represented a repeating pattern, the extraction ratio would be 50%; and if the 40-ft rooms and 20-ft pillars were repeating, the extraction would be 67%. With these low extraction ratios at ambient temperature, the end rooms should show negligible salt flow, and the center rooms, not enough flow to produce roof falls or noticeable floor heaves.

The radioactive and duplicate arrays are contained in the end rooms. The center pillar is heated by 22 heaters with an input of 1546 w each to yield the salt flow data. The temperature-rise pattern in the floor at the heater center-plane after 1-1/2 year of operation (12,800 hr) of the 22 heaters is shown in Fig. 20. It may be noted that the major portion of the pillar base will "see" temperature rises in excess of 70°C. It may also be noted that the temperature rise in the center of the floor in the end rooms will be negligible, and, thus, the heating of the center pillars should not have any thermal effect on the radioactive and duplicate arrays. These arrays, however, will contribute to heating of the two end pillars. (This contribution is not shown in Fig. 20.)

The advantages of this plan over either of the previous plans are: (1) that the area containing the fuel assemblies should be relatively stable even if considerable flow and/or roof falls take place in and around the center pillar, thus not interfering with changeout of the fuel assemblies; (2) that one pillar can be heated sufficiently to produce significant load transfer and salt flows; (3) that the mining pattern is essentially that envisioned for a disposal facility in which space is created specifically for waste storage, and, thus, the flows and load transfers, and the rates at which they take place, will be valuable information which will be useful in the design of a production facility.

6.1.3 Renovation of Lyons Mine for Experiment (W. J. Boegly, Jr.)

The shaft at the Lyons mine of The Carey Salt Company was excavated in 1890 by the Bevis Salt Company, and mining was continued by a number of companies until 1948, when mining was suspended. The main shaft is timber lined and is made up of two hoisting compartments and one airway. The present headframe was installed in 1955 when the old one and the salt-processing equipment were removed. The headframe

UNCLASSIFIED
ORNL-DWG 63-2434

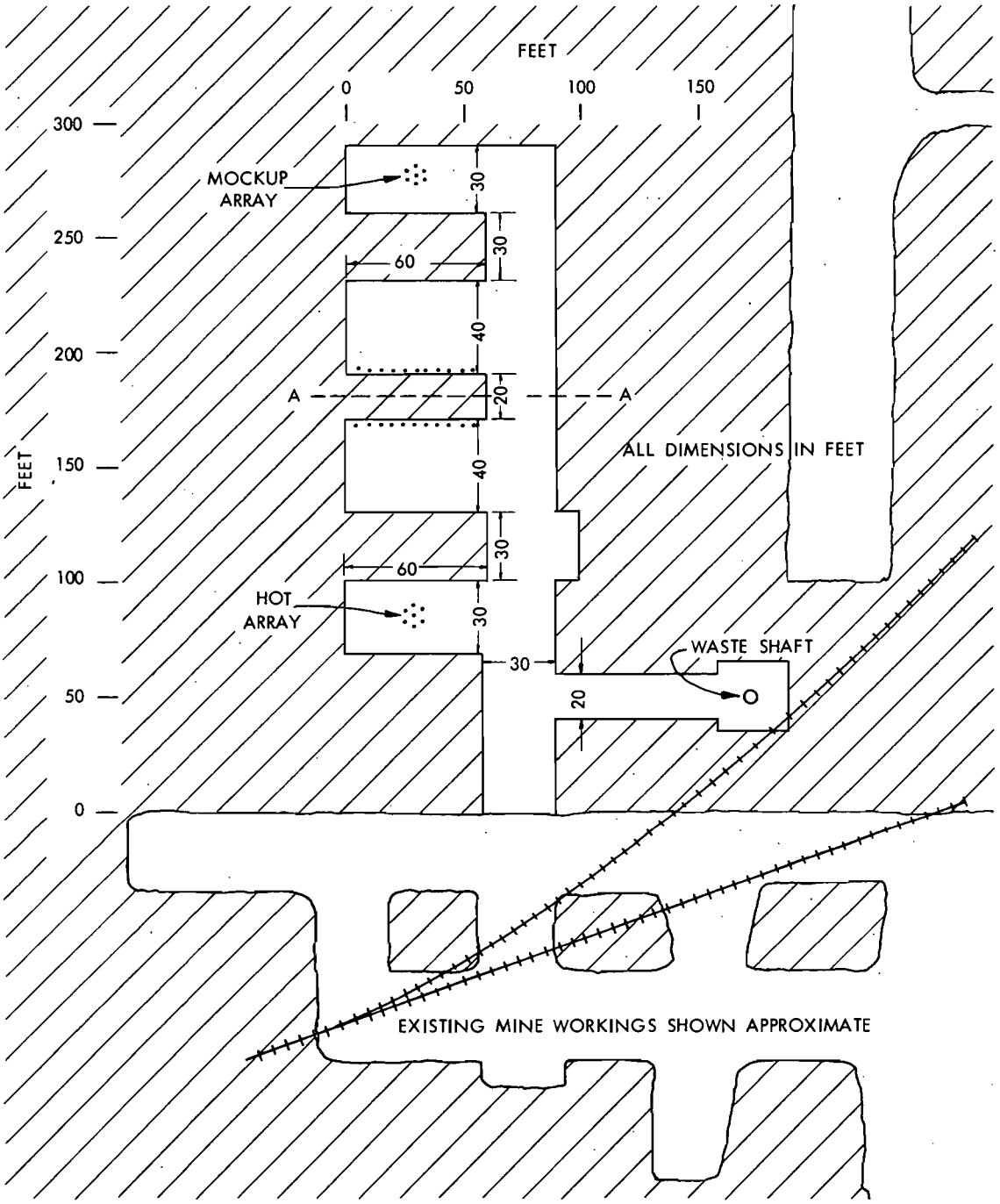

Fig. 19. Proposed Layout for Hot Demonstration Area Room-and Pillar Pattern-Plan III.

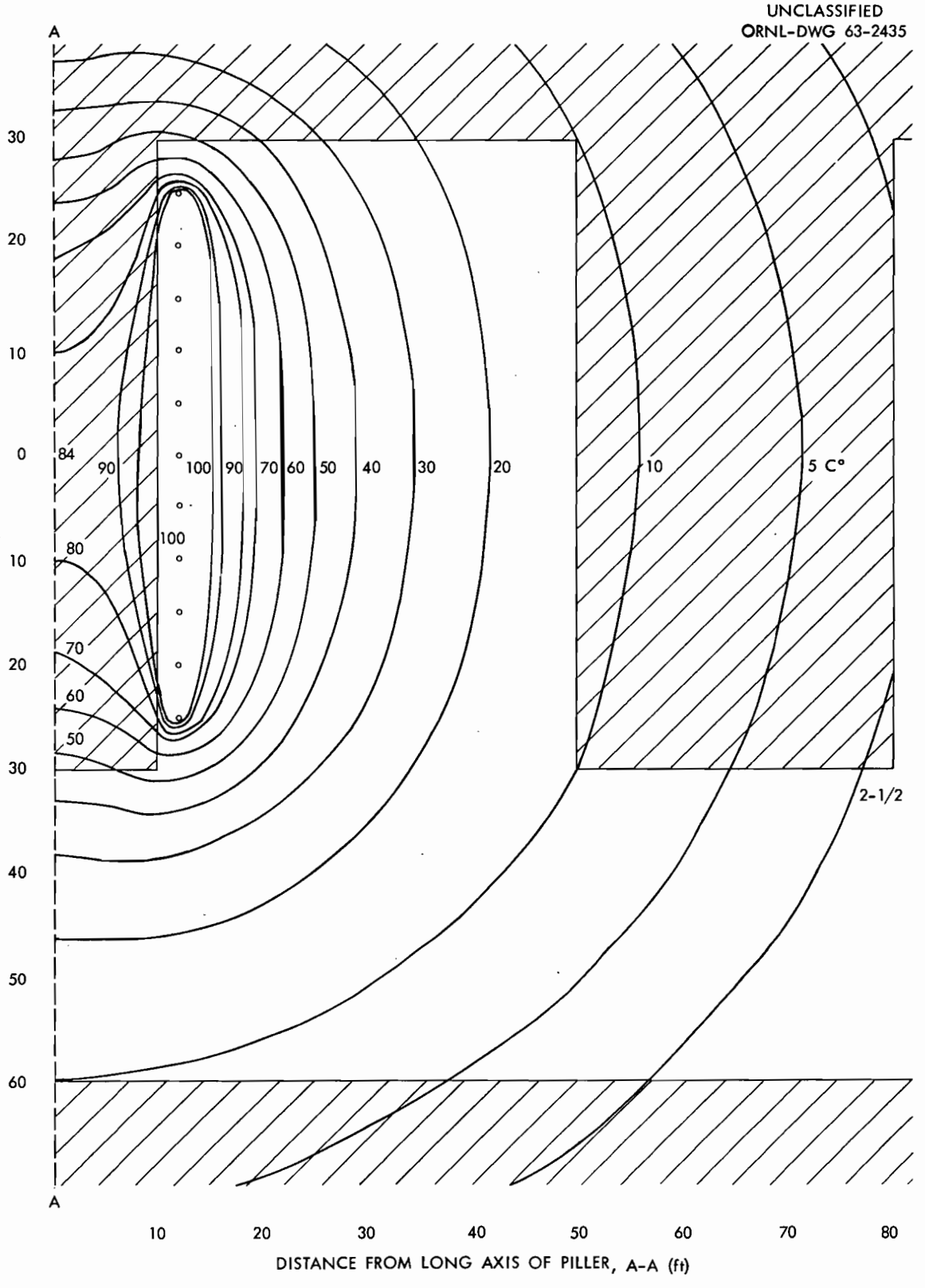

Fig. 20. Nine Feet Below Floor-Level Temperature Rise Isotherms After 12,800 Hours Operation of 22 Heaters at Base of Pillar (1546 w/heater).

is equipped with one sheave wheel, allowing for hoisting in only one compartment. At present, the headframe, man-cage, and hoist combination will handle about a 3000-lb load. The hoist is a converted steam hoist with two cable drums, 8 ft in diameter and 2 ft 9 in. wide.

Since the proposed experiment will necessitate the lowering of larger loads than can be handled by the present equipment, a number of renovations must be made to the hoisting system. The Stearns-Roger Corporation of Denver was requested to make a survey of the mine access facilities and to recommend changes for attaining a hoisting capacity of 7 tons. That hoist capacity can be achieved with the existing hoisting equipment, provided that a skip-and-counterweight hoisting system and a new headframe with the necessary foundations, cables, and sheave wheels are installed. Some work will be required on the topside electrical systems to modernize the electrical switch gear and to provide for the increased electrical requirements of the experiment.

The shaft timbering is in remarkably good shape, considering the age of the mine, and only routine repairs to the timbers, guides, and water-collecting rings will be required. Some replacement of timbers at the bottom of the shaft may be necessary.

Underground, the Lyons mine shows considerable evidence of floor heaves and ceiling sags produced by earth pressure. The major portion of the below-ground renovation will be the removal of these heaves and sags in order to provide safe access to the experimental site and to provide the necessary headroom for the mine transporter carrier. Since the experiment will be located above the mine floor in the perimeter of the mine, it will be necessary to excavate a ramp to reach the higher elevation. The grade on this ramp has been set at 10%, and the new mine floor will be about 12 ft above the present floor.

A new shaft from the surface to the mine will be drilled near the experimental area. The purpose of this shaft will be to lower the fuel-element cans from the topside carrier to the mine carrier. Consideration is being given to equipping this shaft with a temporary man-cage so that the shaft can be considered as a secondary escape exit. The U.S. Geological Survey has established reference points in the mine and at the surface so that the exact spot at which this shaft must be drilled can be located. Fig. 18 shows the approximate location of the experimental area and the waste shaft.

The necessary contractual changes are being made to allow the renovations to begin as soon as possible. A critical-path schedule was developed to define the work sequences during the topside renovations. Items of highest priority at this time are the design of a new headframe, man-cage and counterweight cage, and the development of procurement specifications for power cables, hoisting cables, and topside electrical repairs.

6.1.4 Engineering Design of Demonstration (W. F. Schaffer)

The engineering design of the demonstration for the handling of the radioactive materials requires major effort in the following categories:

1. Encapsulation of the fuel elements.
2. Rail shipment of carrier containing the fuel element capsules.
3. Transfer of the capsules from the fuel carrier at ground surface to the mine floor.
4. Movement of the capsules in a mine transporter within the mine to the demonstration area and transfer of the capsules to the salt environment.
5. Floor-hole liner and associated components.

The design concepts are described in general terms in the following paragraphs:

Encapsulation of the Fuel Elements. Sixty-day-cooled ETR fuel elements after removal of the end boxes will be transferred to the Multi-Cell Facility in Idaho (NRTS) for encapsulation. The fuel element capsule is being designed as a cylindrical container, about 5 in. in diameter and 7-1/2 ft long, for two ETR assemblies in tandem; the present concept incorporates a uranium shield plug at the upper end, which is necessary for certain handling requirements, and four thermocouples and connectors for monitoring the temperatures in the central regions of the fuel elements. The capsule is being designed for mechanical assembly near the midpoint; an interrupted threaded joint to minimize rotation of the parts and damage to the thermocouples is being used. To ensure complete containment of the radioactive materials, the joint design will include provisions for seal welding after mechanical assembly. The thermocouple connections from the outside of the capsule to the temperature recorders will be a plug-in type designed to permit connection after the fuel capsule is in position in the experimental array.

The capsule also includes a connection for the lifting and lowering grapple. Consideration is being given to treating the exterior surfaces of the fuel element to produce a black surface to improve emissivity for heat transfer. A form of anodizing using inorganic materials may be possible. The capsule itself also may be treated in another manner for the same reason. The capsule will be pressure tested for leakage before shipment. Final design of the capsule is contingent upon mechanical strength, procedural mockup, and irradiation tests at ORNL and Idaho.

Shipment of Fuel Capsules from the NRTS, Idaho, to Lyons, Kansas. The carrier proposed for shipping seven fuel capsules (14 ETR fuel elements) is a modification of a carrier at ORNL. The carrier was used for a similar shipment of fuel elements in canisters from Atomic International's SRE reactor on Santa Susana Mountain in California. The modifications include a new water-cooled rotating magazine for holding the fuel capsules, addition of a sleeve in the rear section for the grapple, addition of 2 in. of lead shielding to the body to bring the total shield thickness to 10 in. of lead, or equivalent, and an auxiliary operating door in the front section of the carrier. Forced water circulation through the magazine and an air-cooled external radiator will be used to hold the fuel temperature to approximately 800°F or about 400°F below the melting temperature. The heat generated by the 14 elements, based on 75 days of cooling before shipment, has been calculated as 22,600 Btu/min.

The carrier will be designed for shipment on a railroad gondola, complete with the cooling system, including radiator, pumps, and motor-generator sets.

Transfer of the Capsule from the Ground Surface to the Mine. A vertical charging hole from the ground surface to the receiving area is planned adjacent to an existing railroad spur. The carrier would be elevated to a vertical position over the charging hole by a railroad crane for the movement of the carrier from the gondola to the charging station. Work platforms for personnel will be required at the top and ground level of the carrier. A cable hoist for lowering the fuel capsules from the carrier to the mine is planned. A specially designed grapple, connected to the hoist cable, would be inserted in the upper end of the carrier and operated to lock the grapple and fuel capsule into one unit. The shield door in the lower section of the carrier would be opened to allow passage of the fuel element to the mine. A shield on a specially designed diesel-powered transporter described in the next paragraph would be in a position to receive the fuel capsule. After the fuel capsule enters the shield, the cable is disconnected, and the grapple remains with the shield.

Transfer of the Capsule to the Demonstration Area. Receiving of the fuel capsule, movement within the mine, and discharge to an experimental disposal hole in the floor will be handled by a device known as the HLS Waste Disposal Carrier. This unit is conceived as a standard diesel-powered, two-wheel, rubber-tired tractor and a special trailer equipped with a lead shield. The unit will be designed to be highly maneuverable within the limited confines of a salt mine and is expected to turn (without backing) in a 25-ft-wide corridor. The unit should be able to spot the shield within 1 ft of a given point in the mine. The shield is power driven for limited movement (1-1/2 ft) within the trailer frame in any direction in a plane parallel to the floor; this will permit accurate positioning of the shield above the disposal hole in the floor. Provisions will be made for leveling the shield to make up for floor variations up to 10°. The shield will also have a vertical movement of 2 ft. In order to receive the radioactive waste, the shield must be positioned under the charging hole from the ground surface and elevated to engage with the shadow shields in the roof to protect workers. Doors on the upper end of shield are then opened to receive the capsule. After the capsule is received in the shield, the doors are closed, and the shield is lowered to transport position and secured. The cable is disconnected from the grapple at this point. The carrier is driven to the demonstration area and positioned over the disposal hole. The shield is lowered to the floor and is ready for the transfer of the capsule to the salt environment. A trailer-mounted cable hoist is connected to the grapple cable outside of the shield. The lower shield doors are opened, and the capsule is lowered into the hole. The shield doors are closed, and the shield is raised and moved adjacent to the hole for removal of the grapple. The uranium shield at the upper end of the capsule is expected to minimize the radiation from the disposal hole for limited access during removal of the grapple. A cover plate and supplementary shielding, if required, will then be put in place to close the hole and permit start of the demonstration.

Floor-Hole Liner and Associated Components. The disposal hole for the demonstration with fuel elements differs from the plans for actual waste disposal in salt in

UNCLASSIFIED
ORNL-DWG 63-242

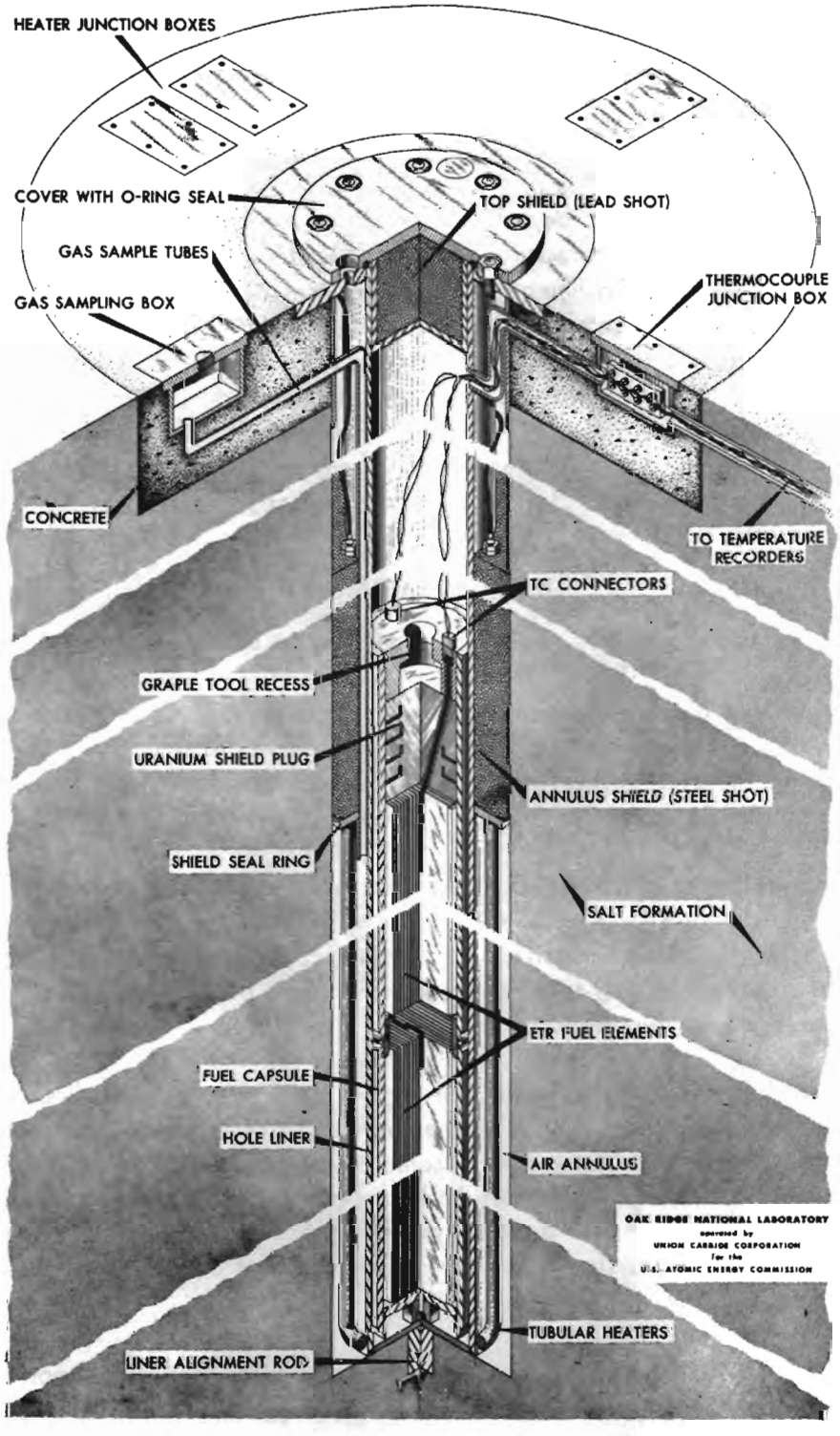

Fig. 21. Concept of Fuel Capsule, Hole Liner and Shielding - Radioactive Solids Disposal Demonstration.

that a metal hole liner is used to avoid contact of the fuel capsule and the salt; this will minimize corrosion problems and prevent closure of the hole by salt flow, thereby ensuring that the fuel capsule may be recovered. A concept of the hole liner and associated components are shown in Fig. 21. In order to measure movement of the salt and to sample the gases released from the salt as a result of the radiation and heat emitted from the fuel capsule, an annulus of approximately 2 in. is allowed in the region surrounding the hole liner adjacent to the fuel elements. Supplemental shielding in the form of steel shot is provided in the annular space above the fuel elements to protect workers at the surface from radiation. Additional shielding above fuel capsule will probably be necessary. The liner with the top cover and seal in place provides a secondary containment vessel to prevent the release of radioactivity to the salt mine. Tubes for sampling gas are brought out to a junction box that provides means for connections to gas samplers. Heaters are provided in the annulus to supplement the heat emitted from the fuel elements and provide closer approximation of the heat generated by solid radioactive waste. The liner and junction boxes will probably be set in concrete to hold the assembly in place, to provide an inexpensive method of sealing the annular space, and to permit sampling of the gases.

6.2 Heated-Model Room

W. J. Boegly, Jr. F. M. Empson R. L. Bradshaw T. W. Hodge

6.2.1 Objectives and Description of Test

It is expected that ultimate disposal of high-level radioactive solids in salt will be carried out in holes in the floor of mined openings. Therefore, knowledge of behavior of rectangular rooms under the influence of elevated temperatures is important.

Theoretical solutions exist for stress distributions around cylindrical openings in an elastic medium and for plastic closure of cylindrical openings at elevated temperatures for certain limited conditions. However, for rectangular openings, the only theoretical solutions known to exist are for the stress distributions in an elastic medium around openings with rounded corners.

Even in the case of cylindrical openings it has not yet been established how well the theoretical solutions will predict the thermal flows that will take place in an actual salt formation where it is not known if some of the assumptions in the theoretical solutions are valid. Thus, it is necessary to heat both cylindrical and rectangular openings to obtain valid data. Since the electrical energy requirements for heating an actual mine room are extremely high, studies of this nature are best carried out on scale-model openings.

To study the effect of temperature on a rectangular room of proportions similar to a mine room, an opening, 8 ft wide by 9-1/2 ft deep by 2 ft high, was created in the face of a large pillar in the Hutchinson, Kansas, mine of The Carey Salt Company. Immediately after the opening was created, electrical transducer-type strain gages, capable of operating at 200°C, were installed to measure the floor-to-ceiling

convergence, the movement of the floor alone, and the convergence of the side walls. Fig. 22 is a plan view of the experimental room showing the location of the gages.

After the gages were installed (June 15, 1962), background creep-closure data was collected for 214 days. The gages were then temporarily removed (February 11, 1963) to permit the installation of heaters. The heaters were turned on March 18, 1963, and heated operation continues to the present.

The heating system selected consists of ten tubular heaters, with diameters of 0.44 in. and active lengths of 7 ft, located inside the cavity. Externally supplied hot-air heat was considered, but it appeared that internal heating would give a more uniform heat pattern with less likelihood of interference with the strain transducers. A sketch of the locations of the heaters as seen from the end of the cavity is shown in Fig. 23. Also shown is the relative radiant heat flux to the surfaces of the cavity. The flux at the center of the floor and ceiling was taken as unity. As may be seen from the figure, the radiant heat flux incident upon the floor and ceiling of the cavity is uniform to within a foot of the side walls. The flux to the side walls is about one-and-a-half times that at the center of the ceiling, tending to make up for the greater heat conduction out into the salt at the sides, and, thus, contributing to a more nearly uniform cavity surface temperature. The heat transferred by convection will also tend to equalize surface temperatures.

Heater power is controlled by a thermostat (exposed to the cavity air but shielded from radiant heat) set for 170°C.

Two radiant-heat-shielded thermocouples monitor the air temperature in the cavity. Six thermocouples are installed in the walls of the cavity, with the junctions being recessed 1/2 in. into the salt. Twenty-four thermocouples are installed in the salt structure around the room at distances from 6 in. to 8 ft from the cavity, as shown in Fig. 24. All thermocouples are in the plane 5 ft back from the front of the room, except at locations 22 and 27, where there are couples located at 1-1/2, 5, and 8-1/2 ft back.

6.2.2 Background Data

Figure 25 shows the floor-to-ceiling movement which took place in the cavity at the various gage locations after it was excavated and before the heating system was installed. The cavity was excavated by slicing into the wall with an undercutter (which was turned on its side to make the vertical cuts) and then breaking off and removing the resulting salt slab. As soon as the slab was removed, the strain gages were installed, and the elapsed time from the first cut to the first set of gage readings (0 time on Fig. 25) was 3 days.

The initial deformation (flow) rates were high but decreased rapidly with time as the salt flowed to relieve the stress concentrations produced by the creation of the cavity. During the period of rapidly decreasing flow rates (up to about 50 days), the gages near the wall (Nos. 8 and 9) indicated slower floor-to-ceiling convergence than

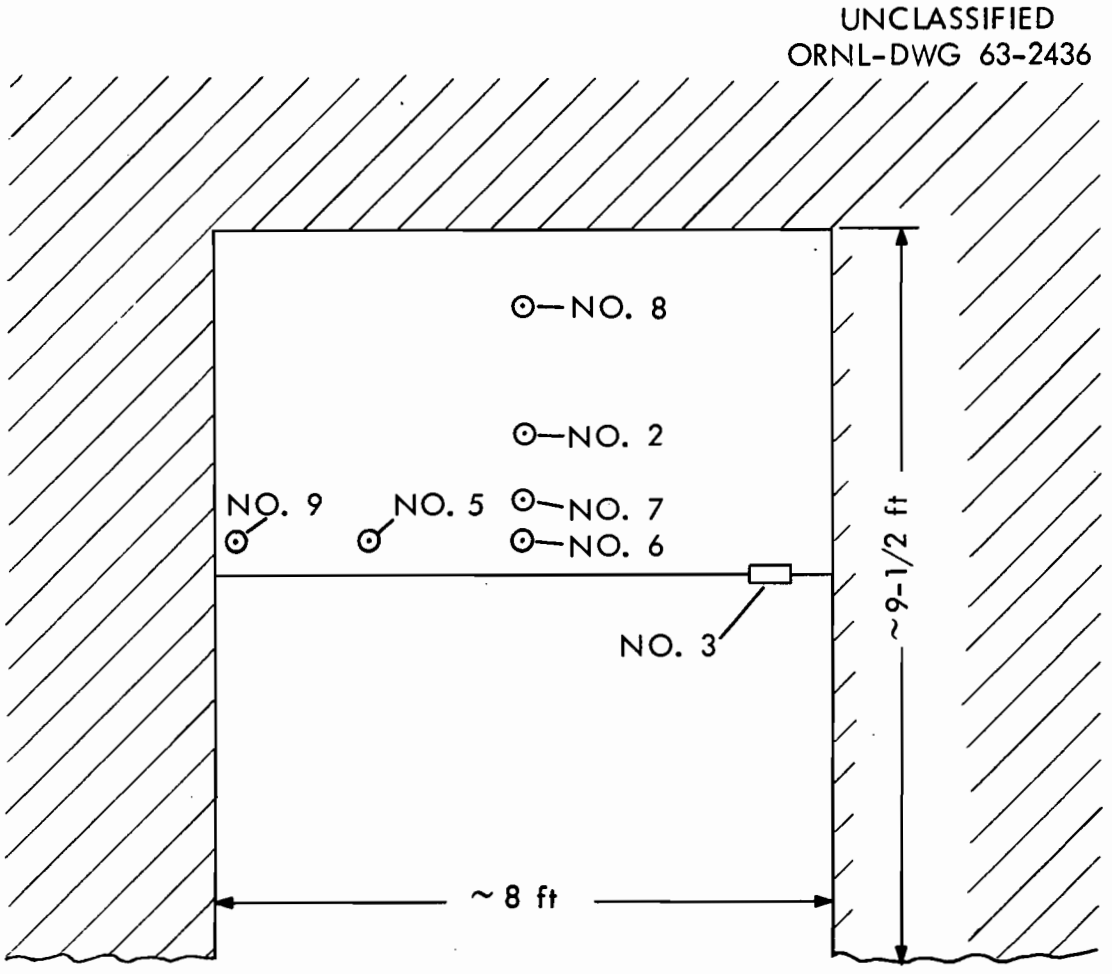

⊙ TRANSDUCER

Transducer No.		
2	Floor to ceiling	CONVERGENCE
3	Wall to wall	CONVERGENCE
5	Floor to ceiling	CONVERGENCE
6	Floor to ceiling	CONVERGENCE
7	Floor	MOVEMENT
8	Floor to ceiling	CONVERGENCE
9	Floor to ceiling	CONVERGENCE

Fig. 22. Plan View of Model Room Showing Locations of Transducer-Type Strain Gages.

UNCLASSIFIED
ORNL-DWG 63-2437

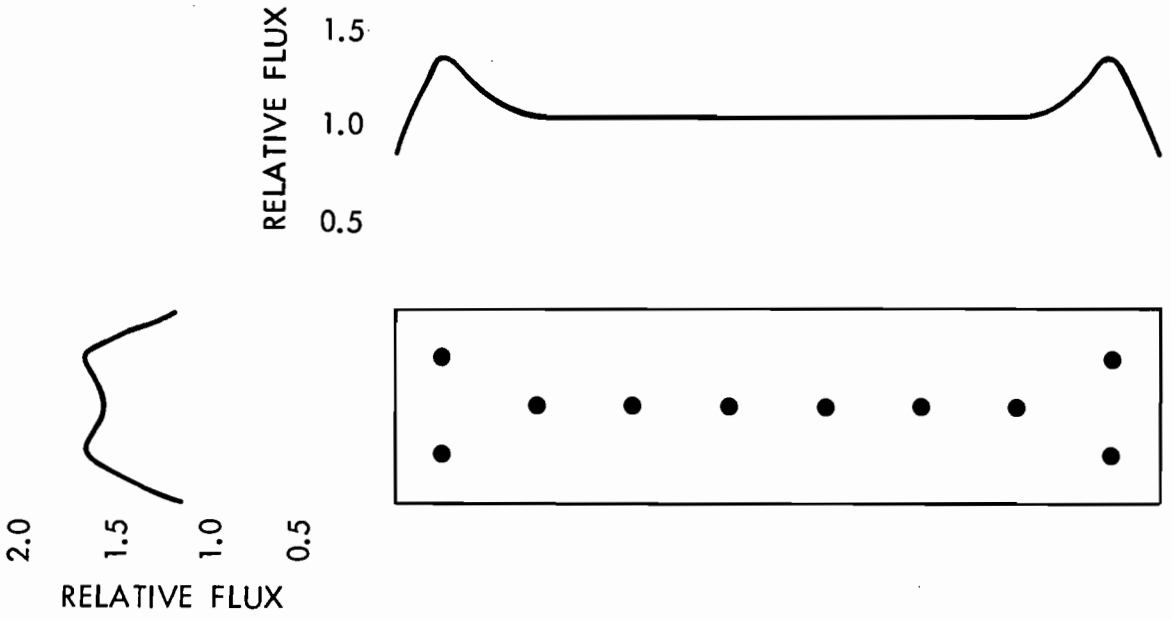

Fig. 23. Elevation View of Cavity Showing Locations of Heaters and Relative Radiant Heat Flux.

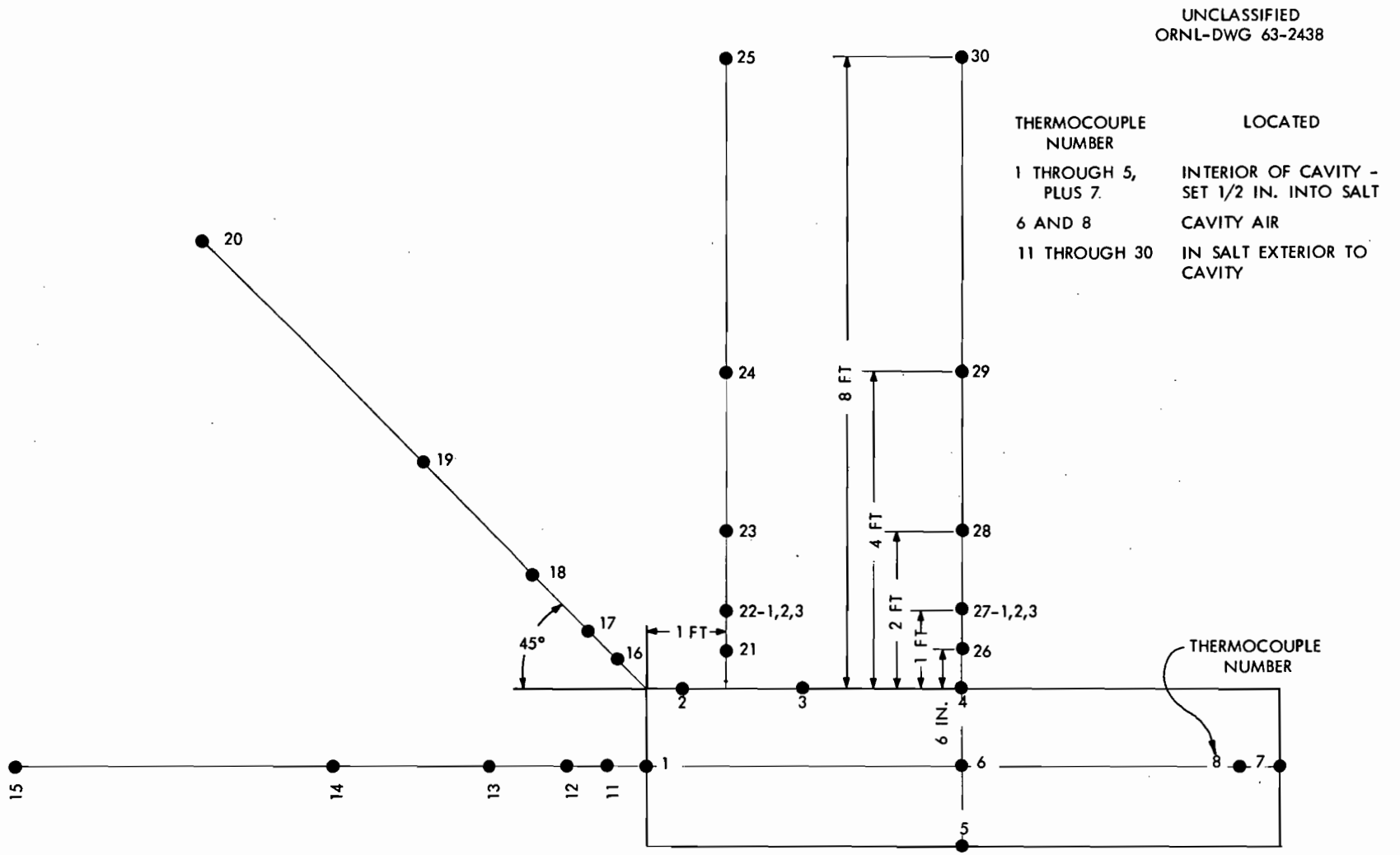

Fig. 24. Elevation View of Heated Room, Showing Thermocouple Locations.

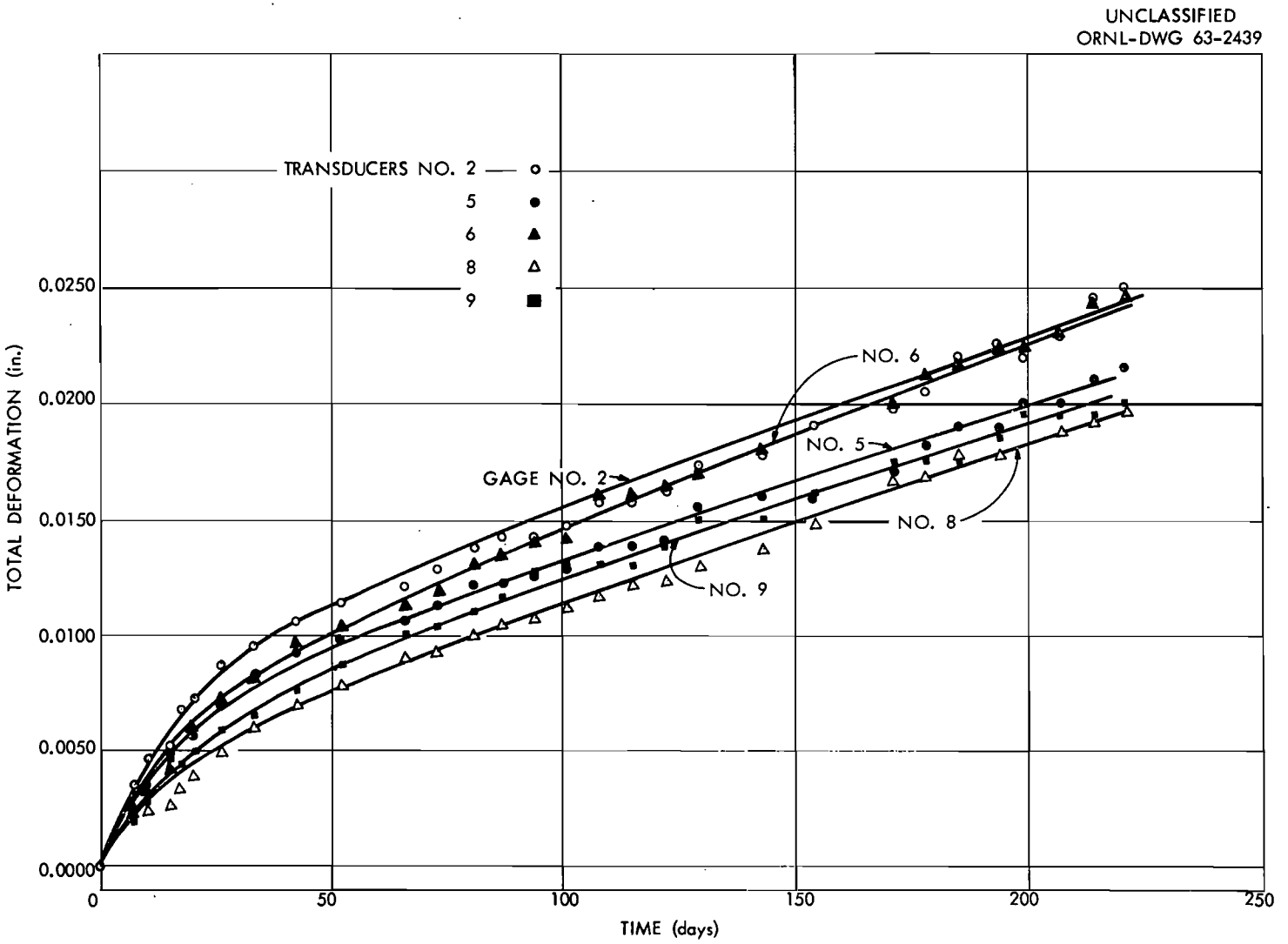

Fig. 25. Floor-to-Ceiling Movement at Ambient Temperature - Heated Room Experiment.

those out in the middle of the room (Nos. 2, 5, and 6). This might be interpreted as a beam deflection of the ceiling, except for the fact that the floor-only gage in the center of the room (No. 7) indicated that the floor movement accounted for about three-fourths of the deformation, as may be noted in Fig. 26. The floor-only gage apparently had a tendency to stick, as indicated by the flat portion in the middle of the curve.

After the initial transients, all the gages indicated steady flow rates, decreasing only slightly with time. The rates of movement for the final 114 days of the background period are shown in Table 20. The unit deformation rates (in. in.$^{-1}$ day^{-1}) were obtained by dividing total rates by the height of the room.

As may be noted from Table 20, the floor-to-ceiling flow rates near the walls (gages 8 and 9) were nearly as large as those in the center of the room. It has also been observed in the measurements made in various locations in the mine that, after the initial transient period in the first few months after the opening is created, the floor-to-ceiling convergence rate near the pillars is almost as large as that out in the center of the openings. For comparison purposes, it may be noted that in Hutchinson mine openings, ranging from about 2 to 30 years in age and from 6 to 12 ft in height, the deformation rates fall within the range of 2×10^{-6} to 7×10^{-6} in. in.$^{-1}$ day^{-1}.

The floor-only gage (No. 7) indicates that the floor is rising a little faster than the ceiling is falling, but the difference may not be significant in view of the erratic behavior of the gage.

The wall-to-wall gage (No. 3) was accidentally connected so that it measured wall-to-wall movement, plus floor movement near the wall. Since there was no floor-only gage near the wall, the readings cannot be readily interpreted and, thus, the data from this gage are not shown.

6.2.3 Heating Data

The heating phase was begun at 12:15 on March 18, 1963, with a power input of 11 kw which was gradually increased to 15 kw at 14:15 on March 20, 1963. At this time the power cycle was running about 30 min on and 5 min off. By March 21, the cavity air temperature had stabilized, reaching a peak of about 175°C during the heater "on" portion of the cycle and falling to about 155°C during the "off" portion. On April 1, 1963, the cycle was 15 min on and 7 min off, and at this time the power was cut back to 14 kw. On April 29, 1963, the cycle was running 15 min on and 8 min off. Figure 27 shows the average power input to the cavity during the first 40 days' operation.

In Fig. 28 is shown the time-temperature-rise curves, for points 5 ft back from the front of the cavity, at distances of 1/2 in., 1 ft, and 8 ft above the center of the cavity. It may be noted that temperatures are beginning to approach equilibrium, and thus the cavity deformation due to thermal expansion should also be approaching equilibrium.

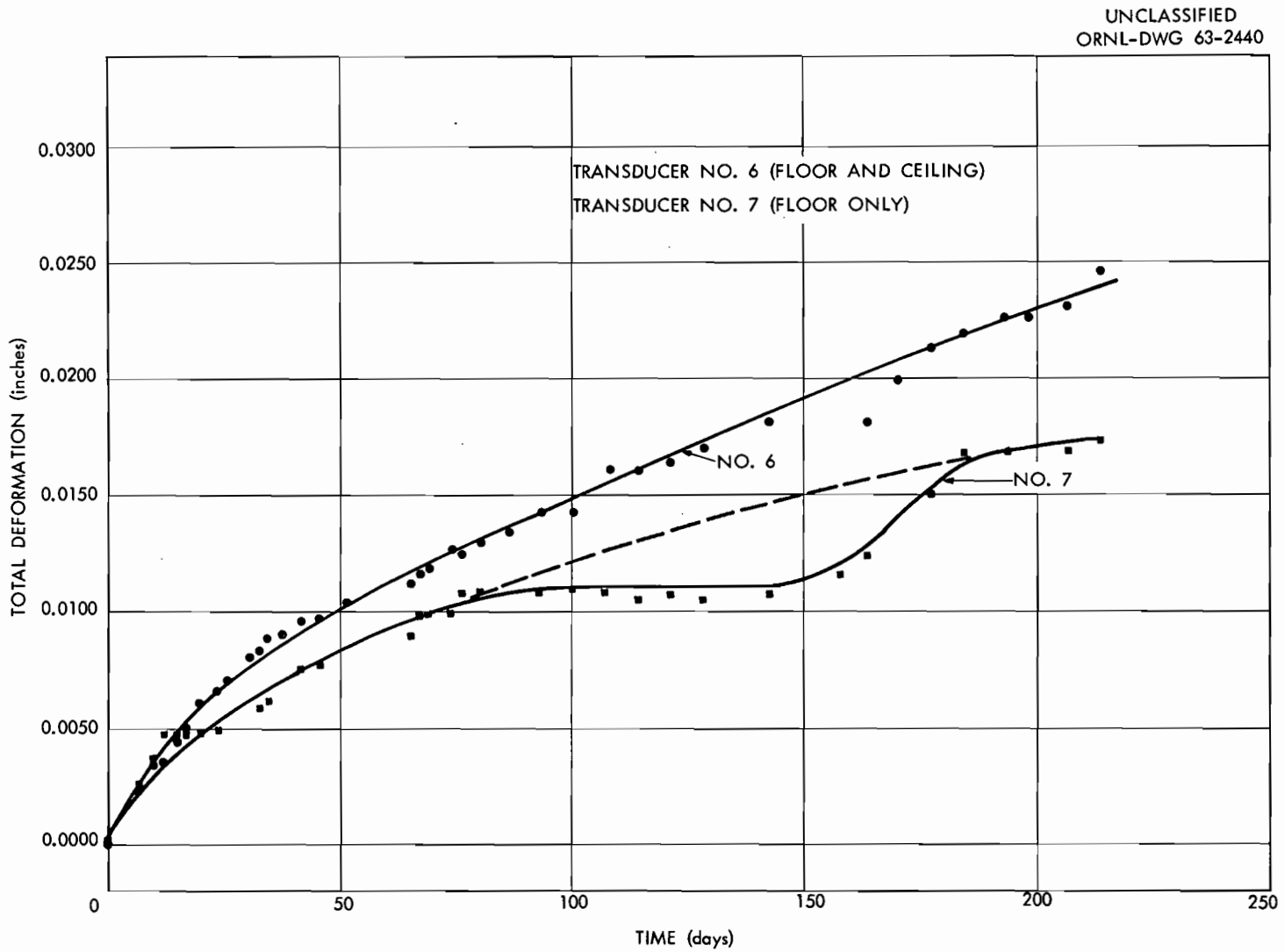

Fig. 26. Deformation at Ambient Temperature - Heated Room Experiment.

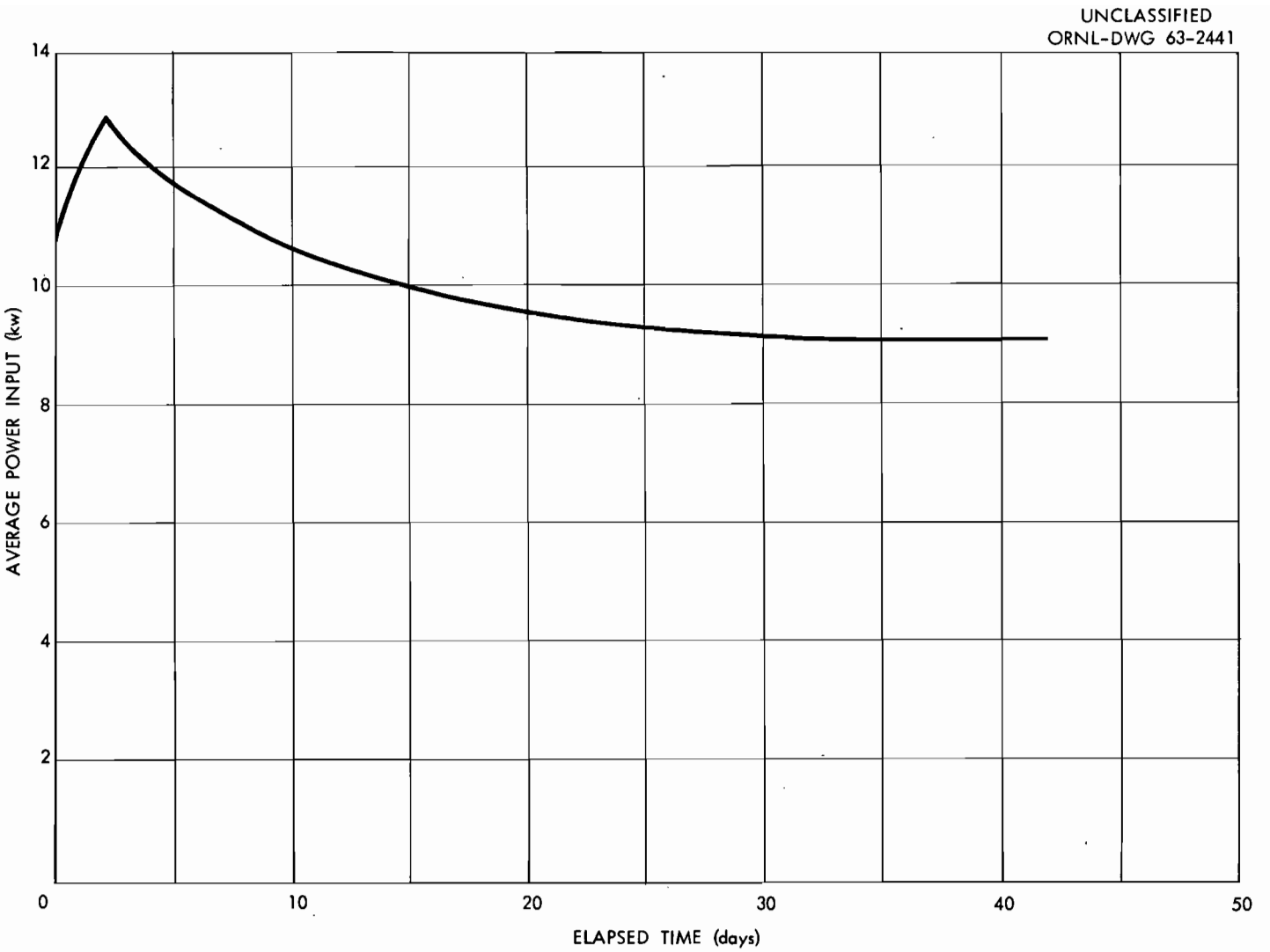

Fig. 27. Average Power Input to Heated Room.

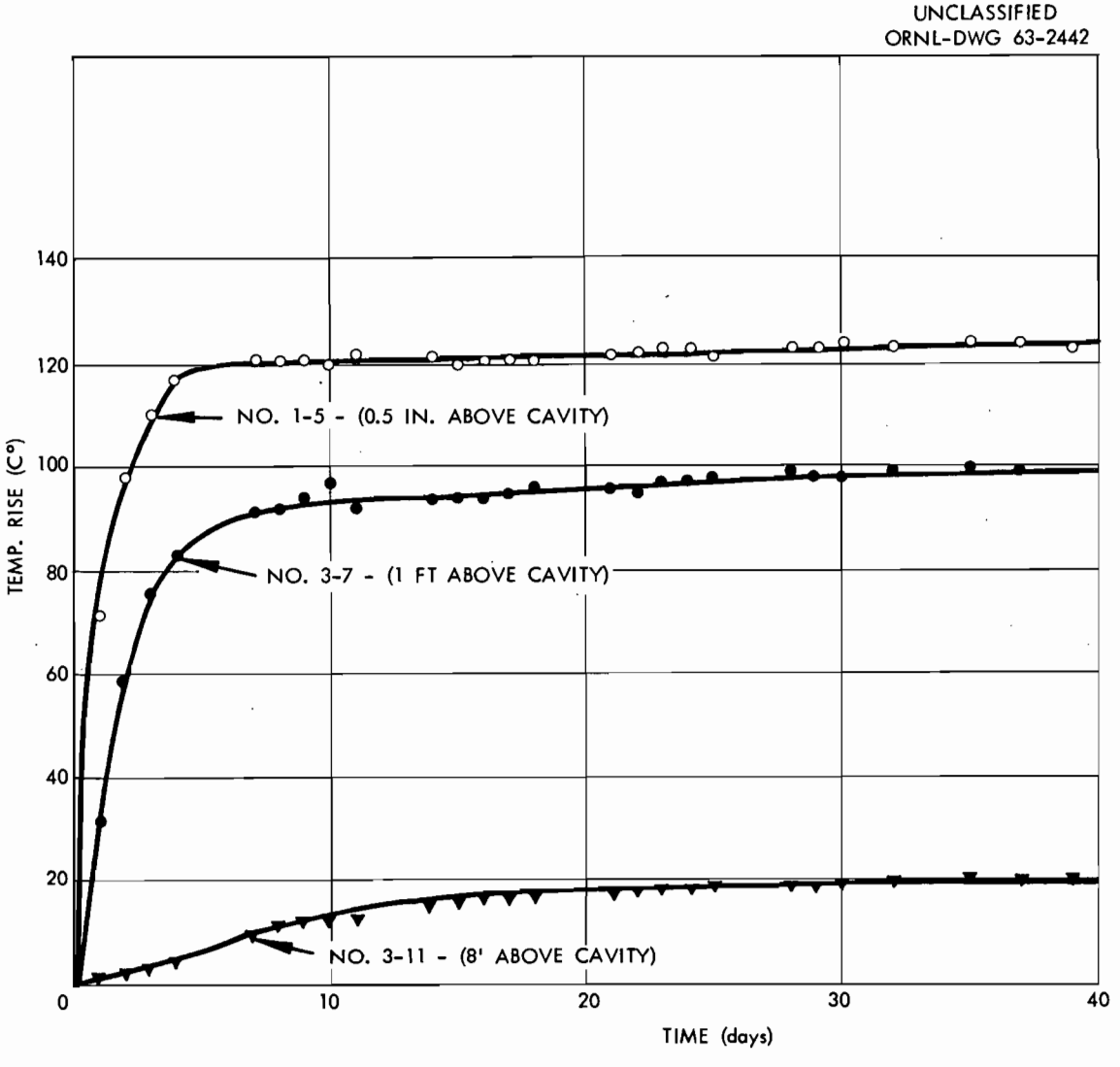

Fig. 28. Heated Room Temperatures Vertical Centerline.

Temperature-rise isotherms around the center of the cavity after 32 days' operation are shown in Fig. 29. As may be noted from the temperature rises 1/2 in. into the salt around the perimeter of the cavity, the heating is reasonably uniform, although the floor and walls are somewhat cooler than the ceiling.

Figure 30 shows the cavity deformations that took place during the first 40 days of heating. Gage 6 is in the center of the room; No. 9 is near a side wall; and No. 3 is wall to wall. It may be noted that the cumulative deformation from wall to wall (about 1 in.) is about the same as that from floor-to-ceiling near the wall, and only about 2/3 as great as the floor-to-ceiling movement in the center of the room (about 1-1/2 in.). The readings from gage 3 end at 24 days, since the limit of travel on the transducer was reached at that point, and No. 3 is not adjustable from outside the cavity in the manner that the others are. The floor-only gage data is not shown, since the gage apparently stuck at 0.35 in. of movement after about 4 days. The data for gage 6 is typical of the other floor-to-ceiling gages that are not shown.

Deformation rates for the period from 30 to 40 days are shown in Table 21. The floor-to-ceiling rates appear to be about the same throughout the cavity, although the accuracy in measuring the flow rates over such short portions of the curves is probably not very good. Comparing the deformation rates with those of the background period (Table 20), it may be noted that the cavity is now closing at a rate a hundred times faster than before heating. Even at this accelerated rate, it would take 12 years for the cavity to completely close. It must be remembered, however, that this is, in effect, an isolated cavity and does not represent the behavior expected for a series of adjacent openings, as in a mine operation.

Table 20. Heated-Room Transducers: Background Closure Data

Gage Number	Cumulative Deformation In Inches at: 100 days	214 days	Rate of Movement During Final 114 Days (in./day)	(in. in.$^{-1}$ day^{-1})
2	0.0153	0.0239	7.5×10^{-5}	3.1×10^{-6}
5	0.0132	0.0209	6.8	2.8
6	0.0146	0.0236	7.9	3.3
8	0.0113	0.0192	6.9	2.9
9	0.0124	0.0201	6.8	2.8
3	---	---	---	---
7[a]	0.0120	0.0173	4.6	1.9

[a]Based on dotted curves shown in Fig. 26.

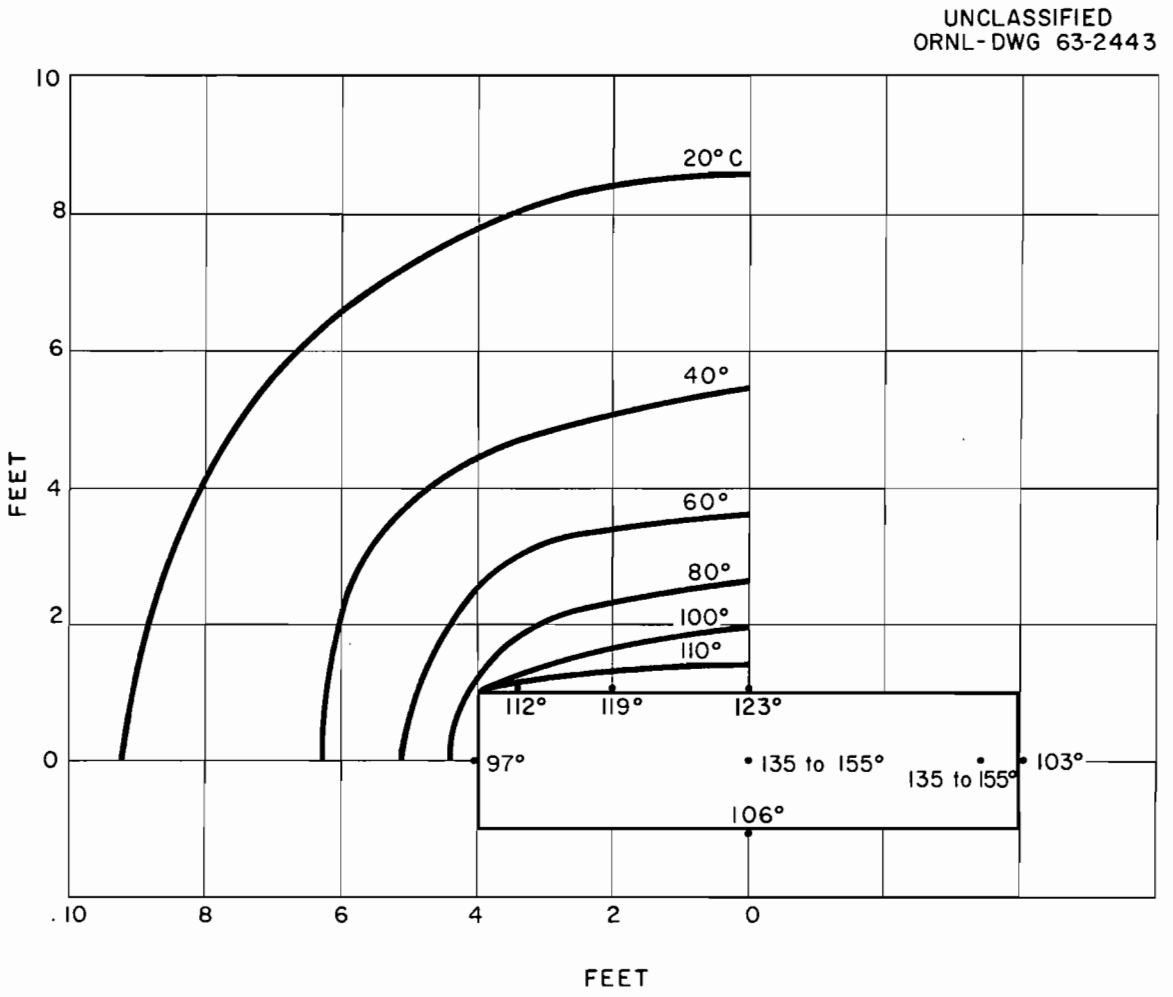

Fig. 29. Heated Room Temperature-Rise Isotherms after 32 Days' Operation.

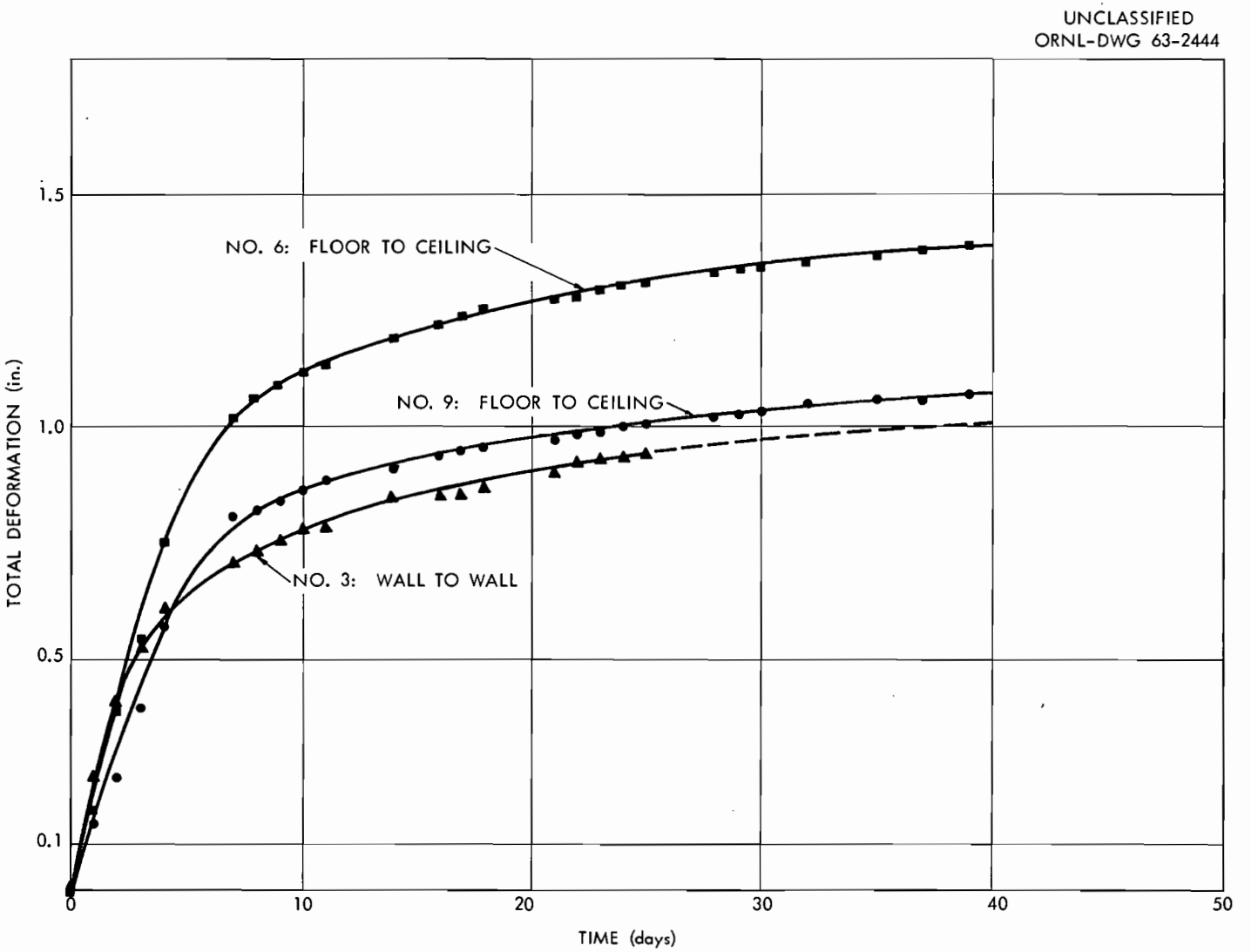

Fig. 30. Deformation During Heating - Heated Room Experiment.

Table 21. Cavity Closure During Heating

Gage Number	Cumulative Deformation In Inches at: 30 days	40 days	Rate of Movement During 30th to 40th Days (in./day)	(in. in^{-1} day^{-1})
2	1.31	1.36	5×10^{-3}	2.1×10^{-4}
5	1.38	1.43	5	2.1
6	1.35	1.40	5	2.1
8	1.19	1.24	5	2.1
9	1.04	1.08	4	1.7
3	>0.94	---	---	---
7	> 0.35	---	---	---

6.3 Chlorine Release from Gamma Irradiated Salt

H. Kubota

Epstein[16] gives quantitative data on the amount of oxidizable substances formed in KCl upon exposure to gamma and beta radiation. The values were obtained by dissolving the salt in water and determining the oxidizing power of the solution either iodometrically or spectrophotometrically. There is considerable uncertainty in the amount of oxidizing substance released to the gas phase, on which he places a maximum of 0.5% of the amount present in the solid escaping to the gas phase. G values are given for this process in the salt, presumably the production of chlorine, and these values are 1.47×10^{-2} at 2×10^{7} rads and 5.1×10^{-4} at 3.27×10^{9} rads. Assuming that the variation in G values obeys a linear relation with respect to dose, and further assuming that the values apply to NaCl as well, the production of chlorine that could be possible from the salt around one disposal hole was calculated, and the values are given in Table 22. The dose was calculated on the basis of a 2-year-old calcined waste contained in a 6-in.-diam can. These values correspond to the total produced in the salt during the lifetime of the activity of the waste. The actural amount that is released to the atmosphere is still problematical, but is expected to be less than 0.5% of the amount produced. The time rate of production is given in Table 23.

The irradiation of NaCl in a Co^{60} source was performed using chemically pure NaCl. The irradiations performed at 35 to 50°C released no free chlorine to the vapor phase which could be detected by the gas chromatograph or chemically by the potassium iodide or o-tolidine reactions. A sample receiving a dose of 3×10^{8} rads released about 2×10^{-6} mole/g of oxidizing substance, corresponding to a G value of about 3×10^{-4}. When salt irradiated at 35 to 50°C is heated to 250°C, a fraction of the oxidizing substance, equivalent to 3×10^{-8} mole/g, is released to the gas phase. The remaining salt, which had been turned black by the irradiation, was annealed back to its original white color, and it contained a residual oxidizing power equivalent to less than 10^{-9} mole/g.

Table 22. Probable Rate of Formation of Chlorine in Solid NaCl

Time After Burial	Dose (rads)	Chlorine Produced (%)
20 days	8.6×10^6	8.5
40 days	1.7×10^7	11.0
80 days	3.4×10^7	14.0
160 days	6.9×10^7	17.0
320 days	1.4×10^8	21.0
1.75 years	3.8×10^8	30.0
3.5 years	7.5×10^8	38.0
7 years	1.5×10^9	49.0
14 years	3×10^9	63.0
28 years	6×10^9	80.0

Irradiations were also performed at 250°C, which approximates the maximum temperatures expected near the periphery of the cans containing the hot wastes. No net change in the color of the salt was observed. Gas chromatography and iodometry revealed no chlorine nor oxidizing material in the gas phase. The oxidizing power released on dissolution to an aqueous medium was 10^{-7} mole/g at a dose of 3×10^8 rads.

The work thus far indicates that under the conditions of a short-term storage of hot wastes in salt, little or no production of free chlorine can be expected. The only question that remains is whether long-term irradiation will result in a slow release of chlorine to the atmosphere, possibly by a slow, diffusion-controlled process.

7.0 CLINCH RIVER STUDY

7.1 Bottom Sediments

P. H. Carrigan, Jr.*

In a study of the distribution of radioactivity in bottom sediments in the Clinch and Tennessee Rivers, the longitudinal distribution patterns for several radionuclides were found to be similar. The longitudinal distributions of seven radionuclides were compared

*On loan from Water Resources Division, U.S. Geological Survey.

Table 23. Yield of Oxidizing Agent with Dose

Dose (rads)	G	Moles of Oxidizing Substance Per Gram of Salt	Mass of Salt Radiated (g)	Total Moles of Oxidizing Agent Produced
10^6	0.1	10^{-7}	1.38×10^7	1.4
10^7	2.3×10^{-2}	2.3×10^{-7}	6.8×10^6	1.6
10^8	5.0×10^{-3}	5.0×10^{-7}	3.6×10^6	1.8
10^9	1.1×10^{-3}	1.1×10^{-6}	1.5×10^6	1.6
1.2×10^{10}	2.3×10^{-4}	2.6×10^{-6}	2.9×10^5	0.8

by using techniques of regression analysis. The results of these comparisons are shown in Fig. 31.

The regression analysis is based on the results of the 1961 annual survey of radioactivity in bottom sediments, made by personnel of the Applied Health Physics Section, ORNL. This survey extended from White Oak Creek on the Clinch River to Kentucky Dam on the Tennessee River. Results of radiochemical analysis of composite samples from the 32 sections of the survey were available for this study.

As shown in Fig. 31, the slope of the curves for the logarithmic correlation of Cs^{137} to Ru^{106}, the trivalent rare earths (excluding Ce^{144} and including Y^{90}), and Co^{60} are nearly the same. Also, the indices of correlations for these curves are extremely good. Thus, the results shown in the figure suggest that similar mechanisms control the longitudinal distribution of these particular radionuclides.

As shown in Fig. 32, the concentration of Cs^{137} in bottom sediments decreases in the downstream direction. The concentrations for the other radionuclides decrease in the downstream direction also. The rate of decrease in concentration in the downstream direction for cobalt, ruthenium, and the rare earths is not as rapid as for cesium, however. The equation for the slope of the curves in Fig. 31 is

$$dy/dx = abx^{b-1},$$

in which

dy/dx = slope,

y = concentration of the dependent variable,

x = concentration of the independent variable,

a = value of y at $x = 1$,

b = slope of straight line on logarithmic plot.

The coefficients are shown in Table 24.

The observed rates of decrease in the concentration of cesium, ruthenium, cobalt, and the rare earths with distance downstream from White Oak Creek are much greater than rates calculated on the basis of flow dilution alone. This lack of relationship between concentration and flow dilution, and the similar longitudinal distribution pattern of the radionuclides, seem to indicate that the mechanism controlling their longitudinal distribution pattern is a sedimentation process, rather than a chemical process, such as equilibration between concentrations in the sediments and radionuclide concentrations in the water.

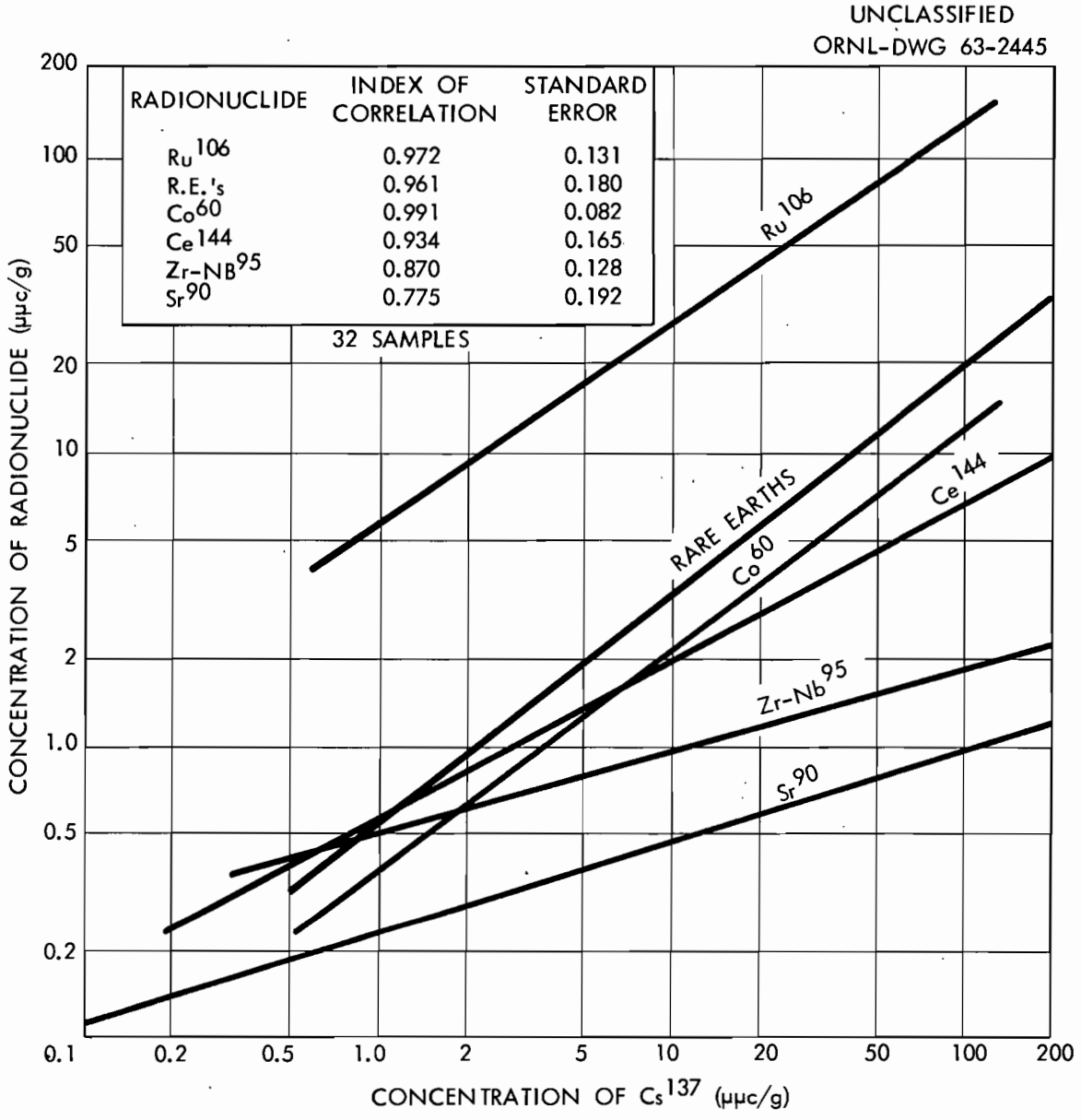

Fig. 31. Correlations Showing Similarity in the Longitudinal Distribution of Radionuclides in the Bottom Sediments of Clinch and Tennessee Rivers.

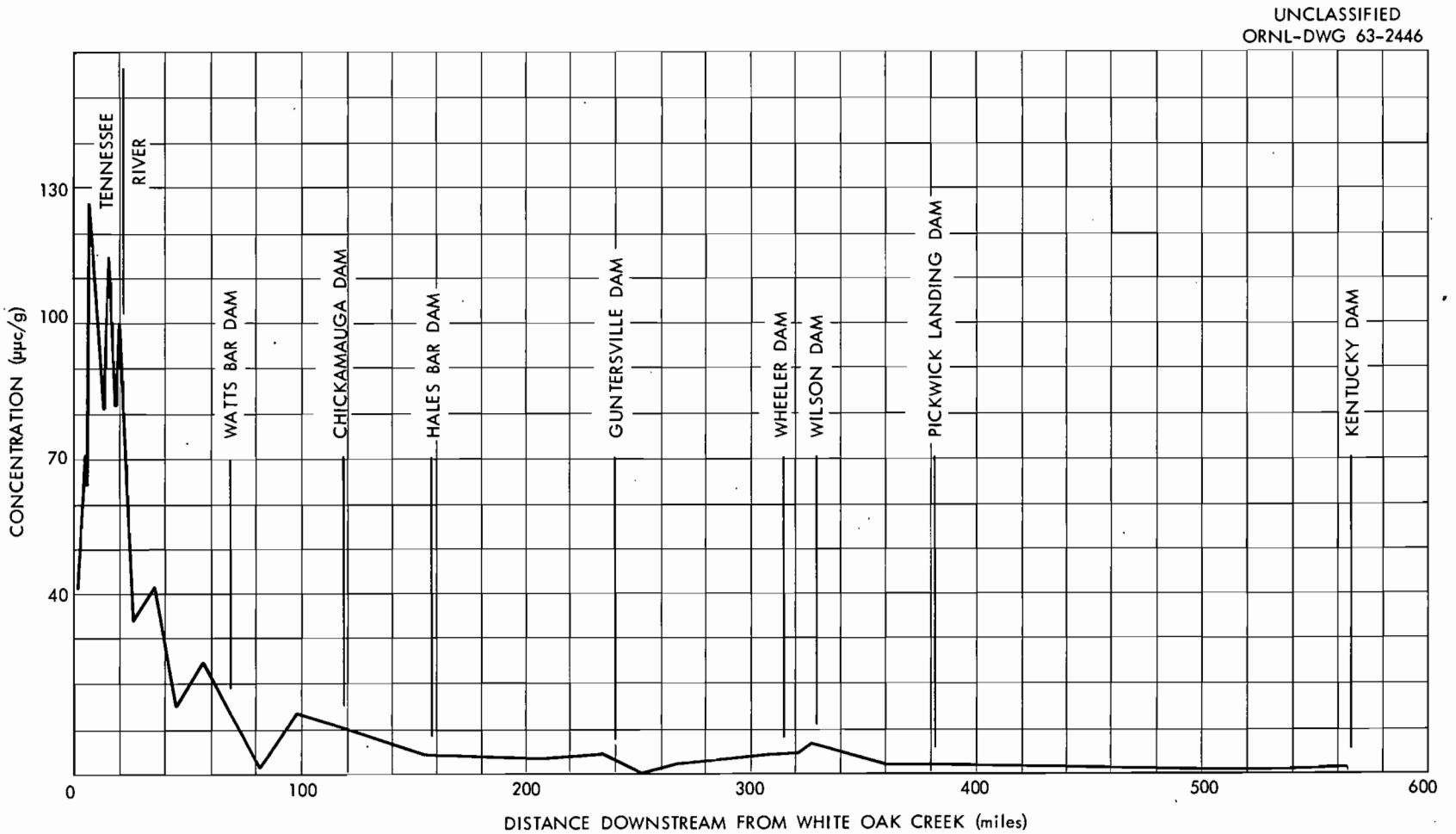

Fig. 32. Longitudinal Distribution of Cesium-137 in Bottom Sediments of Clinch and Tennessee Rivers in 1961.

Table 24. Regression Coefficients for Curves Shown in Figure 31

Correlated Radionuclides	a (μμc/g)	b
Cs^{137} - Ru^{106}	5.50	0.679
Cs^{137} - R.E.'s	0.551	0.778
Cs^{137} - Co^{60}	0.369	0.757
Cs^{137} - Ce^{144}	0.555	0.539
Cs^{137} - Zr-Nb^{95}	0.513	0.282
Cs^{137} - Sr^{90}	0.239	0.295

The slope of the curves for Zr-Nb^{95} and for Sr^{90} in Fig. 31 is less than that for cobalt, ruthenium, or the rare earths. The lesser slope indicates that somewhat different mechanisms may be controlling the longitudinal distribution of zirconium-niobium and strontium in the bottom sediments. The indices of correlation of zirconium-niobium and strontium indicate also that mechanisms affecting the distribution of cesium seem to have a lesser effect on the distribution of these radionuclides.

The index of correlation relating zirconium-niobium to strontium is 0.730, indicating that the mechanisms controlling their distribution are not exactly the same.

Relations demonstrated in Fig. 31 indicate that the longitudinal distribution in the bottom sediments of the concentrations of several radionuclides may be determined on the basis of the distribution of one or two of those radionuclides.

7.2 Calcite Precipitation

R. J. Pickering*

Recent examinations of aluminum plates that have remained submerged in the Clinch River at Miles 19.1, 15.0, and 5.4 for 3 to 4 months[4] have indicated that calcite had not precipitated on the plates during that period. However, calcite had precipitated on the steel bolts and nuts holding the plates to the supporting rope. The rough metal of the bolts and nuts may have provided a surface to which the precipitated calcite could adhere more readily than it could to the polished aluminum surfaces. A coating of calcite has been noted on several metal objects recovered from the river. Additional tests for calcite precipitation in the Clinch River are planned.

* On loan from Water Resources Division, U.S. Geological Survey.

7.3 Sources of Release to Clinch River

R. J. Pickering* B. J. Frederick*

The portion of the Clinch River Study involving the calculation of radionuclide loads in the river is based on the assumption that the only point at which low-level radioactive liquids are released to the Clinch River is the monitored release point at the White Oak Dam gate structure. It is desirable to occasionally provide assurance that no other release points exist. A three-phase investigation for this purpose was conducted during the past quarter.

The gates in White Oak Dam were closed, and fluorescent dye was mixed with White Oak Lake water along the upstream face of the dam. After 24 hr, water samples were collected for fluorescence analysis from very small seeps and small puddles on the creek bank immediately downstream from the dam. No dye was detected in the samples, but flow in the small seeps appeared to have increased slightly, and the creek bank had become more wetted as a result of the higher lake level, thus suggesting a minor amount of seepage through the earth-fill dam structure.

A visit was made to the Tower Shielding Facility, the only facility lying outside White Oak Creek Drainage Basin from which radionuclides might enter the Clinch River. The visit revealed that the reactor cooling water at the facility normally circulates in a closed system and that, when radioactive liquids must be released from the reactor, they are piped into a large closed tank and later transferred to a tank truck for transport to the Oak Ridge National Laboratory area for release. This arrangement appears to rule out contamination of the river from the Tower Shielding Facility.

Several water samples were collected from the drainage areas of small streams adjacent to White Oak Creek Drainage Basin and from streams that drain the Y-12 area. Gross-gamma counting of the samples showed no radioactivity above background.

The data collected in the surveys described above indicate little possibility of introduction of radioactive contamination, other than fallout, through surface drainage into the Clinch River at any point in the Oak Ridge Reservation except White Oak Dam and the area of the Oak Ridge Gaseous Diffusion Plant (ORGDP). Drainage from ORGDP is either within the security fence or is affected by Clinch River waters, and thus could not be readily surveyed. However, it is known that gross quantities of fission products are not handled at the plant.

7.4 Hazards Analyses

K. E. Cowser

Man may be exposed to internal and external sources of ionizing radiation due to the discharge of radioactive fluids to the Clinch River. Based on prior measurements and calculations, it is apparent that the more important exposure pathways are those

*On loan from Water Resources Division, U.S. Geological Survey.

contributing to internal sources. The maximum dose rate by immersion in contaminated water and exposure to contaminated bottom sediments in the Clinch River was calculated to be 0.027 and 12 millirad/day, respectively; from drinking Clinch River water the calculated exposure to the bone ranged from 0.06 to 0.51 of the maximum permissible concentration for water (MPC_w).[4, 17]

The fraction of MPC_w attained for the case of internal dose was calculated according to recommendations of the ICRP.[18] For a mixture of invariant composition and based on a particular organ, x, the fraction of MPC_w that is attained is given by:

$$\sum_i \frac{P_{wi}}{(MPC)^x_{wi}} , \qquad (1)$$

where

P_{wi} = the concentration of the particular radionuclide in water,

$(MPC)^x_{wi}$ = the maximum permissible concentration of the particular radionuclide in water for the organ and individual of interest and for continuous exposure.

The values of P_{wi} are average values, the period of averaging being 1 year, according to the recommendations of ICRP, NCRP, and FRC. All MPC_w values used for data relating to the Clinch River are taken as one-tenth of the occupational MPC_w values for continuous exposure. To obtain MPC_w values relating to the Tennessee River, the MPC_w for continuous occupational exposure has been reduced by a factor of one-hundredth for whole body as critical organ and by one-thirtieth with thyroid, bone, and GI tract as the critical organs.

If the fraction of MPC_w calculated from Eq. (1) is multiplied by the appropriate annual dose rate permitted in the particular organ of interest, an annual dose rate is obtained. A careful interpretation of such values is necessary, since the calculated dose only applies to a long-term and stable situation. The MPC_w values are set by the requirement that the dose rate (rems/week) after 50 years of exposure shall not exceed a recommended limit. During a 50-year exposure period, equilibrium is reached by most of the radionuclides, because their effective half life is short compared to 50 years. However, in the case of Sr^{90}, the allowable annual dose rate is reached only after 50 years of continuous exposure to the MPC_w. For this reason, the calculation of the actual dose received by the ingestion of known concentrations of radionuclides is desirable. As a second interpretation, the calculated dose rate may be considered as the dose that will be received during the next 50 years due to the exposure with P_{wi} for that period. Actually, the dose delivered after various times following the intake period depend upon the effective half-life of the isotope involved.

Because the MPC's which enter into the calculations have been estimated on the basis of so-called "standard man," the dose really represents only that which would be received by a person of physical characteristics and habits resembling standard man. Thus, the doses estimated should be considered as average values for typical adults. Very little is known at present concerning differences in metabolic rates or processes of children and adults as they relate to important radionuclides. However, dose-correction factors that take into account differences due to intake and organ size can be estimated.[19,20,21]

During ingestion of water, the activity present in a critical organ of the body at time, t (after the start of ingestion), can be expressed as:[18,22]

$$Q = f_w RX \int_0^t e^{-\lambda_e t'} \, dt' \, , \qquad (2)$$

where

Q = μc present in critical organ,

f_w = fraction of ingested radionuclide that is retained in the critical organ,[18]

R = rate of intake of water,

X = concentration of radionuclide in water during exposure,

λ_e = effective half life of radionuclide (year), and

t' = a time variable.

By assuming the concentration of a radionuclide in water is the average annual concentration and the rate of water intake is 2.2 liters/day (standard man), Eq. (2) is integrated over a time period of 1 year giving:

$$Q(I)_t = \frac{f_w R \bar{X}_t}{\lambda_e} \left[1 - e^{-\lambda_e} \right] \, , \qquad (3)$$

where

$Q(I)_t$ = μc present in the critical organ due to the intake of water during a particular year, t, and,

$\bar{X}_t$ = average annual concentration of a radionuclide in water during a particular year, t.

After the exposure period t, the quantity of radionuclide remaining in the critical organ is given by:

$$Q(A)_{t\tau} = Q(I)_t \, e^{-\lambda_e \tau} , \tag{4}$$

where

τ = the years after a particular intake period, t, and $1 \leq \tau \leq n$. Since the quantity of water consumed by an individual is a function of the individual's age, the critical-organ burden is also a function of the individual's age. Thus, an intake correction factor, i_γ (where γ is the individual's age during a particular intake period), must be applied to Eqs. (2) and (4). For example, assume that an individual of age γ = 10 began to consume contaminated water at the beginning of year, t = 1, the critical-organ burden of a particular radionuclide each year for a period of 3 years would be determined as follows:

Period	Body Burden (μc)
t = 1	$i_{10}Q(I)_1$
t = 2	$i_{11}Q(I)_2 + i_{10}Q(A)_{11}$
t = 3	$i_{12}Q(I)_3 + i_{10}Q(A)_{12} + i_{11}Q(A)_{21}$ (5)

The dose received by the critical organ during the period of intake, t, is

$$D(I) = \frac{MPD}{qf_2} \int_0^t Q dt' , \tag{6}$$

where

MPD = the maximum permissible dose rate to a particular organ,

$qf_2 = \dfrac{MPC_w \, R \, f_w}{\lambda_e} \left[1 - e^{-\lambda_e 50} \right]$, the fraction of radionuclide in the critical organ after 50 years of continuous exposure.

By substituting Eq. (2) in Eq. (6) and integrating over an exposure period of 1 year, the dose received by the critical organ during a particular exposure year, t, is

$$D(I)_t = \frac{MPD \, g_t}{1 - e^{-\lambda_e 50}} \left[1 - \frac{1 - e^{-\lambda_e}}{\lambda_e} \right] , \tag{7}$$

where

$g_t = \dfrac{\bar{X}}{MPC_w}$, the fraction of MPC_w in water during a particular year, t.

After the exposure period t the critical organ will continue to be irradiated by the radionuclide retained from the exposure period. The length of time for such

residual exposure depends on the effective half life of the radionuclide. The dose after exposure is

$$D(A)_{t\tau} = \frac{MPD\, g_t \lambda_e}{1 - e^{-\lambda_e 50}} \int_0^t e^{-\lambda_e t'} dt' \int_{\tau-1}^{\tau} e^{-\lambda_e t''} dt'' \quad , \quad (8)$$

where

t'' = a time variable.

Integration of Eq. (8) over an exposure period of 1 year and post exposure period, τ, gives

$$D(A)_{t\tau} = \frac{MPD\, g_t \left[1 - e^{-\lambda_e}\right]}{\lambda_e \left[1 - e^{-\lambda_e 50}\right]} \left[e^{-\lambda_e (\tau - 1)} - e^{-\lambda_e \tau}\right] . \quad (9)$$

The total dose received by a particular critical organ due to a particular radionuclide after a number of years of exposure is then the sum of Eqs. (7) and (9). A dose-correction factor must be applied to Eqs. (7) and (9) to account for differences in the intake and organ size of the individuals under consideration. The dose correction factor is

$$h_\gamma = \frac{R_\gamma / M_\gamma}{R_{sm} / M_{sm}} \quad ,$$

where

R_γ = the rate of water intake of an individual of age, γ,

R_{sm} = the rate of water intake of standard man,

M_A = the weight of the critical organ of an individual of age, γ, and

M_{sm} = the weight of the critical organ of standard man.

For an individual of age, γ = 10, who began to consume contaminated water at the beginning of year, t = 1, the dose received each year for a period of 3 years would be determined as follows:

Period

$t = 1 \qquad h_{10}\, D(I)_1$

$t = 2 \qquad h_{11}\, D(I)_2 + h_{10}(M_{10}/M_{11})\, D(A)_{11}$

$$t = 3 \qquad h_{12}\, D(I)_3 + h_{10}(M_{10}/M_{12})\, D(A)_{12} + h_{11}(M_{11}/M_{12})\, D(A)_{21} \qquad (11)$$

A code has been developed for Data Control 1604 that permits machine computation of critical-organ burdens and dose received. It will be instructive to compare the critical-organ burden and dose received by the so-called "standard" man and that of individuals of various age groups who hypothetically begin consuming Clinch River or Tennessee River water at various times.

7.5 Desorption of Radionuclides from River Sediments

T. Tamura W. P. Bonner

To ascertain the conditions under which the radionuclides associated with the Clinch River sediments might be desorbed, several leaching agents were applied to a contaminated sediment sample. The sediment was obtained at the mouth of White Oak Creek (CRM 20.8) with a Petersen dredge; a count exceeding 100,000 counts/min when measured with a Geiger-Mueller counter gave reasonable assurance that sufficient activity was present for detecting radionuclides removed by the treatments. The collected sediment was thoroughly mixed and kept in a tightly closed jar in its original moist state prior to use.

The radiochemical analysis of the sediment is (dis/min/50 g, oven dry basis): Ce^{144}, 4145; Sr^{90}, 2405; TRE, 24,190; $Ru^{103-106}$, 129,000; Cs^{137}, 118,000; Co^{60}, 16,600. Cesium-137 and ruthenium-103 and -106 are the principal contributors to the activity. The relative order of contribution by the radionuclides agree in general with earlier results obtained in the vicinity of CRM 20.8. The exception is ruthenium, which, in this sample, is present in higher concentrations than in the earlier samples.

For desorption, duplicate samples of the wet sediment equivalent to 25 g of oven-dry weight were weighed and contacted with 200 ml of solution. The pH of the solution was adjusted prior to contact and immediately thereafter; another adjustment followed 4 hr later. After 24 hr standing, the samples were centrifuged. The supernatant from the duplicate samples was combined after preliminary tests had shown that the desorbed activity was extremely low. The combined volume was acidified with HNO_3 and reduced in volume by heating prior to radiochemical analysis.

In Table 25, leaching results by acid, salt, and basic solutions are given. Up to 1 M solutions of salts, such as NaCl, KCl, and $CaCl_2$ between pH 6 and 8, removed less than 10% of the Co^{60}, Ru^{106}, and Cs^{137}. This behavior suggests that these ions

Table 25. Removal of Cobalt, Cesium, and Ruthenium from Clinch River Sediment by Various Solutions

50 g - oven dry equivalent - CRM 20.8; 400 ml solution; 24 hr standing

Reagent	Concentration (M)	pH	Co^{60}	Cs^{137} (% removed)	Ru^{106}
HNO_3		6	2.8	---[a]	3.0
HNO_3		2	64.6	---	3.1
HNO_3		1	78.1	3.3	5.5
HCl		6	---	---	3.5
HCl		2	65.6	---	4.1
$NaHSO_2$	0.1	6	16.8	---	9.8
$K_2Cr_2O_7$	0.1	5.6	5.9	1.7	4.7
$CaCl_2$	0.1	7	6.4	---	4.1
$CaCl_2$	1.0	7	4.7	---	4.4
NaCl	0.1	6	3.5	0.8	4.1
NaCl	0.1	8	---	5.7	6.8
NaCl	1.0	6	---	0.7	3.9
NaCl	1.0	8	---	0.6	5.1
KCl	0.1	6.2	---	0.7	2.8
KCl	1.0	6.2	3.0	1.7	2.5
NaOH		8	---	0.4	5.9
NaOH		12	16.5	3.1	46.6
NH_4OH		8	---	0.7	8.2
NH_4OH		11.8	17.2	4.5	45.1
Tap Water		7.7 (natural pH)	---	---	4.5
Ethyl Alcohol			---	---	0.9
Acetone			---	---	1.0

[a] Refers to concentrations below detectable limits.

are not held in the sediment by simple ion exchange. The higher value of 5.7% of cesium desorbed by 0.1 M NaCl at pH 8 was not confirmed by later tests. In acid systems of HNO_3 or HCl, ruthenium is not removed from the sediment but cobalt is released. If ion exchange fixation was responsible for cobalt retention and the acid treatment destroyed the clays responsible for the fixation, cesium would be expected to have been higher in the supernatant. The cobalt was suspected to be in a colloidal form.

In basic media, cobalt is only moderately leachable; ruthenium removal is highest in NaOH or NH_4OH media. It may be noted in passing that the pits into which ruthenium is released is highly basic; the river sediment pH is approximately 7.5; and the presence of ruthenium in the sediment may be due to the reduction in pH in the river. Note that cesium is not removed from the sediment by salts, acids, nor bases after 24 hr contact. The extremely high affinity exhibited by certain clay minerals for cesium have been demonstrated and is likely the reason for the nonremovable nature of this element in the sample.

Although strontium analysis is not available, it is believed that it is desorbable by neutral salt solutions since previous laboratory tests have shown this ion to be easily exchangeable when sorbed on sediments.

Behavior of Cobalt in Demineralized and Tap Water. Solutions containing Co^{60} at approximately 10^{-7} M were prepared with demineralized and tap water. The water was first acidified to prevent possible cobalt hydroxide precipitation when the cobalt tracer was added. The amount of cobalt removed from the solution was calculated by dividing the activity of the centrifuged sample after overnight contact by the initial activity of the solution at pH 2.0 after 15 min of stirring. The results of these tests are shown in Fig. 33 for contact times of 16 and 18 hr. With increasing pH up to 9, both demineralized and tap water solutions show a gradual decrease in cobalt content in the liquid. Above pH 9, the demineralized water sample shows a slight increase, whereas the tap water solution continued to decrease in cobalt content in the liquid phase.

Observation of the tap water sample showed definite flocculated colloids in the bottle above pH 9. Due to the composition of tap water (hardness), it is believed that the precipitate is calcium carbonate; the disappearance of cobalt from solution is likely caused by coprecipitation. At the concentration of cobalt added to the water, no precipitation of cobalt hydroxide is expected until the pH is at least above 9.5. A possible explanation of the removal of cobalt from demineralized water is adsorption on the glass sides. The apparent lower removal from tap water may be an argument for this type of removal, since the tap water contains dissolved ions, such as calcium and magnesium, which could substitute for cobalt adsorption on the sides.

In Table 26, the influence of adding Clinch River sediment to the tap water solutions at three different pH's are shown. Since the pH of Clinch River water is approximately 7.5, the results at this pH may be most meaningful. The large removal at pH 7.5 may explain the high concentration of cobalt in the sediment very near the mouth

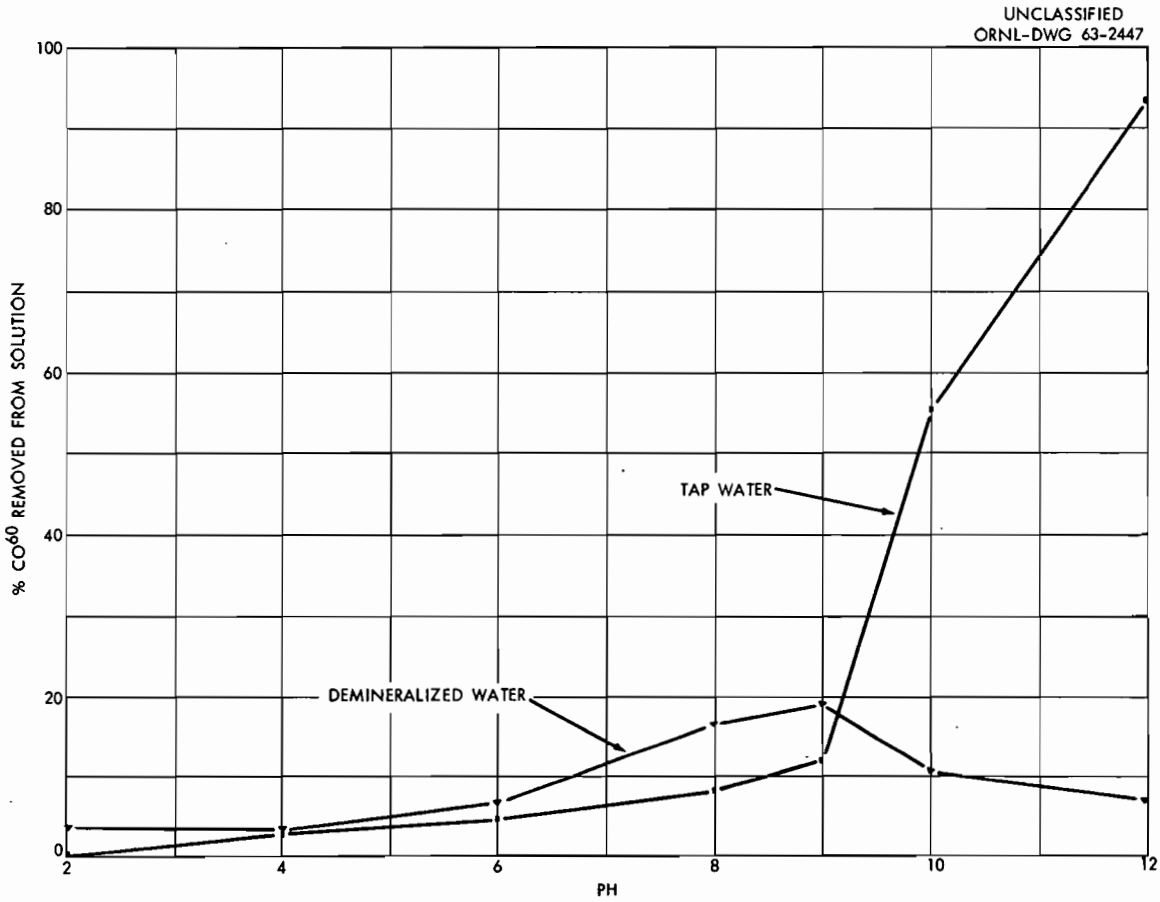

Fig. 33. Removal of Cobalt from Tap and Demineralized Water as a Function of pH.
50 ml Tap Water + Co^{60} - 16 hrs Standing
50 ml Demineralized Water + Co^{60} - 18 hrs Standing

of the White Oak Creek in the Clinch River. Much work remains to be done before the behavior of cobalt is understood, and work is still in progress to elucidate the mechanism of cobalt reaction with Clinch River sediment.

Table 26. Uptake of Cobalt by Clinch River Sediment at pH 4, 6, and 7.5

Solution: 50 ml tap H_2O + Co^{60}

	pH 4		pH 6		pH 7.5	
Time	% Cobalt Removed from Solution	pH Range	% Cobalt Removed from Solution	pH Range	% Cobalt Removed from Solution	pH Range
40 min	39.9	3.98-5.01	73.0	5.98-6.30	91.0	7.50-7.52
1 hr	38.5	3.98-4.34	74.4	6.00-6.13	93.5	7.52-7.58
22 hr	38.2	4.00-4.41	79.3	6.00-6.51	94.6	7.50-7.71
4 hr	38.2	3.98-4.16	80.8	5.95-6.21	95.2	7.51-7.68
24 hr	45.9	3.98-5.30	84.8	6.00-6.78	96.8	7.50-7.82
48 hr	39.7	4.00-4.37	87.0	6.00-6.48	97.8	7.48-7.72

8. MINERAL EXCHANGE STUDIES

8.1 Cesium Exchange by Potassium-Treated Vermiculite

D. G. Jacobs

Previous studies showed that potassium treatment of Zonolite BO-4 (hydrobiotite obtained from American Zonolite Company, Travelers' Rest, South Carolina), an interlayered hydrobiotite of approximately 40% biotite and 60% vermiculite lattices with a particle size range of 20 to 65 mesh, results in an increase of the distribution coefficient for trace cesium exchange from high-sodium-salt systems by a factor of 2.7 when determined by slurry techniques.[23] This increased sorption is attributed to the increased number of collapsed (10-A) lattices which provide exchange sites at the edges of the basal spacings which are sterically favorable for cesium, compared with sodium. However, when column techniques are employed to measure sorption of trace quantities of cesium from 0.5 M $NaNO_3$, the continued leaching action of the sodium nitrate is effective in removing the interlayer potassium. As a result, the lattices collapsed to 10-A by potassium treatment rehydrate upon sodium saturation and expand to 14-A; thus the exchange sites at the edges of the basal spacing lose their specific attractiveness for cesium, and the beneficial effects of potassium treatment are negated.

Zonolite BO-4 was treated with 1 M KCl to induce lattice collapse. The excess salt was removed by elutriation with ethanol (95%). The treated Zonolite had a sharp x-ray diffraction maximum at 10 A and an exchange capacity of 5.9 meq/100 g. Eight

liters of 0.5 M $NaNO_3$ containing traces of cesium (1.7×10^{-7} M) were passed through columns filled with 10 g of the treated vermiculite. Various amounts of potassium were added to the influent to maintain the collapsed lattice structure. The results (Table 27) show that optimum cesium removal was obtained with an influent potassium concentration of 0.0005, which gave a Cs K_d of 366 ml/g and a final exchange capacity of 46.8 meq/100 g. Higher concentrations of potassium were more effective in maintaining collapsed lattices, as indicated by a lower final exchange capacity; but the increased numbers of favorable exchange sites were not sufficient to counteract the increased competition caused by the greater concentration of potassium.

8.2 Strontium Exchange by Vermiculite with Potassium Added to the Influent

Addition of potassium to 0.5 M $NaNO_3$ influent to raise the potassium concentration above 0.01 M results in collapse of vermiculite lattices and the interlayer fixation of trace concentrations of cesium by physical entrapment of the cesium held at exchange sites on the basal surface of the vermiculite.[26] No appreciable quantities of strontium could be fixed in this manner, however (Table 28). The uptake of strontium was reduced by increased concentrations of potassium, although the reduction was not proportional to the reduction in final exchange capacity. In addition, the major portion of the strontium remained in an exchangeable form.

Table 27. Effect of Addition of Potassium to the Influent on the Sorption of Cesium by Potassium-Treated Vermiculite from 0.5 M $NaNO_3$ Containing the Mass Equivalent of 2 μc of Cs^{137} per ml

Potassium Concentration (M)	Cesium K_d (ml/g)	Cesium Leached (%)	Final CEC (meq/100 g)
0.0000	252	15.0	67.0
0.0001	311	16.2	63.7
0.0002	352	10.5	56.2
0.0005	366	9.8	46.8
0.001	358	10.8	37.9
0.002	262	9.5	16.7
0.005	180	10.2	9.1
0.01	147	9.6	10.0
0.05	65	10.2	9.0

Table 28. Effect of Addition of Potassium to the Influent on the Sorption of Trace Quantities of Strontium by Vermiculite from 0.5 M $NaNO_3$

Potassium Concentration (M)	Strontium K_d (ml/g)	Strontium Leached (%)	Final CEC (meq/100 g)
0.00	43.8	84.1	86.0
0.01	46.9	76.2	65.5
0.02	36.0	86.1	44.6
0.04	24.1	70.7	22.8

9. WHITE OAK CREEK BASIN STUDY*

9.1 Distribution and Transport of Radionuclides in the Bed of Former White Oak Lake

T. F. Lomenick

A series of core samples was taken in the bed of former White Oak Lake to determine the quantity and distribution of radionuclides within the area.[4] In general, it is observed that most of the Cs^{137} is associated with the relatively thin layer of recent lacustrine sediment that covers the lake bed. Thus, in areas near the shore line where the sediment is thinnest, the smallest quantities of activity are found. Maps showing concentrations of Cs^{137} for the 0- to 6-in. and 6- to 12-in. layers of lake bed soil are presented as Figs. 34 and 35. For the first 6 in. of soil (Fig. 34) it is noted that concentrations vary from less than 1×10^{-3} μc/g to 77×10^{-3} μc/g, and the areas of maximum concentrations lie roughly adjacent to the course of White Oak Creek through the bed and in the present impoundment area behind the dam. The greatest depth of lacustrine sediment in the lake bed is also found in these areas.[4] In the soil section 6 to 12 in. below the surface, it is seen (Fig. 35) that the concentrations of Cs^{137} at most of the sample points are much less than those observed in the upper layer of soil. The higher values are restricted to sites where the lake sediment is greater than 6 in. deep.

The concentrations of Sr^{90} for the upper 6 in. of soil over the lake bed are shown in Fig. 36. It is of interest that, with the exception of a few narrow zones parallel to

*This project, entitled, "Environmental Radiation Studies: Evaluation of Fission Product Distribution and Movement in White Oak Creek Drainage Basin" (AEC Activity 060501000), is supported by the U.S. Atomic Energy Commission's Division of Biology and Medicine. All other projects covered in this report are supported by the Division of Reactor Development (AEC Activity 04640011).

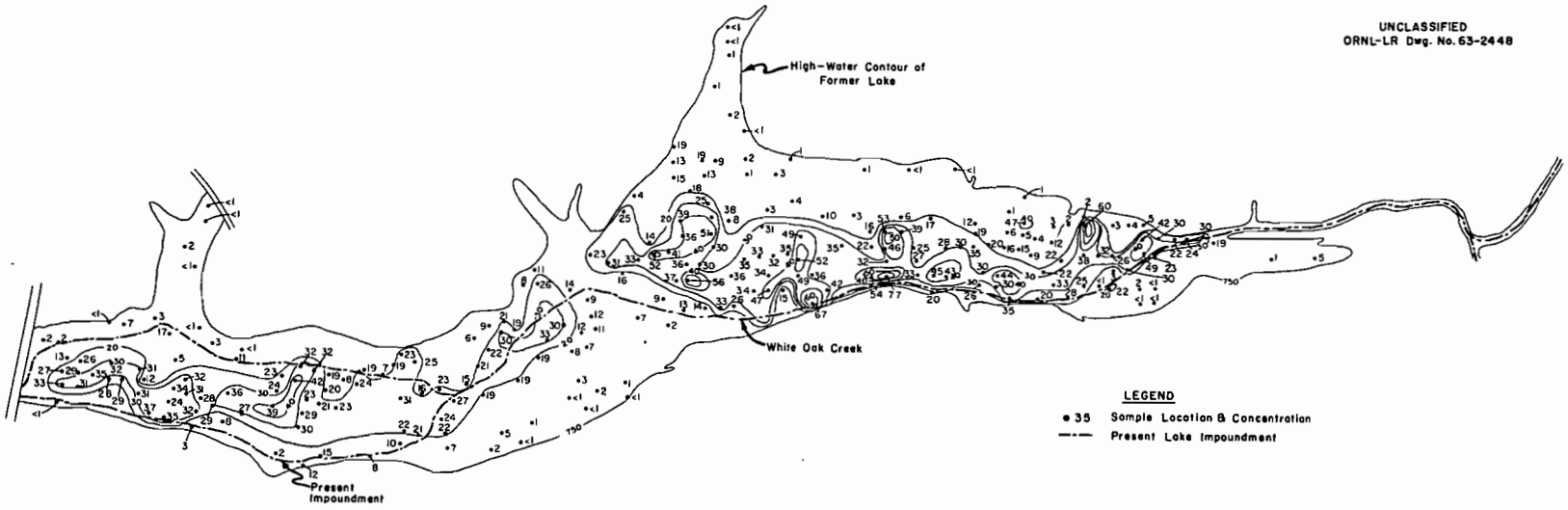

Fig. 34. Map of White Oak Lake Bed Showing Cs^{137} Concentrations in 10^{-3} μc/gm for 0-6 Inches Soil Layer

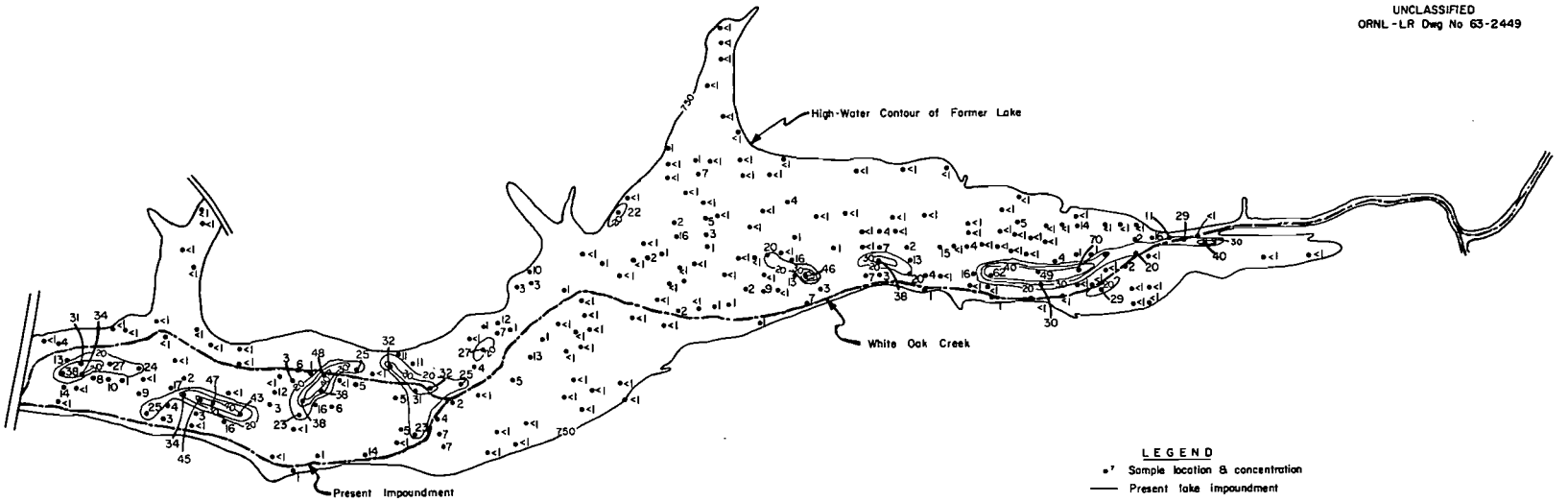

Fig. 35. Map of White Oak Lake Bed Showing Cs^{137} in 10^{-3} μc/gm for 6 to 12 Inches Soil Layer

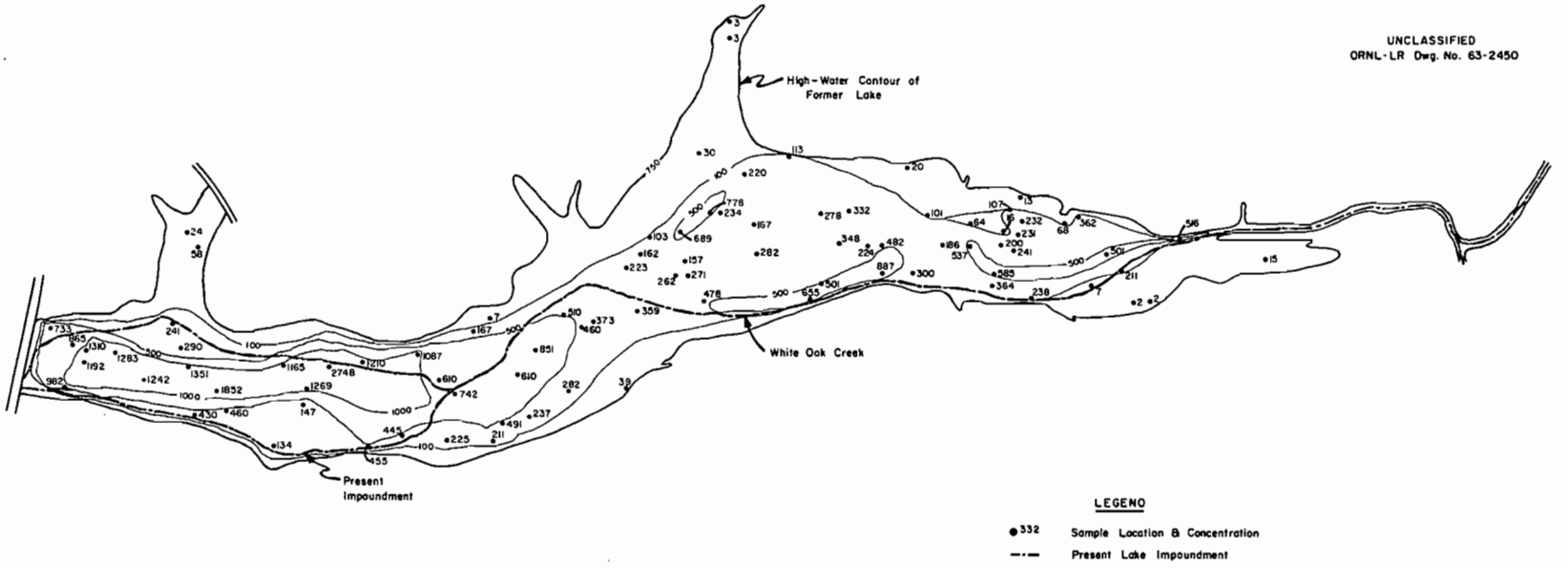

Fig. 36. Map of White Oak Lake Bed Showing Sr^{90} Concentrations in μμc/gm for 0-6 Inches Soil Layer

the creek in the upper part of the bed, the highest concentrations of Sr^{90} are found within the inundated area behind the dam. This indicates that strontium is presently being removed from the lake water and is accumulating in the bottom sediments. It is also observed that the concentrations of Sr^{90} in the soil are roughly a hundredth of those of Cs^{137}.

9.2 Movement of Radionuclides in White Oak Creek

A preliminary investigation of the bed of White Oak Creek and its flood plain revealed that bottom sediments to a depth of 18 in. at mile 2.3 contain Sr^{90}, Cs^{137}, Co^{60}, and the rare earths (exclusive of Y^{90}) in concentrations that range from 100 to 3450 μμc/g, 4000 to 76,900 μμc/g, 290 to 2200 μμc/g, and 0 to 14,100 μμc/g, respectively. In general, for Sr^{90} and the rare earths the highest concentrations occur in the uppermost few inches of the sediment; whereas, for Cs^{137} and Co^{60} the higher concentrations were found at a depth of 6 to 12 in. The concentrations of radionuclides found in the flood plain along the bank of the creek are roughly the same as those observed in the creek bed.

9.3 Geology and Hydrology of White Oak Creek Basin

W. M. McMaster* R. M. Richardson*

Heavy rains occurring on March 5 and again on March 11-12 caused extensive flooding in White Oak Creek basin. On March 5, when 2.68 in. of rain fell at ORNL according to the U. S. Weather Bureau, discharge measurements were made at most of the White Oak Creek basin gaging stations, and water samples were collected at each station for chemical quality and sediment analyses. Sediment samples collected at gaging stations on White Oak Creek were taken continuously at closely spaced intervals as the stream stage changed. Results of analyses of these samples will add to the knowledge of stream discharge-sediment transport relations in White Oak Creek basin.

On March 11 to 12, when 4.47 in. of rain fell at ORNL, a flood time-of-travel study was made in White Oak Creek at a time near the peak discharge, which was about 200 cfs at the gaging station White Oak Creek below ORNL. Two liters of 40% Rhodamine β dye was poured into the stream at a point about 500 ft above the main laboratory area, and samples were collected for measurement of fluorescence at three stations during passage of the dyed water. Results of this flood time-of-travel study are shown in Fig. 37 for stations White Oak Creek at ORNL and White Oak Creek below ORNL. No data were obtained at the station, White Oak Creek at White Oak Dam, due either to dilution of the dye or failure to sample during passage of the dye.

---

*On loan from Water Resources Division, U.S. Geological Survey.

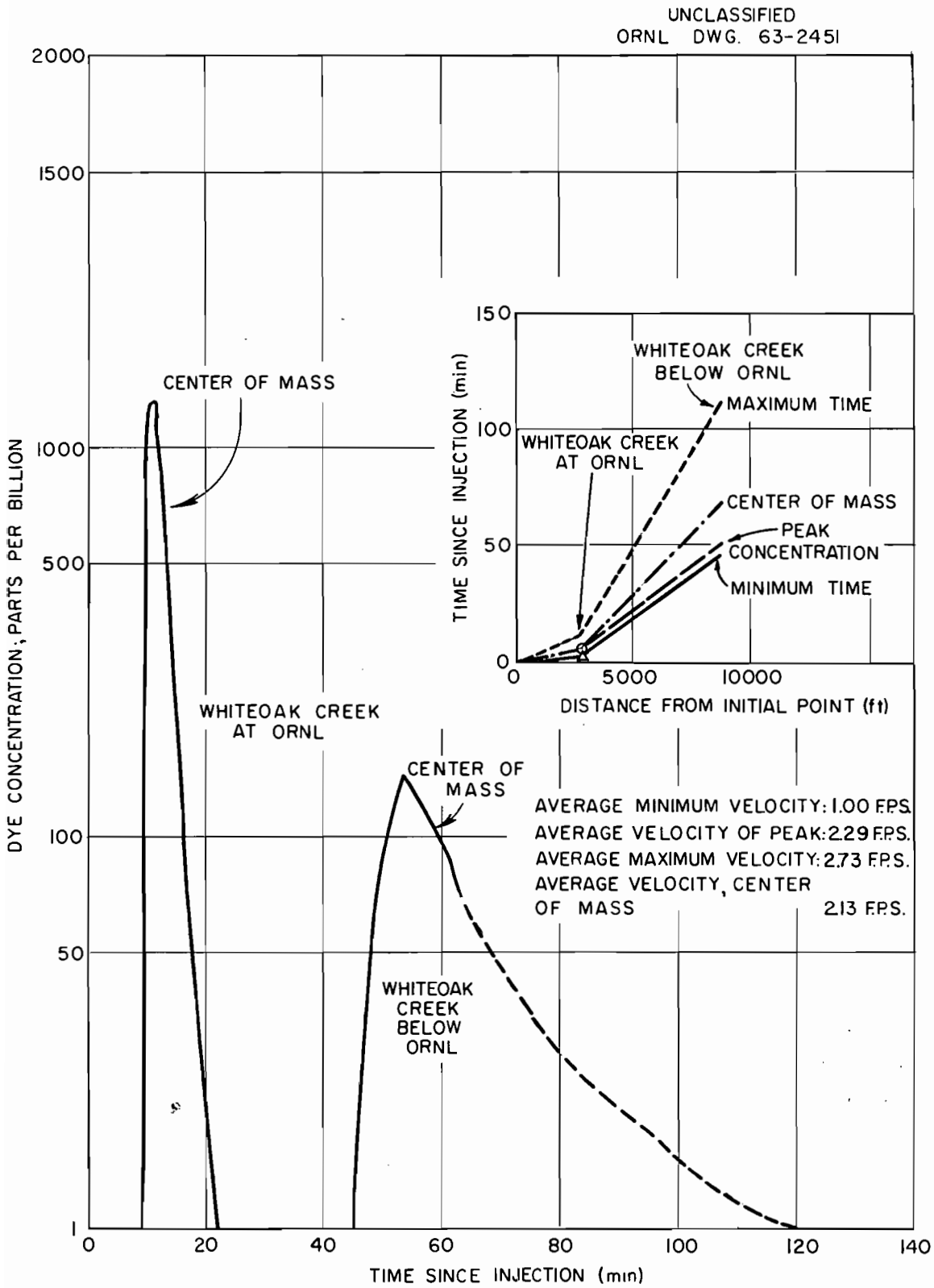

Fig. 37. Time of Travel Study White Oak Creek, March 15, 1963.

The results of this flood time-of-travel study contrast markedly with results obtained from studies made under base flow conditions. When discharge was 4.7 cfs, in October, about 3.5 hr was the minimum time required for water to travel from the Laboratory area to the station, White Oak Creek below ORNL. However, only 37 min were required during the March 15 flood.

During the week of March 18 to 22, water levels were measured in most of the permanent wells in White Oak Creek basin. A water-table contour map, drawn on the basis of the nearly 250 wells measured, was constructed, representing the water-table high for the 1963 water year.

REFERENCES

1. Unit Operations Section Monthly Progress Report for February 1963, ORNL-TM-581 (in press).

2. Unit Operations Section Monthly Progress Report for March 1963, ORNL-TM-586 (in press).

3. Unit Operations Section Monthly Progress Report for April 1963 (in press).

4. Waste Treatment and Disposal Progress Report for November 1962-January 1963, ORNL-TM-516 (June 12, 1963).

5. Chemical Technology Division Monthly Progress Report for Chemical Development Section B, March 1961, ORNL-CF-61-4-108.

6. J. T. Roberts and R. R. Holcomb, A Phenolic Resin Ion-Exchange Process for Decontaminating Low-Radioactivity-Level Process Water Wastes, ORNL-3036 (May 22, 1961).

7. R. R. Holcomb, Low-Radioactivity-Level Waste Treatment. Part I. Laboratory Development of a Scavenging-Precipitation Ion-Exchange Process for Decontamination of Process Water Wastes, ORNL-3322 (in press).

8. R. E. Brooksbank, et al., Low-Radioactivity-Level Waste Treatment. Part II. Pilot Plant Demonstration of the Removal of Activity from Low-Level Process Wastes by a Scavenging-Precipitation Ion-Exchange Process, ORNL-3349 (May 13, 1963).

9. P. Hamer, J. Jackson and E. F. Thurston, Industrial Water Treatment Practice, pp. 22-37, Butterworths in association with Imperial Chemical Industries Limited, London, 1961.

10. E. Schonfeld, R. Sanford, G. Mozella, D. Ghosh, and S. Mook, The Removal of Strontium and Cesium from Nuclear Waste Solutions by Foam Separation, NYO-9577 (July 26, 1960).

11. E. Rubin and E. Schonfeld, Foam Separation, Quarterly Progress Report, October 1, 1962 to December 31, 1962, Radiation Applications, Inc., RAI-110 (March 15, 1963).

12. R. M. G. Boucher and A. L. Weiner, "Sonic Defoaming - It's Present Status," Food Processing (October 1962).

13. R. M. G. Boucher, "Ultrasonics in Processing," Chemical Engineering, p. 83-100 (October 2, 1961).

14. Anonymous, "Defoaming by Sound Waves Explained," Chem. Engr. Prog., 57, No. 11, p. 169-70 (November 1961).

15. American Petroleum Institute, Oil-Well Cementing Practices in the United States, API, 50 West 50th Street, New York 20, New York (1959).

16. L. M. Epstein, Formation of Chemically Free Halogen by Radiolysis of Solid Potassium Chloride, Westinghouse Electrical Corporation Research Laboratories, Pittsburg, Pennsylvania, WERL-0100 (June 1962).

17. R. E. Blanco and F. L. Parker, Waste Treatment and Disposal Quarterly Progress Report August-October 1962, ORNL-TM-482 (Mar. 25, 1963).

18. Report of Committee II on Permissible Dose for Internal Radiation, International Committee on Radiological Protection, Publication 2, Pergamon Press, London (1959).

19. E. C. Albritton, Standard Values in Nutrition and Metabolism, W. B. Saunders Company (1954).

20. Department de la Protection Sanitaire Contrat de' association, C.E.A./Euratom, Donnees Biologiques de Base pour l'etude des Niveaux de Contamination Applicables aux Enfants, Supplied to ICRP by Dr. Jammet (February 1962).

21. William S. Spector (ed.), Handbook of Biological Data, Wright Air Development Center (October 1956).

22. Harry Levin, "Some Aspects of Inhalation Dose Calculation from Single Exposures," Health Physics. 9, 41-44 (1963).

23. D. G. Jacobs, "The Effects of Collapse-Inducing Cations on the Cesium Sorption Properties of Hydrobiotite," to be published in the Proceedings of the 1963 International Clay Conference, August 12-16, 1963, Stockholm, Sweden.

INTERNAL DISTRIBUTION

1. ORNL - Y-12 Technical Library Document Reference Section
2-4. Central Research Library
5-14. Laboratory Records Department
15. Laboratory Records, ORNL-RC
16-17. R. E. Blanco
18. J. O. Blomeke
19. W. J. Boegly, Jr.
20. R. L. Bradshaw
21. J. C. Bresee
22. R. E. Brooksbank
23. F. N. Browder
24. K. B. Brown
25. P. H. Carrigan, Jr.
26. W. E. Clark
27. K. E. Cowser
28. F. L. Culler
29. W. Davis, Jr.
30. W. De Laguna
31. F. M. Empson
32. D. E. Ferguson
33. E. J. Frederick
34. H. W. Godbee
35. H. E. Goeller
36. J. M. Googin
37. P. A. Haas
38. C. W. Hancher
39. C. E. Haynes
40. R. F. Hibbs
41. R. R. Holcomb
42. J. M. Holmes
43. D. G. Jacobs
44. W. H. Jordan
45. H. Kubota
46. T. F. Lomenick
47. K. Z. Morgan
48. R. J. Morton
49. E. L. Nicholson
50-51. F. L. Parker
52. J. J. Perona
53. R. M. Richardson
54. J. T. Roberts, IAEA, Vienna
55-56. E. G. Struxness
57. J. C. Suddath
58. J. A. Swartout
59. T. Tamura
60. J. W. Ullmann
61. M. E. Whatley

EXTERNAL DISTRIBUTION

62. E. L. Anderson, AEC, Washington, D. C.
63. W. G. Belter, AEC, Washington, D. C.
64. H. Bernard, AEC, Washington, D. C.
65. Arnold B. Joseph, AEC, Washington, D. C.
66. J. A. Lieberman, AEC, Washington, D. C.
67. W. H. Regan, AEC, Washington, D. C.
68. Robert F. Reitemeier, AEC, Washington, D. C.
69. Vincent Schultz, AEC, Washington, D. C.
70. John N. Wolfe, AEC, Washington, D. C.
71. H. M. Roth, AEC, ORO
72. C. S. Shoup, AEC, ORO
73. J. R. Horan, AEC, Idaho
74. K. K. Kennedy, AEC, Idaho
75. J. A. Buckham, Phillips Petroleum Company
76. J. A. McBride, Phillips Petroleum Company
77. C. M. Slansky, Phillips Petroleum Company
78. H. J. Carey, Jr., Carey Salt Company, Hutchinson, Kansas
79. C. W. Christenson, Los Alamos Scientific Laboratory
80. J. C. Frye, State Geological Survey, Div., Urbana, Ill.

81. W. B. Heroy, Sr., Geotechnical Corp., Dallas, Texas
82. E. F. Gloyna, University of Texas, Austin
83. W. J. Kaufman, University of California, Berkeley
84. L. Silverman, Harvard Graduate School of Public Health
85. G. M. Fair, Harvard University, Pierce Hall
86. H. A. Thomas, Jr., Harvard University, Pierce Hall
87. John Geyer, Johns Hopkins University
88. C. R. Naeser, George Washington University
89. W. A. Patrick, Johns Hopkins University
90. H. C. Thomas, University of North Carolina
91. L. P. Hatch, Brookhaven National Laboratory
92. H. H. Hess, Princeton University
93. Abel Wolman, Johns Hopkins University
94. O. F. Hill, Hanford
95. C. R. Cooley, Hanford
96. E. R. Irish, Hanford
97. A. M. Platt, Hanford
98. W. H. Reas, Hanford
99. G. Rey, Hanford
100. R. L. Moore, Hanford
101. W. H. Swift, Hanford
102. J. H. Horton, Savannah River
103. R. M. Girdler, Savannah River
104. Harvey Groh, Savannah River
105. C. H. Ice, Savannah River
106. J. W. Morris, du Pont, Savannah River
107. C. M. Patterson, du Pont, Savannah River
108. W. B. Scott, Savannah River
109. E. B. Sheldon, Savannah River
110. D. S. Webster, Savannah River
111. V. R. Thayer, du Pont, Wilmington
112. A. A. Jonke, Argonne National Laboratory
113. S. Lawroski, Argonne National Laboratory
114. W. A. Rodgers, W. R. Grace and Company, Naperville, Ill.
115. J. J. Weinstock, RAI
116. J. F. Honstead, IAEA, Vienna
117. D. W. Pearce, IAEA, Vienna
118. R. L. Nace, USGS, Washington, D. C.
119. P. H. Jones, USGS, Washington, D. C.
120. C. P. Straub, U. S. Public Health Service, Cincinnati, Ohio
121. Dade Moeller, U. S. Public Health Service, Winchester, Mass.
122. W. J. Lacy, Office of Civil Defense, Washington, D. C.
123. J. E. Crawford, U. S. Bureau of Mines, Washington, D. C.
124. J. W. Watkins, U. S. Bureau of Mines, Washington, D. C.
125. L. C. Watson, AECL, Chalk River, Canada
126. John Woolston, AECL, Chalk River, Canada

127. AECL, Chalk River, Canada, Attn: C. A. Mawson, I. L. Ophel
128. AEC, Sidney, Australia, Attn: R. C. Cairns, L. Keher
129. AERE, Harwell, England, Attn: H. J. Dunster
130. AERE, Harwell, England, Attn: R. H. Burns, K. D. B. Johnson
131. CEA, Grenoble, France, Attn: G. Wormser
132. CEA, Saclay, France, Attn: F. Duhamel, A. Menoux, C. Gailledreau
133. Peter A. Krenkel, Vanderbilt University, Nashville, Tennessee
134. Yehuda Feige, Ministry of Defense, Atomic Energy Commission, Rehovoth, Israel
135. CEA, Fontenay-aux-Roses, Attn: P. Regnaut, P. Faugeras, M. Bourgeois
136. Centre d'Etude Nucleaire, Mol, Belgium, Attn: L. Baetsle
137. Centre d'Etude Nucleaire, Mol, Belgium, Attn: P. de Jonghe
138. Euratom (ISPRA), Casella Postale No. 1, Attn: M. Lindner
139. Eurochemic, Mol, Belgium, Attn: R. Rometsch, T. J. Barendregt, F. Marcus
140. Jitender D. Sehgal, Bombay, India

141-155. DTIE